ROLES OF A CORE SEPTIN PROTEIN Cdc3 AND A SEPTIN ASSOCIATED PROTEIN Nap1 IN *CANDIDA ALBICANS* POLARIZED GROWTH AND CELL CYCLE

ZHAO PAN

A THESIS SUBMITTED FOR

THE DEGREE OF DOCTOR OF PHILOSOPHY

NATIONAL UNIVERISTY OF SINGAPORE GRADUATE SCHOOL FOR INTEGRATIVE SCIENCES AND TECHNOLOGY

INSTITUTE OF MOLECULAR AND CELL BIOLOGY

2011

Acknowledgements

I would like to give my heartfelt thanks to my supervisor, Professor Wang Yue, for his invaluable guidance and enormous support, especially for taking me in during the difficult time of my PhD years. He selflessly shared his life experience and his visions in science. To me, he is not just a supervisor, but also a role model in life. I am also in debt to my TAC members, A/P Uttam Surana and Prof. Yang Xiaohang, for their constructive discussions and constant encouragement.

I am very grateful to Dr. Zeng Guisheng for training me to become the researcher I am today. I would like to extend my gratitude to both the past and present members in WY lab, Dr. Yap Wai Ho, Dr. Li Changrun, Dr. Bai Chen, Dr. Zou Hao, Dr. Li Wanjie, Dr. Zhu Yong, Dr. Wang Honghua, Dr. Anand Tiwari, Ms. Xu Xiaoli, Ms. Wang Yanming, Ms. Chan Fong Yee, Ms. Au Yong Jie Ying, Mr. Daniel Schindler and Mr. Jamie Greig, for creating such a conducive working environment and for caring about me as their friend.

My family is the source of my strength and determination. I thank my parents for their understanding and their faith in me. My deepest thanks go to my beloved husband, Mr. Huang Zhenxing, for sharing the same passion in science, for keeping me together through the toughest time, and for always being there for me.

This work is dedicated to my grandfather, who died of fungal lung infection.

Zhao Pan

July, 2011

Table of Contents

List of Figures

List of Tables

Abbreviations

1NM-PP1	1-(1,1-dimethylethyl)-3-(1-naphthalenylmethyl)-1H-pyrazolo[3,4-d]pyrimidin-4-amine
2D WB	2 dimension Western blot
5-FOA	5-fluoro orotic acid
Ala (A)	Alanine
Asp (D)	Aspartic acid
ATP	Adenosine-5’-triphosphate
AUC	Area under curve
bp	Base pair or base pairs
cAMP	3’-5’-cyclic adenosine monophosphate
Cys	Cysteine
DAPI	4',6-diamidino-2-phenylindole
DTT	Dithiothreitol
g	gram
GFP	Green fluorescence protein
Glu (E)	Glutamic acid
HFM-	6×His-Flag-6×Myc tag
hr	hour or hours
HSG	Hypha-specific gene
Kb	Kilo bases
KD	Kilo Dalton
MAPK	Mitogen-activated protein kinase

Met	Methionine
mg	Milligram
min	Minute
ml	Millilitre
ng	Nanogram
OD	Optical density
ORF	Open reading frame
PAGE	Polyacrylamide gel electrophoresis
PBS	Phosphate buffered saline
PCR	Polymerase chain reaction
Pro (P)	Proline
s	Seconds
UV	Ultraviolet
µl	Microliter
µM	Micromolar

Summary

Septins play important roles in morphogenesis, cell cycle progression and cytokinesis in yeast. Their organization and function are regulated in a cell cycle dependent manner. However, the mechanisms of control remain unclear. This thesis consists of two projects on the study of one septin Cdc3 and a septin associated protein Nap1 in the fungus *Candida albicans*.

The first project is on a septin protein Cdc3. I uncovered that the *Candida albicans* septin Cdc3 undergoes cell cycle dependent phosphorylation and that phosphorylation at a single amino acid Ser422 is critical for Cdc3 functions. Hyperphosphorylated isoforms are detected in early G1 followed by a period of dephosphorylation; and after the START, Cdc3 phosphorylation increases gradually through the rest of the cell cycle. Phospho-mapping by mass spectrometry identified phosphorylation on S422 near the C terminus. The phosphomimetic S422D mutation causes disorganization of septin structures, severe cytokinetic defects, dramatic cell elongation, and inability of Cdc3 to localize to the neck. In contrast, the nonphosphorylatable S422A mutation produces a much weaker phenotype. Co-immunoprecipitation experiments demonstrate that the S422D mutation greatly weakens Cdc11's association with the septin complex and causes premature dissociation of Cdc11 from the ring. The Nim1 kinase Gin4 is involved in the phosphorylation of Cdc3, but the Cdk Cdc28 is not. These findings reveal that controlling the phospho-regulation at a single residue S422 on Cdc3 may play a crucial role in regulating septin assembly/disassembly and stability.

The second project focuses on a septin-associated protein Nap1. I report that deletion of *C. albicans NAP1* leads to constitutive filamentous growth, higher sensitivity to hyphal induction, and defective septin organization. FCF, a compound known to stabilize septin filaments, can rescue the defects caused by *NAP1* deletion. Fluorescence recovery after photo-bleaching (FRAP) analysis of Cdc3-GFP uncovers a more dynamic septin ring in *nap1*Δ compared to that in WT. In *nap1*Δ cells, Cdc3 deposits randomly on the cell cortex as spots or partial rings and experiences impairment of phosphorylation. Double deletion of *NAP1* and *CDC10*, another septin protein, results in exacerbated temperature sensitivity, defective septin ring formation and scattered Cdc3 localization. Phospho-mapping by mass spectrometry identified phosphorylation on 10 Thr/Ser residues in the N-terminus of Nap1. Mutation of these 10 residues to non-phosphorylatable Ala results in pseudohyphal growth and affects Nap1 neck localization. Conversely, mutation of these ten residues to phospho-mimetic Glu does not affect cell morphology, but causes random deposition of Cdc3. My findings unveil the roles of Nap1 in septin stabilization and Cdc3 phosphorylation control.

Chapter 1 Introduction

Candida albicans is an opportunistic fungal pathogen of human, commonly residing in the oral cavity, gastrointestinal and genital-urinary tracts (Odds, 1985). Although benign in healthy subjects, it frequently causes life-threatening systemic infections in immuno-compromised patients (Rabkin et al., 2000; Richards et al., 1999). Largely due to the AIDS pandemic in the past 30 years, *C. albicans* is today the most prevalent fungal pathogen, posing a great challenge to medicine (Berman and Sudbery, 2002). Thus, there is an urgent need to understand the mechanism of its virulence, in order to eventually develop therapies to treat *C. albicans* infections.

In addition to its medical significance, *C. albicans* is an excellent model to study certain fundamental biological processes. For example, although well known for its stringent diploidy, its unusual sexual cycle can happen under certain special conditions (Hull and Johnson, 1999; Hull et al., 2000; Magee and Magee, 1997; Magee, 2010; Perepnikhatka et al., 1999; Soll, 1997). Another example is the morphogenesis aspect of this organism. *C. albicans* can grow under 3 vegetative morphological forms: yeast, pseudohyphae and hyphae. Great efforts in the field of *C. albicans* have been devoted to understanding its ability to switch between several different morphological forms in response to environmental stimuli (Odds, 1985). The various morphological forms play different roles to account for its virulence, and the transition between them has been shown to be essential for a successful infection (Sudbery et al., 2004). To accomplish a proper morphological transition, *C. albicans* deploys multiple mechanisms, some of which are highly conserved pathways in eukaryotes. Thus, elucidation of the mechanisms underlying the transition will not only contribute to a deeper understanding of fungal

pathogenesis and virulence, but also improve our knowledge in cell morphogenesis, polarity control and cell cycle regulation.

In the following introduction section, I will first review the pathogenicity and polymorphism of *C. albicans*, its cell cycle progression, and currently known mechanisms that control its morphogenesis. Then I'll review previous studies on two proteins Cdc3 and Nap1 which I have found to play important roles in *C. albicans* morphogenesis.

1.1 Polymorphism in the pathogenesis of *C. albicans*

1.1.1 Pathogenicity of *C. albicans*

Virtually all of us carry *C. albicans* in our gastrointestinal and genitourinary tracts, and to a lesser extent, on our skin. The integral host tissue and intact immune system help to maintain a commensal relationship between *C. albicans* and the host (Calderone and Fonzi, 2001). *Candida* infection can be classified as candidiasis, referring to the infection of mucosal surfaces, and candidaemia, referring to infection in the blood stream. Mucosal candidiasis in healthy subjects is normally not life-threatening. However, recurrent oral candidiasis, such as in immune-compromised patients, sometimes lead to death from advanced esophageal colonization. Candidemia, caused by tissue invasion or contamination of indwelling catheters, can progress to the growth of fungal masses in the kidney, heart and brain (Berman and Sudbery, 2002).

C. albicans is one of the most common hospital-acquired infections. The estimated cost of treating *Candida* infection in the US alone is 1.7 billion annually (Wilson et al., 2002). Candidemia-related hospitalization incidence rose by 52% from 2000 to 2005 (Zilberberg et al., 2008). Because *C. albicans* shares some highly conserved biological processes with humans, most fungicidal drugs cause deleterious side effects. Moreover, the capacity to rapidly develop resistance to anti-fungal drugs, such as to amphotericin B, flucytosine, and a series of azoles, means that continued development of new fungicides remains of great importance. Thus, research on *C. albicans* biology would help to identify more appropriate treatment targets.

C. albicans develops various tactics to efficiently infect a host and evades the host defense mechanism. Biofilm formation is a sophisticated first step of infection. The yeast

form cells readily adhere to the host surface, followed by developing a meshwork of yeast, hyphal, pseudohyphal cells and extracellular polymers (Hawser and Islam, 1996). The ability of *C. albicans* to grow filamentously plays a critical role in the development of the spatially organized architecture seen in biofilms (López-Ribot, 2005). Deletion of the transcription factor Epidermal Growth Factor (*EFG1*) renders the cells in locked yeast form, resulting in inability of biofilm formation (Ramage et al., 2002).

The next step is tissue invasion, involving *C. albicans* cells penetrating either mucosal surfaces or blood vessel epithelial cells (Gow et al., 2003; Malic et al., 2007). To accomplish this, *C. abicans* cells utilize a combination of anchoring proteins and proteases, or mechanisms to induce endocytosis by host epithelial cells. Membrane anchoring proteins like hypha-specific wall protein 1 (Hwp1) (Staab *et al.*, 1999), and secreted aspartyl proteinases (SAP proteins) (Naglik *et al.*, 2004) have been extensively studied. *C. albicans* hyphae interact with endothelial cells *in vitro* by binding to N-cadherin on the endothelial cell surface. This binding triggers rearrangement of endothelial cell microfilaments, which results in the organism being engulfed by endothelial cells (Filler and Sheppard, 2006).

It is evident that every step of a *Candida* infection involves the intricate collaboration between its yeast and filamentous forms. Accumulated evidence from years of research points directly to the ability of *C. albicans* to switch between different growth forms being key to its virulence and pathogenicity. It is clear that a detailed understanding of this ability is essential for the control and treatment of this opportunist pathogen.

1.1.2 Host defense system and vaccination

Thanks to the considerable amount of work done on host defense against *C. albicans*, a comprehensive understanding has been achieved. The first line of defense is the intact host tissue surface. After a successful invasion by mechanisms elaborated in **Chapter 1.1.1**, leukocytes from innate immunity forms the primary protection against this organism (Fidel, 1999). Macrophages, being an important arm of phagocytic leukocytes, are the major engulfer due to the expression of mannose receptors that can recognize the cell wall of *Candida* (Seider et al., 2010; van de Veerdonk et al., 2010). However, by switching from yeast to filamentous form, *C. albicans* can not only escape from inside the host macrophage but also lyse and destroy the phagocyte (Lo et al., 1997). T cells and cell-mediated immunity (CMI) are activated a few days after *Candida* invasion. Interferon γ (IFN-γ) is a prototypic cytokine generated by T-helper1 (Th1) response. It also facilitates the killing by macrophages and the production of *Candida*-specific antibodies (Káposzta et al., 1998).

Vaccination is one of the most extraordinary achievements in human medical history, and its protective power against infectious diseases is evident. Unfortunately, no effective vaccine against *Candida* is currently available for human, and antibodies that can neutralize or opsonize the microbe are still under clinical trials (Ferwerda et al., 2010). The discovery that bacterial peptidoglycan is the active compound in the serum to induce hyphal development is ground-breaking in the understanding of the morphological switch in this organism (Xu et al., 2008), and presents a new angle for antibody targeting. By scavenging the peptidoglycans in the serum, the morphological switch of *C. albicans* might eventually be blocked, resulting in avirulent *C. albicans*.

1.1.3 Polymorphism of *C. albicans* and controlling signal transduction pathways

As introduced above, polymorphism underlies the pathogenicity of *C. albicans* and contributes greatly to its ability to evade the host's immune surveillance. Morphogenesis refers to the ability of *C. albicans* to switch between 3 vegetative morphological forms: yeast, pseudohyphae and hyphae (**Fig. 1.1**). The shape of yeast cells is round to ovoid, and the daughter and mother cells are readily separated from each other after cytokinesis. At the mother daughter junction, where the nuclear division occurs, the septin ring serves as both a scaffold and a diffusion barrier (Sudbery et al., 2004). At the tip of the growing bud, the crescent-shaped polarisome helps to establish polarized growth. During pseudohyphal growth, both the polarisome and septin ring localize properly, except the cells themselves are elongated and are not separated after cytokinesis. Different from pseudohyphal cells, no obvious septal constrictions can be observed in true hyphae. At the tip of a growing germ tube, both the polarisome and the Spitzenkorper can be found (Crampin et al., 2005). Nuclear division happens across the septum within the elongated germ tube, usually 10-15 micron from the base of the germ tube (Sudbery, 2001). *C. albicans* can switch between these different morphologies responding to environment cues. As discussed in **Chapter 1.1.1**, each growth form provides essential functions to the pathogenicity of *C. albicans*, and the ability to switch growth forms accounts for its virulence (Sudbery et al., 2004). Mutants defective in morphological transition have shown to be less virulent than wild type strain or avirulent (Lo et al., 1997; Zheng and Wang, 2004).

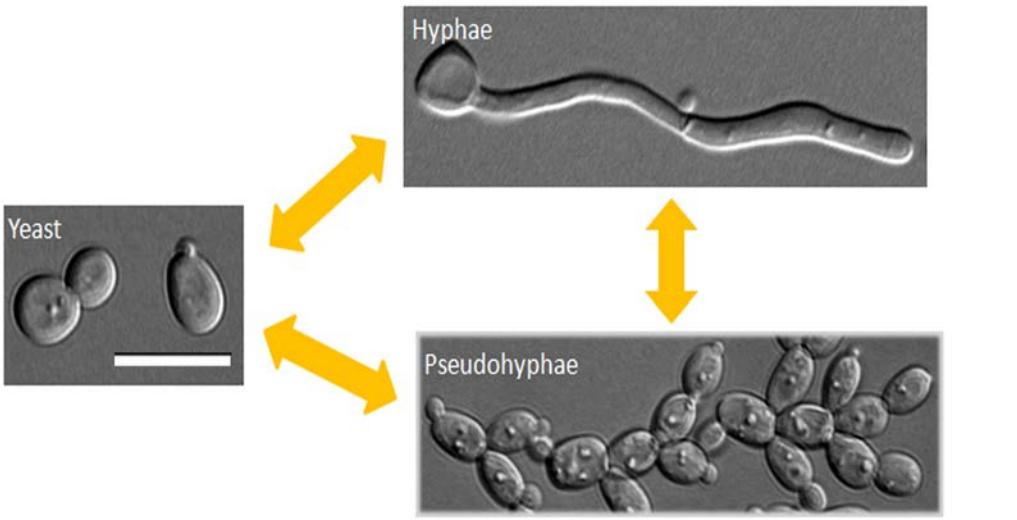

Figure 1.1 Polymorphism of *C. albicans*

C. albicans can switch among different morphological forms as indicated by yellow arrows upon external triggering. Grey bar=10 μm

The yeast to hyphal transition can be triggered by a wide range of growth conditions and chemicals, such as serum, *N*-acetyl-glucosamine, high temperature, CO_2, starvation, pH, genotoxic and oxidative stress (Biswas et al., 2007). Different inducers exhibit varied degrees of potency and penetration. Serum is found to be the most potent and physiologically relevant hyphae inducer (Ernst, 2000). In laboratories, the routine practice for hyphal induction is media containing 5-20% serum at 37^{o}C, which mimics physiological conditions. Xu *et al.* have recently identified the bacterial peptidoglycan-like molecules as the active ingredient in serum, showing high potency in triggering *C. albicans* hyphal growth (Xu et al., 2008).

Numerous studies have been devoted to the understanding on how the external signals are relayed into the cell to induce cellular response. Multiple pathways and genes involved in controlling the yeast-hyphal transition have been identified. Among them, Cph1-mediated MAPK and the Efg1-mediated cAMP pathways are well-understood (**Fig. 1.2**). *CPH1* (*Candida* PseudoHyphal 1) is a transcription factor homologous to *S. cerevisiae STE12* (STErile 12), which is targeted by MAPK (Mitogen-Activated Protein Kinase) cascade. Its deletion results in suppression of hyphal formation on solid but not in liquid media containing serum (Liu et al., 1994). Farnesol, an autoregulatory quorum sensing molecule, has been shown to inhibit hyphal formation through the MAPK pathway (Sato et al., 2004). Other triggers, such as oxidative stress, nitrogen starvation and low pH, are also likely to act through the MAPK pathway (Alonso-Monge et al., 1999; Eisman et al., 2006). *EFG1* (Enhanced Filamentous Growth 1), homologous to *S. cerevisiae PHD1* (PseudoHyphal Determinant 1), is a transcriptional regulator targeted by cAMP metabolism. Deletion of *EFG1* again results in defective hyphal formation on solid media. In fact, absence of *CDC35/CYR1* that encodes the sole adenylyl cyclase responsible for cAMP production, also renders the yeast cells unresponsive to hyphal induction (Rocha et al., 2001). It has been demonstrated that muramyl dipeptides, subunits of peptidoglycan, can bind to Cdc35/Cyr1 directly and activate it (Xu et al., 2008). Both Cph1and Efg1 subsequently regulate a group of hyphal-specific genes that orchestrate the hyphal growth in response to induction (**Fig. 1.2**).

Among the hypha-specific genes (HSGs), *HGC1* (Hypha-Specific G1 Cyclin) is essential for hyphal growth (Zheng and Wang, 2004). The CDK/cyclin complex Cdc28/Hgc1 has been demonstrated to phosphorylate Rga2, a GTPase activating protein

(GAP) of the master polarity regulator Cdc42. Consequently, the localization of Rga2 to the hyphal tips is inhibited, thus Cdc42 is locked in the active form at the tip (Zheng et al., 2007). Cdc28/Hgc1 also targets the above mentioned transcription factor Efg1 (Wang et al., 2009). The phosphorylated Efg1 exhibits strong affinity for the promoters of Ace2 activated genes, which are involved in the post-cytokinetic septum degradation. The complex has also been shown to phosphorylate Sec2 to regulate secretory vesicles (Bishop et al., 2010), and mediate the transcription factor *UME6* regulated filamentous growth (Carlisle and Kadosh, 2010).

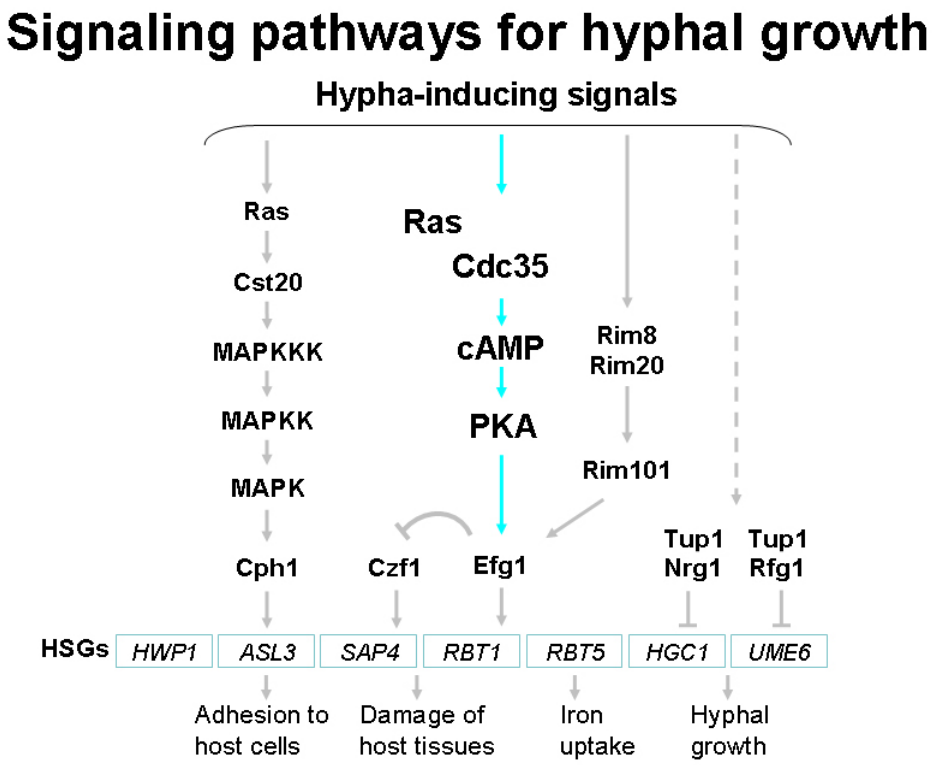

Figure 1.2 Signalling pathways responsible for hyphal induction

Figure modified from review slides by Dr. Wang Y.

Other hyphal inducers, such as alkaline pH and *N*-acetyl-glucosamine are effectuated by transcription factor Rim101 (Davis et al., 2000) and a group *N*-acetyl-glucosamine catabolic genes (Kumar et al., 2000) respectively. With the increased amount of regulatory factors that have been identified over the years, a network of signal transduction pathways is unveiling, which greatly enhances our understanding of *C. albicans* morphogenesis and related pathogenicity.

1.2 Septins in the regulation of cell cycle

1.2.1 Mitosis and its regulation

Cell division is a fundamental biological process that underlies the survival and perpetuation of all living things, from prokaryotes to eukaryotes, from single to multi cellular organisms. Prokaryotic cells duplicate themselves by binary fission. In eukaryotes, cell division is a precisely controlled series of events, usually in a cyclic manner termed the cell cycle. When the DNA content is replicated and equally segregated into the two resultant cells, the cell cycle is termed mitosis. I will focus on mitosis in this thesis. In each mitotic cell cycle, the DNA content is faithfully duplicated and accurately segregated into two cells. It is quite clear now that the regulators of cell cycle are similar in essence in all eukaryotes, ranging from the budding yeast to human somatic cells (Enserink and Kolodner, 2010; Satyanarayana and Kaldis, 2009).

The complicated process of cell cycle passage is controlled and driven by protein phosphorylation dependent activation or degradation. The most crucial group of proteins that orchestrate the cell cycle are called cyclin-dependent-kinases (CDKs) (Enserink and

Kolodner, 2010; Satyanarayana and Kaldis, 2009). Interestingly, their expression levels do not fluctuate with the progression of cell cycle. However, their kinase activities exhibit cell cycle dependency due to a group of the activator proteins called cyclins. Different cyclins associate with designated CDKs at specific stages of the cell cycle. They not only activate the kinase activity of CDKs, but also determine the substrate specificity. The activation or inhibition of the target proteins involved in cell cycle progression is achieved by the cyclin-CDK complexes phosphorylating their specific regulatory sites at the appropriate time. Two ubiquitin ligases, Skp1–Cul1–F-box-protein (SCF) and anaphase promoting complex (APC/C), are also essential for cell cycle progression (Skaar and Pagano, 2009). They control the ubiquitination and thus degradation of the phospho-inactivated proteins targeted by cyclin-CDKs. Moreover, they also control the degradation of cyclin-CDKs at the end of their designated phase, thus forcing the cell to traverse the cell cycle unidirectionally.

Mitosis can be briefly divided into interphase and mitosis (M) phases. Interphase is generally a preparation stage and cells go through G1 (G indicates Gap), S (S indicates synthesis), and G2 phases. During G1 phase, the cell size enlarges and G1 cyclin-CDKs are activated. They subsequently phosphorylate and activate transcription factors controlling the genes required for DNA synthesis. S-phase cyclin-CDKs are assembled in late G1 and accumulate very fast due to G1 cyclin-CDKs phosphorylating S-phase cyclin-CDK inhibitors, which are subsequently ubiquitinated by SCF. When S-phase cyclin-CDKs phosphorylate and activate proteins for DNA replication, cells enter S phase. Mitotic cyclin-CDKs are assembled during S and G2 phase, but their activity is suppressed until DNA synthesis is faithfully completed. Once activated, cells enter the

complicated M phase, which is divided into prophase, metaphase, anaphase and telophase. In prophase, several events occur, such as nuclear envelope breakdown, chromosome condensation, and formation of mitotic spindle apparatus by microtubules. In metaphase, chromosome kinetochores are attached to the spindle apparatus. Daughter chromatids are pulled towards opposite spindle poles by the shortening of spindle microtubules. Anaphase is marked by the separation of sister chromatids. This is promoted by APC/C mediated destruction of securin. Securin is the protector of the proteins linking the sister chromatids together. Cdc14 is a protein phosphatase essential for the late mitotic progression (De Wulf et al., 2009). It is released from the nucleolus by the coordinated action of FEAR (CDC Fourteen Early Anaphase Release) and MEN (Mitotic Exit Network) during anaphase. Cdc14 together with APC/C the ubiquitin ligase direct the dephosphorylation and degradation of mitotic cyclin-CDKs at late anaphase. The consequence is that the targets of mitotic cyclin-CDKs are dephosphorylated soon after the kinase activity drops, leading to the onset of telophase. During telophase, events such as chromosome decondensation, nuclear envelope re-assembly, remodeling of daughter cell cytoskeleton and eventual cytokinesis, mark the end of mitosis.

Saccharomyces cerevisiae, also known as budding yeast and baker's yeast, has had irreplaceable value in food and fermentation products for thousands of years. Together with *Schizosaccharomyces pombe*, also known as fission yeast, they have proven to be enormously beneficial eukaryotic model organisms, especially in the understanding of the eukaryotic cell cycle. The 2001 Nobel Prize in Physiology or Medicine was awarded to Sir Paul Nurse and Leland Hartwell for the discovery and elucidation of cell cycle regulation by cyclins and CDKs in yeast since the 1970s. They

identified the *cdc* (cell-division cycle) mutants by screening temperature sensitive mutations, which later led to the rapid isolation of genes regulating human cell cycle. They initiated the field of cell cycle control study using yeast models and laid the foundation of our current understanding of the cell cycle in eukaryotes.

In animal cells, the nuclear envelope is broken down during mitosis, which is termed "open" mitosis. In *S. cerevisiae* and *C. albicans*, the nuclear envelope stays intact throughout the cell cycle, and the chromosome segregation is accomplished inside the nuclear envelope. This is termed "closed" mitosis. Both *S. cerevisiae* and *C. albicans* cells replicate by budding. Apart from differences in the bud formation and the breakdown of the nuclear envelope, the basic events and their regulation are quite similar in yeast and mammalian cells (Lodish et al., 6^{th} ed). During G1 phase, the cell has to enlarge to a critical size, after which the cell enters S phase irrevocably and traverses the entire cell cycle. This point of commitment is called START (**Fig. 1.3**). A small bud emerges after START and DNA replication begins during S phase. In G2 phase, the nucleus migrates towards mother daughter neck region and starts to elongate. During M phase, the chromosomes align at the metaphase plane inside the nucleus and sister chromatids segregate, followed by cytokinesis, resulting in a larger mother cell and a smaller daughter cell.

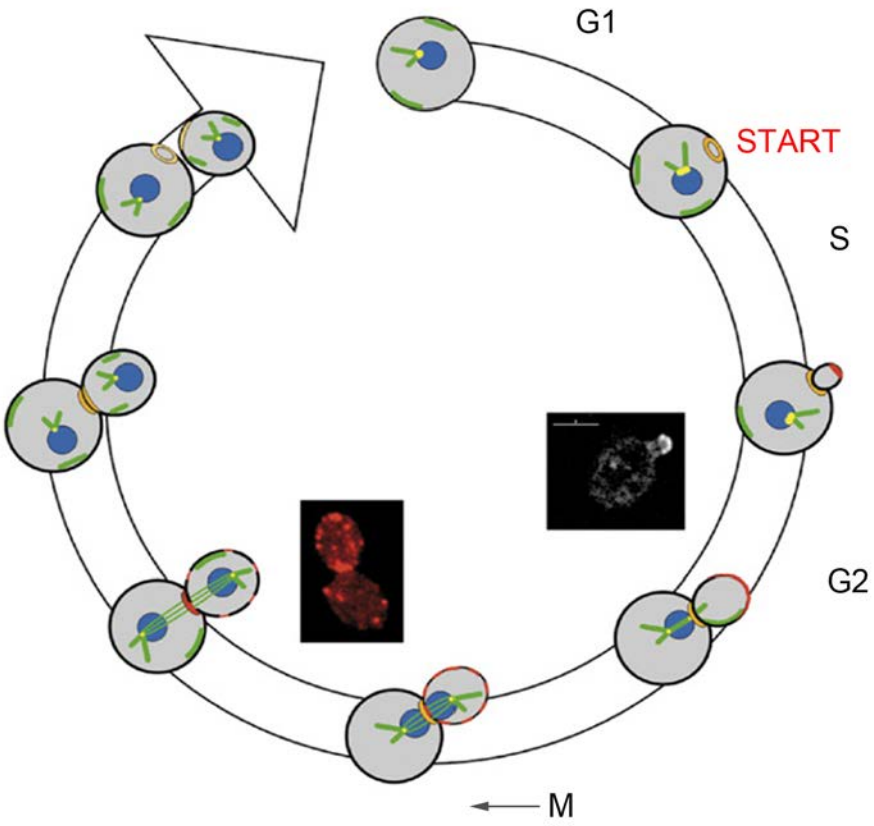

Figure 1.3 The cell cycle progression in *S. cerevisiae* and *C. albicans*

The septin ring is represented by the orange ring, polarisome by the red crescent, spindle pole body by yellow dots, astral microtubule by green lines, and nucleus by blue spheres.

1.2.2 Cell cycle in *C. albicans*

S. cerevisiae has six CDKs: Cdk1 (also known as Cdc28) (Lörincz and Reed, 1984), Pho85 (similar to mammalian Cdk5) (Toh-e et al., 1988), Kin28 (mammalian Cdk7 homologue) (Simon et al., 1986), Ssn3 (mammalian Cdk8 homologue) (Liao et al., 1995), Ctk1 (Lee and Greenleaf, 1991) and Bur1 (Yao et al., 2000) (both are homologues

of mammalian Cdk9). Cdk1/Cdc28 is the only necessary and sufficient CDK to drive the cell cycle (Liu and Kipreos, 2000). Stage specific cyclins include 3 G1 cyclins (Cln1, 2 and 3) (Tyers et al., 1993), 6 B-type cyclins (Clb5 and 6 in early S phase (Jackson et al., 2006); Clb3 and 4 in late S and early M phase (Mendenhall and Hodge, 1998; Richardson et al., 1992); Clb1 and 2 in late M phase (Seufert et al., 1995)). Similar to *S. cerevisiae, C. albicans* has one CDK Cdc28 (Damagnez and Cottarel, 1996), 3 G1 cyclins (Ccn1 and Cln3 for yeast growth G1 phase (Chapa y Lazo et al., 2005; Sherlock et al., 1994); Hgc1 for hyphal growth (Zheng and Wang, 2004)). Unlike *S. cerevisiae, C. albicans* has only 2 B-type cyclins (Clb2 and 4) (Bensen et al., 2005; Damagnez and Cottarel, 1996). The cell cycle progression in *C. albicans* is similar to that of *S. cerevisiae*, though the players vary (**Fig. 1.3**) (Berman, 2006). Cell size threshold has to be reached for START, after which septins form a ring at the neck and the polarisome concentrates to the tip of the bud to direct bud growth. Growth becomes more isotropic with the enlargement of the bud. The nucleus moves to the neck region during G2 and divides across the neck at anaphase. At telophase, with the disassembly of spindle, septin ring splits into two. The old septin ring will be disassembled before the formation of a new ring in the next G1.

Pseudohyphal and hyphal growth forms of *C. albicans* have distinctive cell cycles. The features of pseudohyphal growth are: polarized growth persists longer, G2 phase is prolonged resulting in large daughter cell and cytokinetic defect results in chains of cells. The features of hyphal growth are: germ tube evagination and elongation occur before START, hyphal growth is independent of cell cycle (Hazan et al., 2002) and is directed by the Spitzenkörper and polarisome, both of which are constitutively present at the tip of the germ tube (Crampin et al., 2005). During early hyphal development, septins form a

faint cap at the tip of the germ tube and a band structure at the base of the germ tube. Both the cap and the band structures become diffuse as the germ tube elongates. A septin ring is formed at the presumptum along the germ tube, and the nucleus divides across the metaphase plane. After cytokinesis, the daughter cell, which is in the shape of a cylindrical germ tube, is still attached to the mother cell without a constriction between them. Furthermore, the septin ring is not disassembled and stays at the septum (Sudbery et al., 2004).

1.2.3 Septins

Septins are a group of highly conserved GTP binding proteins found in yeast and animal cells. Septins were first identified by Hartwell (Hartwell, 1971) as temperature sensitive cell cycle division (*cdc*) mutants in *S. cerevisiae*. *S. cerevisiae* encodes seven septins, of which 5 (*CDC3*, *CDC10*, *CDC11*, *CDC12* and *SHS1*) are expressed in mitosis, and 2 (*SPR3* and *SPR28*) in meiosis (De Virgilio et al., 1996; Ozsarac et al., 1995). The same number of septin genes was found in fission yeast and *C. albicans* (Pan et al., 2007; Warenda and Konopka, 2002). There are 2 septins in *C. elegans*, 14 in humans, 13 in mouse, and 17 in zebrafish (Pan et al., 2007). Despite the varied number of isoforms, septins share a common structure: a flexible N-terminal extension (NTE), a polybasic region that facilitates plasma membrane binding and a conserved GTP binding domain (**Fig. 1.4**). Most septins also have a C-terminal flexible end (CTE), which contains a coiled-coil (CC) domain.

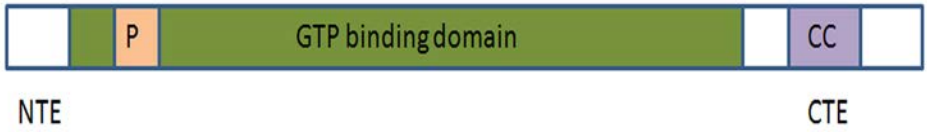

Figure 1.4 The common structure of septins

NTE=N terminal extension; CTE=C terminal extension; P=poly basic domain; CC=coiled coil domain.

Although every septin has a GTP-binding domain, not all possess the ability to hydrolyze GTP. For example, mammalian Sept2 and Sept7, but not Sept6, share the conserved Thr78, which is involved in GTP binding and hydrolysis (Sirajuddin et al., 2007; Sirajuddin et al., 2009). In *S. cerevisiae*, only Cdc10 (Thr74) and Cdc12 (Thr75), but not Cdc3, Cdc11 or Shs1, display GTPase activity(Versele and Thorner, 2004). Therefore, the ability of septins to bind to GTP appears to play mainly a structural role, as many works have substantiated (Farkasovsky et al., 2005; Field et al., 1996; Kinoshita et al., 2002; Nagaraj et al., 2008; Vrabioiu et al., 2004).

Though the number of players varies, the fundamental mechanism of septin complex formation is similar across species. Septin units can hetero-oligomerize into rod-shaped complexes which then polymerize end-to-end into paired long filaments. Electron microscopy pictures show septins purified from yeast, *C. elegans* and human form similar rod-shaped hetero-oligomers in vitro (**Fig. 1.5**) (Bertin et al., 2008; John et al., 2007; Sirajuddin et al., 2007). The filaments can assemble into higher order structures such as rings at the mother-daughter neck in yeast. Two types of interaction interfaces G and NC alternate to link the septin monomers in a rod (**Fig. 1.5**). The G interface involves the

GTP-binding domain of adjacent monomers, and the NC interface involves residues in the N- and C-terminal segments. Most septins have a variable C-terminal extension (CTE) that often contains a segment with coiled-coil-forming potential thought to mediate protein-protein interaction. The CTE is essential for *S. cerevisiae* Cdc3 and Cdc12 functions in vivo (Bertin et al., 2008; Bertin et al., 2010; John et al., 2007; Rodal et al., 2005; Versele et al., 2004; Versele and Thorner, 2004). The two septins associate through the G interface in septin rods and their CTEs form a coiled-coil helix bundle (Bertin et al., 2008). Under low salt conditions the CTEs coiled-coils projecting from one filament associate with those from a parallel filament, forming lateral bridges that cross-link the filaments into a 'rail-track'-like structure (Bertin et al., 2010). Thus, the CTEs of Cdc3 and Cdc12 play key roles in the assembly and stabilization of septin structures. The CTE of Cdc11 has also been shown to associate in a homotypic manner which mediates the end-to-end assembly of septin rods into long filaments and further into mesh-like structures (Bertin et al., 2008). It is thus tempting to speculate that the CTEs might be the points of control by protein modifications to regulate septin architectures. The reported regulatory phosphorylation of ScCdc3 and CaCdc11 by CDKs in the CTE supports this hypothesis (Tang and Reed, 2002; Sinha et al., 2007).

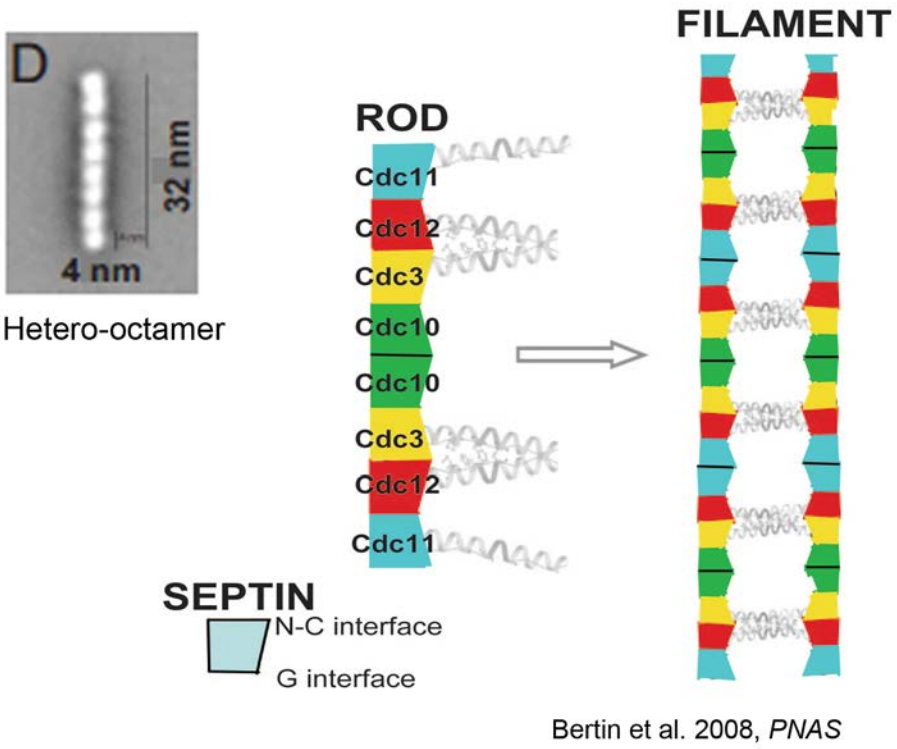

Figure 1.5 Electron microscopic photo of septin hetero-octamer in *S. cerevisiae* and schematics of the septin filament organization

D: electron microscope picture of the septin hetero-octamer in vitro. The formation of the octamer requires the interaction between alternating N-C interface of one septin and G interface of another. The helices represent the C terminal extension of Cdc3 and Cdc12.

The septin complex at the bud neck serves two major functions: a scaffold that recruits proteins involved in cell cycle progression to the neck; and a diffusion barrier that maintains the distinct protein repertoires of mother and daughter cells. For example, in the budding yeast, the p21-activated kinase (PAK) Cla4 is recruited to septin filaments at G1 to S phase before bud emergence through its septin-binding domain, and directly phosphorylates Cdc10 to promote septin collar formation (Versele and Thorner, 2004). In

C. albicans, the Nim1 kinase Gin4 has been shown to be phospho-activated by the B-type cyclin-CDK to phosphorylate Sep7 at mitosis, but it can associate with septin complex since G1 phase through its non-kinase region. This association during G1 is likely to play a structural role in the septin ring assembly (unpublished data by Dr. Wang Yue's lab). The barrier formed by the septin complex serves to prevent the free diffusion of nuclear envelope proteins (Shcheprova et al., 2008) and endoplasmic reticulum (Luedeke et al., 2005), as well as to compartmentalize the plasma membrane (Barral et al., 2000; Dobbelaere and Barral, 2004; Takizawa et al., 2000). An unambiguous result of this septin filament barrier is the maintenance of growth polarity. In fact, in budding yeast cells with a disrupted septin collar in combination with the deletion of cell cycle check point *SWE1*, cell growth is mis-directed to the mother cell instead of to the daughter bud (Barral et al., 2000).

1.2.4 Septin organization, dynamics and regulation in *S. cerevisiae*

In budding yeast, 5 septins (Cdc3, Cdc10, Cdc11, Cdc12 and Shs1/Sep7) are expressed during mitosis. Mutations in all but Shs1 cause temperature sensitive cell division cycle defects (Hartwell, 1971). Deletion of *CDC3* or *CDC12* is lethal (Flescher et al., 1993). All septins contain a conserved GTP-binding domain, with variable N- and C- terminal extensions. As discussed in **Chapter 1.2.3**, the function of GTP binding is mainly structural, since the ability to hydrolyze GTP is not absolutely required (Versele and Thorner, 2004). The longest N-terminal extension (NTE) is found in Cdc3, and longest C-terminal extension (CTE) is found in Shs1. A coiled-coil domain is located in the CTE of all septins except Cdc10. The CTEs are essential for the function and

association of Cdc3 and Cdc12 *in vivo* (Versele et al., 2004). The four essential septins (Cdc3, Cdc10, Cdc11 and Cdc12) form a linear octameric rod in the sequence of Cdc11-Cdc12-Cdc3-Cdc10-Cdc10-Cdc3-Cdc12-Cdc11 (**Fig. 1.5**). This non-polar feature of the octamer enables end-to-end assembly into filaments through the NTE of Cdc11 (Bertin et al., 2008). The lateral association between filaments is speculated to be mediated by the CTEs of Cdc3 and Cdc12, however, this has not been tested since octamers cannot form in the absence of them (Bertin et al., 2008; Versele et al., 2004).

One hallmark of the septin ring in the budding yeast is the cell cycle "regulatedness". As discussed in **Chapter 1.2.2**, the old septin ring disassembles in early G1 and a nascent ring marking the incipient budding site is formed in late G1. Septin complex stays at the septum from S until late anaphase as a single ring. The ring splits into two at telophase and the two rings eventually separate with the two resultant cells. The disassembly is thought to be triggered by the phosphorylation of Cdc3 at its CTE by G1 cyclin-Cdk1 complex (Tang and Reed, 2002). The assembly of a new ring is controlled by Cdc42, the master regulator of polarity. Three steps are executed: septin recruitment, ring assembly and ring maturation. The recruitment of septins to the presumptive budding site can operate through either Gic1/Gic2 (GTPase interactive component 1/2) (Iwase et al., 2006) at high temperature or Bni1 (Bud neck involved 1) (Park and Bi, 2007) at low temperature, both of which are effecter pathways of Cdc42. The ring assembly requires the GTPase-activating proteins (GAPs) for Cdc42, which help to unload the septin complex from recruitment pathways (Caviston et al., 2003; Gladfelter et al., 2002; Kadota et al., 2004). Another Cdc42 effecter protein Cla4 has been shown to directly phosphorylate a subset of septins and promote septin collar

formation (Versele and Thorner, 2004). Ring maturation refers to the formation of a stable septin hourglass at the neck after bud emergence. The mechanism is still unclear. Elm1 (Bouquin et al., 2000) and one of its target kinases, the Nim1 kinase Gin4 (Asano et al., 2006) are thought to be involved.

Using FRAP (Fluorescence Recovery After Photobleaching), the dynamics of the ring has also been shown to be cell cycle dependent (Dobbelaere et al., 2003). The septin ring appears static during bud growth and telophase, while highly dynamic during bud emergence and M phase till the onset of cytokinesis. Phosphorylation of Shs1 by Cla4 and Gin4 triggers septin immobilization. While dephosphorylation of Shs1 by Rts1, a regulatory subunit of PP2A, induces fluidity at telophase (Dobbelaere et al., 2003). Together, even though the overall events are not quite clear, it is very likely that phospho-regulation of septins is the mechanism controlling the ring organization and dynamics.

1.2.5 Septin organization, dynamics and regulation in *C. albicans*

Similar to *S. cerevisiae*, there are 5 mitotic septins (Cdc3, Cdc10, Cdc11, Cdc12 and Sep7) in *C. albicans*, of which Cdc3 and Cdc12 are essential for survival. All septin members have variable N- and C- terminal extensions. Cdc3, Cdc11 and Cdc12, but not Cdc10, have a coiled-coil domain at the C-terminus. Deletion of *CDC10* causes very mild cell elongation at 30^{o}C, while the effect of *CDC11* deletion is slightly stronger. The aberrant phenotype is exacerbated with the increase of temperature. Deletion of *SEP7* causes no observable phenotype under yeast growth condition (Warenda and Konopka, 2002). Upon hyphal induction, *CDC10* and *CDC11* null mutants exhibit abnormally

curved germ tubes and reduced pathogenicity (Warenda et al., 2003; Warenda and Konopka, 2002). On the other hand, *sep7*Δ mutants are able to form normal germ tubes, but the daughter hyphal compartment, which usually remains attached to the mother cell, separates from the mother compartment after cytokinesis. The cause for the separation is the abnormal recruitment of Cdc14, the phosphatase promoting mitotic exit, to the septum in the hyphal tube (Gonzalez et al., 2009).

During *C. albicans* yeast growth, the localization of septins is indistinguishable from that in *S. cerevisiae*, i.e. at incipient budding site and later the neck of the mother-daughter septum. The ring slowly disassembles after cytokinesis but before new bud emergence. Upon hyphal induction, septins localize to the cortical site of germ-tube emergence, then form a cap at the tip and a band at the base of the germ tube (Warenda and Konopka, 2002). As the germ tube elongates, the band at the base is disassembled and septins are concentrated at the septum between hyphal compartments. At telophase, the ring splits into two rings, which are maintained after cytokinesis. The septin dynamics under yeast growth condition in *C. albicans* has been reported to be different from hyphal growth (González-Novo et al., 2008). During yeast growth, the pattern is similar to that of *S. cerevisiae*. No exchange of septins is observed in cells with small buds or split rings. On the other hand, under hyphal induction condition, Cdc3, Cdc12 and Sep7 exhibit no observable exchange with cytoplasmic pool, whereas Cdc10 is quite dynamic. Cdc28-Hgc1, the hyphal-specific CDK-G1 cyclin complex, has been implicated in the phosphorylation of Sep7, and conversion of the septin ring to hyphal-specific state (González-Novo et al., 2008). Therefore, the septin complex is likely to be differentially regulated under different growth modes with phospho-regulation as a major controlling

mechanism. One study by Sinha *et al.* has elegantly illustrated the differential control of Cdc11 under yeast and hyphal growth. Gin4, a Nim1 kinase known to regulate septins, phosphorylates Cdc11 at Ser349 at the end of mitosis. This event primes Cdc11 for the phosphorylation by Cdk1/Ccn1, the CDK- G1 cyclin complex, at Ser395 during G1 phase of the next cell cycle. Cdc11 is dephosphorylated at the G1/S transition and stays dephosphorylated until the end of mitosis. In contrast, under hyphal induction, both S394 and S395 are locked in a phosphorylated state independent of cell cycle phases, which is achieved through coordinated actions of three kinases: Gin4, Cdc28-Ccn1 and the hyphal-specific Cdc28-Hgc1 (Sinha et al., 2007).

Compared to the septins in *S. cerevisiae*, the structural organization of the complex in *C. albicans* is less well understood. However, due to the high sequence homology, very similar behavioral pattern and dynamics, it is likely that the structure of *C. albicans* septins also resembles that of *S. cerevisiae*. Thus, combining their highly conserved nature and the current understanding of septins in *C. albicans*, the key regulation of septin complex in *C. albicans* most likely lies in the intricate interplay between kinases and phosphatases. Furthermore, the understanding of septins in *C. albicans* can also reciprocate and complement the current knowledge in *S. cerevisiae* and other organisms.

1.3 Nucleosome assembly protein 1

Nucleosome assembly protein 1 (Nap1), as the name suggests, was first identified as a chaperone protein that can assemble nucleosomes in mammalian cells *in vitro* (Ishimi and Kikuchi, 1991; Ishimi et al., 1987; Ishimi et al., 1985). Since then, homologues of Nap1 have been identified in yeast (Ishimi and Kikuchi, 1991), *Drosophila* (Ito et al., 1996), soybean (Yoon et al., 1995), tobacco and rice (Dong et al., 2003), nematode (Gal et al., 2005), and *Xenopus* (Steer et al., 2003). Nap1 is a highly conserved protein among all these organisms. While yeast has only one NAP family protein, multi-cellular organisms have more than one NAP1 homologue, including NAP1 like proteins (NAP1L), template activating factor 1 (TAP1, also known as SET), testis specific protein Y encoded (TSPY), and CASK (calcium/calmodulin-dependent serine protein kinase)-interacting nucleosome assembly protein (CINAP). Many members of the NAP family display tissue or cell type specific expression patterns. The functions of this family of proteins are ubiquitous and seemingly unrelated. They have been implicated in nucleo-cytoplasmic shuttling, chromatin assembly and remodeling, transcription and translation, silencing, cell cycle control, and cell wall synthesis (Park and Luger, 2006a; Zlatanova et al., 2007). In this thesis, I will focus on Nap1's involvement in cell cycle and morphogenesis control.

The central domain of all nucleosome assembly proteins, which is called the NAP domain, is highly conserved. This NAP domain is necessary and sufficient for their nucleosome assembly function (Fujii-Nakata et al., 1992); and the N- and C-terminal extensions are highly variable. The structure of yeast Nap1 reveals a possible mechanism by which the nucleo-cytoplasmic shuttling is regulated. Nap1 exists as homo-dimers,

which are mediated by a 47 amino acid long dimerization helix (McBryant and Peersen, 2004). A nuclear export signal (NES) resides at the tip of the helix and is masked by an accessory domain that contains potential target sites for casein kinase II (Park and Luger, 2006b). Indeed, a later study has demonstrated that casein kinase II can phosphorylate Nap1 at 3 Ser sites, and the phosphorylation promotes import of Nap1 into the nucleus (Calvert et al., 2008). Mutating these Serines to either non-phosphorylatable or phospho-mimetic residues causes prolonged S phase, but exerts no effect on normal bud formation.

Due to its involvement in numerous cellular functions, especially in gene transcription regulation, deletion of *NAP1* in *S. cerevisiae* causes altered gene expression patterns of over 10% of the whole genome (Ohkuni et al., 2003). Interestingly, loss of the gene does not result in any significant phenotype in the budding yeast. In contrast, deletion of *NAP1* in *Drosophila* and mouse results in embryonic lethality (Lankenau et al., 2003; Rogner et al., 2000). The diverse functions of Nap1 are likely to be achieved by binding to a vast number of partners. Compared to the understanding of Nap1 in chromatin assembly and histone binding, other aspects, such as cell cycle regulation are largely unclear. Its involvement in cell cycle was first discovered by Kellogg *et al.* for its specific interaction with the B type cyclins, Clb2 in the budding yeast and cyclins B1 and B2 in *Xenopus* (Kellogg et al., 1995). Without Nap1, Clb2 cannot carry out its full range of functions, such as the regulation of microtubule dynamics, or the induction of isotropic bud growth, which results in elongated buds (Kellogg and Murray, 1995). It was later uncovered that Nap1, together with Clb2-Cdk1 and Gin4, a Nim1 kinase promoting mitosis, are in the septin complex (Altman and Kellogg, 1997; Longtine et al., 2000; Okuzaki et al., 1997). Gin4 is hyperphosphorylated and activated upon entering mitosis.

The activation of Gin4 kinase activity is dependent on Nap1 and Clb2-Cdk1. In addition, the bud neck localization of Gin4 is lost in the absence of *NAP1*. Thus, it is highly likely that Nap1 acts upstream of Gin4. However, Nap1 has later been shown to affect septin organization in the budding yeast. In the absence of the gene, instead of forming a clear band structure at the neck, the septin complex is either "fuzzy" or forms parallel bars at the neck (Longtine et al., 2000). Therefore, it is also possible that Nap1 and Gin4 act on septins in separate pathways, and the efficient recruitment of Gin4 to the neck is impaired by the misorganized septin complex. This hypothesis is supported by the observation that the phenotype and degree of septin complex misorganization of *nap1Δgin4Δ* are more severe than either *nap1Δ* or *gin4Δ* (Longtine et al., 2000).

In *C. albicans*, in contrast to the mild filamentous growth phenotype in budding yeast *gin4Δ* mutants, deletion of *GIN4* results in severe cell elongation, cytokinetic defects and irresponsiveness to serum induction (Wightman et al., 2004). Similar to *S. cerevisae*, CaGin4 is also activated by hyperphosphorylation during mitosis, as well as hyphal development (Sinha et al., 2007). Recent findings have shown that Gin4 is activated by mitotic Clb2-Cdk1, and the activated Gin4 kinase can then phosphorylate Sep7 in the septin complex (unpublished data in Dr. Wang Yue's lab). Therefore, Nap1 becomes a primary candidate as one of Gin4's activators.

1.4 Objectives of studies

As discussed in **Chapter 1.2**, the septin complex is essential for cell polarity and cell cycle progression. The organization of the septin complex is in turn regulated by cell cycle and polarity determinants. In the event of septin complex assembly/disassembly, the exact mechanism of how these events are triggered and controlled is not fully understood in either *S. cerevisiae* or *C. albicans*. Cdc3 is an essential protein and a core septin unit in both organisms. Surprisingly, little is known about this protein in the budding yeast except that it is a substrate of G1 cyclin-Cdk1 during the disassembly of the old septin ring, and a likely substrate of Cla4 during the septin ring assembly. Less is known about Cdc3 in *C. albicans*. The first half of the thesis focuses on CaCdc3, The objectives of this project are: 1. characterize the protein; 2. identify the regulatory mechanism and its cell cycle dependency; 3. identify the target residues of the regulation and establish their physiological significance.

Since the mechanism of Gin4 activation seems quite conserved in both *S. cerevisiae* and *C. albicans*, and since Gin4 carries more physiological importance in *C. albicans* than in *S. cerevisiae*, it is of pragmatic interest to determine whether Nap1 is part of the activation pathway. Since Ca*NAP1* has not been characterized before, the objectives of this study are: 1. characterize *NAP1* and the physiological functions of the protein; 2. identify its relevance in Gin4 activation; 3. elucidate its involvement in septin complex organization and morphogenesis.

Chapter 2 Materials and Methods

2.1 Reagents

All laboratory chemicals were purchased from Sigma-Aldrich Co. (St. Louis MI, USA) and Bio-Rad Ltd. (Hercules CA, USA). Enzymes were purchased from New England Biolabs (Boston MA, USA) and Fermentas International Inc. (Canada). Antibodies were purchased from Santa Cruz Biotechnology Inc. (Santa Cruz CA, USA) and Roche (Switzerland). Kits for plasmid and gel purification were purchased from Qiagen (USA). Kits for genomic DNA purification were purchased from Pierce (now own by Thermo Fisher Scientific Inc.). Site directed mutagenesis kit was purchased from Stratagene (USA). The isoelectric focusing machine and dry gel strips for 2D western blot were purchased from GE Healthcare (UK). Oligonucleotides were synthesized by 1st Base Ltd. (Singapore). Calf serum was purchased from JR Science (USA). 1NM-PP1 was purchased from EMD Chemicals (USA).

2.2 Strains and culture conditions

C. albicans strains in this study are listed in Table 2.1. Strains were routinely cultured in YPD medium (1% yeast extract, 2% peptone, and 2% glucose), or GMM (1× yeast nitrogen base without amino acids and 2% glucose), or GMM with required amino acids. All strains were grown at 30^{o}C or 37^{o}C water-baths with shaking. For hyphal induction, yeast cells were inoculated into YPD or GMM supplemented with 20% newborn calf serum and incubated at 37^{o}C.

Table 2.1 *C. albicans* strains used in this study

Strains	Genotype	Sources
SC5314	Wild type, clinically isolated	(Fonzi and Irwin, 1993)
BWP17	*ura3Δ/ura3Δ his1 Δ/ his1 Δarg4Δ/arg4 Δ*	(Enloe et al., 2000)
nap1Δ/Δ	Same as BWP17 except *nap1Δ::hisG/nap1Δ::hisG*	This study
nap1Δ/Δ::NAP1-MYC	Same as *nap1Δ/Δ* except *NAP1-MYC URA3*	This study
nap1Δ/Δ::NAP-GFP	Same as *nap1Δ/Δ* except *NAP1-GFP URA3*	This study
nap1Δ/Δ::NAP1 -HA	Same as *nap1Δ/Δ* except *NAP1-HA ARG4*	This study
BWP17::CLB2-MYC	Same as BWP17 except *CLB2 MYC URA3*	This study
nap1Δ/Δ::CLB2-MYC	Same as *nap1Δ/Δ* except *CLB2-MYC URA3*	This study
NAP1-HA::CLB2-MYC	Same as BWP17 except *NAP1 HA ARG4::CLB2 MYC URA3*	This study
BWP17::GIN4-GFP:: CDC3-MYC::NAP1-HA	Same as BWP17 except *NAP1 HA ARG4::CLB2 MYC URA3::GIN4 GFPHIS1*	This study
nap1Δ/Δ::CCN1-MYC	Same as *nap1Δ/Δ* except *CCN1-MYC URA3*	This study
BWP17::HGC1-MYC	Same as BWP17 except *HGC1-MYC URA3*	This study
nap1Δ/Δ::HGC1-MYC	Same as *nap1Δ/Δ* except *HGC1-MYC URA3*	This study
nap1Δ/Δ::NAP1-GFP	Same as *nap1Δ/Δ* except *NAP1-GFP URA3*	This study
nap1Δ/Δ::NAP1 N-MYC	Same as *nap1Δ/Δ* except *NAP1*(1-860nt)-*MYC URA3*	This study
nap1Δ/Δ::NAP1 N-HA	Same as *nap1Δ/Δ* except *NAP1* (1-860nt)-*MYC URA3*	This study
nap1Δ/Δ::NAP1 C-MYC	Same as *nap1Δ/Δ* except *NAP1*(861-1307nt)-*MYC URA3*	This study
nap1Δ/Δ::NAP1 C-HA	Same as *nap1Δ/Δ* except *NAP1* (861-1307nt)-*MYC URA3*	This study
nap1Δ/Δ::NAP1 N-GFP	Same as *nap1Δ/Δ* except *NAP1*(1-860nt)-*GFP URA3*	This study
nap1Δ/Δ::NAP1 C-GFP	Same as *nap1Δ/Δ* except *NAP1*(861-1307nt)-*GFP URA3*	This study

nap1Δ/Δ::NAP1 N-MYC::PMET3 NAP1 C-HFM	Same as *nap1Δ/Δ* except *NAP1*(1-860nt)-*MYC URA3::PMET3 NAP1* (861-1307nt)-*HFM ARG4*	This study
nap1Δ/Δ::HOF1-GFP	Same as *nap1Δ/Δ* except *HOF1-GFP URA3*	This study
nap1Δ/Δ::PMET3 GFP-CDC42 URA3	Same as *nap1Δ/Δ* except *PMET3-GFP-CDC42 URA3*	This study
nap1Δ/Δ::SEP7-GFP	Same as *nap1Δ/Δ* except *SEP7-GFP URA3*	This study
nap1Δ/Δ::MYO1-GFP	Same as *nap1Δ/Δ* except *MYO1-GFP URA3*	This study
nap1Δ/Δ::SPA2-GFP	Same as *nap1Δ/Δ* except *SPA2-GFP URA3*	This study
gin4Δ/PMET3 GFP-GIN4 K57A /NAP1-MYC	Same as BWP17 except *gin4Δ::HIS1::PMET3 GFP-GIN4 K57A ARG4::NAP1-MYC URA3*	Li Changrun
BWP17::PMET3 GFP-GIN4 ::NAP1 MYC	Same as BWP17 except *PMET3 GFP-GIN4 ARG4::NAP1-MYC URA3*	Li Changrun
BWP17::PMET3GFP-GIN4 K57A ::NAP1 MYC	Same as BWP17 except *PMET3 GFP-GIN4 K57A ARG4::NAP1-MYC URA3*	This study This study
nap1Δ/Δ::NAP1 ^{6A} MYC	Same as *nap1Δ/Δ* except *NAP16A-MYC URA3*	This study
nap1Δ/Δ::NAP1^{10A} MYC	Same as *nap1Δ/Δ* except *NAP110A-MYC URA3*	This study
nap1Δ/Δ::NAP1 ^{6A} HA	Same as *nap1Δ/Δ* except *NAP16A-HA URA3*	This study
nap1Δ/Δ::NAP1 ^{10A} HA	Same as *nap1Δ/Δ* except *NAP110A-HA URA3*	This study
gin4Δ/MAL2 GIN4/NAP1-GFP	Same as BWP17 except *gin4Δ:: ARG4::MAL2 GIN4 HIS1::NAP1-GFP URA3*	This study
nap1Δ/Δ::NAP1^{6A}-GFP	Same as *nap1Δ/Δ* except *NAP16A-GFP URA3*	This study
nap1Δ/Δ::NAP1^{10A}-GFP	Same as *nap1Δ/Δ* except *NAP110A-GFPURA3*	This study
cdc10Δ/Δ	Same as BWP17 except *cdc10Δ::HIS1/cdc10Δ::ARG4*	Li Changrun
cdc11Δ/Δ	Same as BWP17 except *cdc11Δ::HIS1/cdc11Δ::ARG4*	Li Changrun
cdc10Δ/Δ::NAP1-GFP	Same as *cdc10Δ/Δ* except *NAP1-GFP URA3*	This study
BWP17::cdc28Δ::CDC28as	Same as BWP17 except cdc28*Δ:: HIS1::CDC28^{F58G}-ARG4*	Li Changrun

BWP17::cdc28Δ::CDC28as ::NAP- HA	Same as BWP17 except cdc28*Δ:: HIS1::CDC28*^{F58G}*-ARG4::NAP1-HA URA3*	This study
NAP1^{6A} *MYC::CDC3-GFP*	Same as *nap1Δ/Δ* except *NAP16A-MYC URA3::CDC3-GFP ARG4*	This study
nap1Δ/Δ::NAP1^{3E} *MYC*	Same as *nap1Δ/Δ* except *NAP13E-MYC URA3*	This study
nap1Δ/Δ::NAP1^{3E} *GFP*	Same as *nap1Δ/Δ* except *NAP13E-GFP URA3*	This study
nap1Δ/Δ::NAP^{7E} *MYC::CDC3-GFP*	Same as *nap1Δ/Δ* except *NAP17E-MYC URA3::CDC3-GFP ARG4*	This study
nap1Δ/Δ::NAP1^{10E} *MYC::CDC3 GFP*	Same as *nap1Δ/Δ* except *NAP110E-MYC URA3::CDC3-GFP ARG4*	This study
nap1Δ/Δ::NAP1^{7E} *GFP*	Same as *nap1Δ/Δ* except *NAP17E-GFP URA3*	This study
nap1Δ/Δ::NAP1^{10E} *GFP*	Same as *nap1Δ/Δ* except *NAP110E-GFP URA3*	This study
BWP17::CDC3 GFP	Same as BWP17 except *CDC3-GFP AGR4*	This study
nap1Δ/Δ::CDC3 GFP	Same as *nap1Δ/Δ* except *CDC3-GFP ARG4*	This study
BWP17::CDC11 GFP	Same as BWP17 except *CDC11-GFP URA3*	Zeng Guisheng
nap1Δ/Δ::CDC11 GFP	Same as *nap1Δ/Δ* except *CDC11-GFP URA3*	This study
BWP17::GIN4 HFM	Same as BWP17 except *GIN4-HFM URA3*	Zeng Guisheng
nap1Δ/Δ::GIN4 HFM	Same as *nap1Δ/Δ* except *GIN4-HFM URA3*	This study
nap1Δ/Δ::CLB4 MYC	Same as *nap1Δ/Δ* except *CLB4-MYC URA3*	This study
NAP1-HA::CLB4 MYC	Same as BWP17 except *NAP1 HA ARG4::CLB4 MYC URA3*	This study
*cdc3*Δ*::PMET3 CDC3*	Same as *BWP17* except *cdc3*Δ*::FRT1::* P_{MET3} *CDC3 HIS1*	Yap Wai Ho
*cdc3*Δ*::PMET3 CDC3 ::CDC3 HFM*	Same as *cdc3*Δ*::PMET3 CDC3* except *CDC3 HFM ARG4*	Yap Wai Ho
*cdc3*Δ*::PMET3 CDC3 ::CDC3 S422A HFM*	Same as *cdc3*Δ*::PMET3 CDC3* except *CDC3S422A HFM ARG4*	Yap Wai Ho
*cdc3*Δ*::PMET3 CDC3 ::CDC3 S422D HFM*	Same as *cdc3*Δ*::PMET3 CDC3* except *CDC3 S422D HFM ARG4*	Yap Wai Ho
*cdc3*Δ*::PMET3 CDC3 ::CDC3 S422A GFP*	Same as *cdc3*Δ*::PMET3 CDC3* except *CDC3 S422A GFP ARG4*	This study
*cdc3*Δ*::PMET3 CDC3*	Same as *cdc3*Δ*::PMET3 CDC3*	This study

::CDC3 S422D GFP	except *CDC3 S422D GFP ARG4*	
cdc28as::CDC3 GFP	Same as cdc28*Δ::HIS1::CDC28*^{F58G}*-ARG4* except *CDC3 GFP URA3*	This study
cla4 Δ/Δ::CDC3 GFP	Same as *cla4 Δ/Δ* except *CDC3 GFP ARG4*	This study
GIN4 K57A::CDC3 GFP	Same as *GIN4 K57A* except *CDC3 GFP ARG4*	This study
*rts1*Δ*/*Δ*::CDC3 GFP*	Same as *rts1*Δ*/*Δ except *CDC3 GFP ARG4*	This study
*cdc14*Δ*/*Δ*::CDC3 GFP*	Same as *cdc14*Δ*/*Δ except CDC3 GFP ARG4	This study
cdc3Δ::PMET3 CDC3::CDC3HFM::CDC10 GFP	Same as *cdc3*Δ*::PMET3 CDC3 ::CDC3 HFM* except *CDC10 GFP URA3*	Yap Wai Ho
cdc3Δ::PMET3 CDC3::CDC3HFM::CDC11 GFP	Same as *cdc3*Δ*::PMET3 CDC3 ::CDC3 HFM* except *CDC11 GFP URA3*	Yap Wai Ho
cdc3Δ::PMET3 CDC3::CDC3HFM::CDC12 GFP	Same as *cdc3*Δ*::PMET3 CDC3 ::CDC3 HFM* except *CDC12 GFP URA3*	Yap Wai Ho
cdc3Δ::PMET3 CDC3::CDC3^{S422A} *MYC::CDC10 GFP*	Same as *cdc3Δ::PMET3 CDC3::CDC3HFM::CDC10 GFP* except S422A	Yap Wai Ho
cdc3Δ::PMET3 CDC3::CDC3^{S422D} *MYC::CDC10 GFP*	Same as *cdc3Δ::PMET3 CDC3::CDC3HFM::CDC10 GFP* except S422D	Yap Wai Ho
cdc3Δ::PMET3 CDC3::CDC3^{S422A} *MYC::CDC11 GFP*	Same as *cdc3Δ::PMET3 CDC3::CDC3HFM::CDC11 GFP* except S422A	Yap Wai Ho
cdc3Δ::PMET3 CDC3::CDC3^{S422D} *MYC::CDC11 GFP*	Same as *cdc3Δ::PMET3 CDC3::CDC3HFM::CDC11 GFP* except S422D	Yap Wai Ho
cdc3Δ::PMET3 CDC3::CDC3^{S422A} *MYC::CDC12 GFP*	Same as *cdc3Δ::PMET3 CDC3::CDC3HFM::CDC12 GFP* except S422A	Yap Wai Ho
cdc3Δ::PMET3 CDC3::CDC3^{S422D} *MYC::CDC12 GFP*	Same as *cdc3Δ::PMET3 CDC3::CDC3HFM::CDC10 GFP* except S422D	Yap Wai Ho
cdc3Δ::PMET3 CDC3::CDC3HFM::GIN4 GFP	Same as *cdc3*Δ*::PMET3 CDC3 ::CDC3 HFM* except *GIN4 GFP URA3*	This study
cdc3Δ::PMET3 CDC3::CDC3^{S422A} *MYC::GIN4 GFP*	Same as *cdc3Δ::PMET3 CDC3::CDC3HFM::GIN4 GFP*	This study

	except S422A	
cdc3Δ::PMET3 CDC3::CDC3^{S422D} *MYC::CDC11 GFP*	Same as *cdc3Δ::PMET3 CDC3::CDC3HFM::GIN4 GFP* except S422D	This study
gin4Δ/gin4^{K57A} *ARG4*	Same as BWP17 except *gin4Δ::gin4*^{K57A} *ARG4*	Li Changrun
gin4Δ/gin4^{K57A} *ARG4::CDC3 GFP*	Same as *gin4Δ/gin4*^{K57A} *ARG4* except *CDC3 GFP*	This study
cdc3Δ::PMET3 CDC3::CDC3^{S422A} *GFP*	Same as *cdc3Δ::PMET3 CDC3* except *CDC3*^{S422A} *GFP*	This study
cdc3Δ::PMET3 CDC3::CDC3^{S422D} *GFP*	Same as *cdc3Δ::PMET3 CDC3* except *CDC3*^{S42D} *GFP*	This study

2.3 *C. albicans* manipulation

2.3.1 Heat shock transformation

The overnight culture of yeast cells were harvested to obtain a cell pellet of 40-50 µl. The pellet was washed once with 1 ml dH_2O and resuspended into 100 µl 1X LiAc-TE for 10 min at 30°C. 600 µl 50% PEG 5000 was then added in together with 20 µl salmon sperm DNA and 30-80 µl of digested DNA. The mixture was vortexed briefly, and then incubated at 30°C for 1 hr. Heat shock was carried out at 45°C for 15 min. The cells were spun down at 4000 rpm for 1 min, PEG was then removed. After being washed once with dH_2O, the cells were re-suspended in 100 µl of water and plated out on selection plates.

2.3.2 Electroporation transformation

Cells were harvested from 10 ml over night culture, followed by washing once with water. Cells were then suspended in 4 ml 1X LiAc-TE and incubated at 30°C for 45 min. 100 µl 1M DTT was added in and the mixture was incubated at 30°C for another 15 min. Cells were wash twice with 15 ml ice cold water and once with 2 ml of 1 M sorbitol. The cell pellet was re-suspended in equal volume of 1 M sorbitol. Aliquot of 40 µl cells was mixed with pre-digested and purified DNA, and loaded into 0.2 mm cuvette. The electroporation was carried out at a voltage of 1.65 KV, resistance 200 Ω and capacity 25 µF. The cells were then suspended into 100 µl water and plated out onto selection plates.

2.3.3 Preparation of *C. albicans* genomic DNA

Pierce Y-DER Yeast DNA Extraction Reagent Kit was used to extract the genomic DNA. 50 µl of cell pellet were harvest from the overnight culture and

resuspended in 200 µl Y-PER. The mixture was incubated at 65°C for 10 min. After spinning at 13,000 rpm for 5 min, the supernatant was discarded, and 200 µl DNA Releasing Reagent A and 200 µl DNA Releasing Reagent B were added in. The solution was vortexed briefly and incubated at 65°C for 10 min. 100 µl Protein Removal Reagent was then added and the tube was inverted several times. The solution was then centrifuged at 13,000 rpm for 5 min and the supernatant was transferred to a new tube containing 400 µl isopropanol. The tube was inverted several times and spun at 13,000 rpm for 10 min to precipitate the genomic DNA. The supernatant was removed and the remaining DNA was washed once with 1 ml 70% ethanol. The pellet was air dried for 5 min and resuspended in 50 µl dH_2O.

2.3.4 Preparation of *C. albicans* total cell lysates

Cells were spun down from overnight culture by centrifugation at 4000 rpm for 5 min. Cell pellets were resuspended in 5 times the volume of ice-cold lysis buffer containing 1% Triton X-100, 50mM Tris (pH7.4), 150mM NaCl, 2µM DTT, and 1× protease inhibitor mixture tablet (Roche). The suspension was subsequently transferred to a 2-ml screw-cap tube. An equal volume glass beads were added, and the cells were broken by the Mini-Beadbeater (Biospec Products Inc.) at 5000rpm for 5 cycles of 1 min beating at 4°C. The supernatant lysates were collected by spinning at 13,000 rpm for 10 min in an Eppendorf centrifuge. Protein concentration was measured by either the Bradford assay (BioRad) or the Nanodrop (Thermo Scientific).

2.4 DNA work

2.4.1 Oligonucleotides primers and PCR

Primers used in this study are listed in **Table 2.4.1**. Restriction sites added are underlined. Additional bases were added to the 5' end to ensure a complete enzymatic digestion at the ends of the PCR products. Mutations of primers used in mutagenesis are highlighted in red.

Table 2.2 Oligonucleotide primers used in this study

No.	Primer	Sequence (5' to 3')
1	NAP1-A	TGC GGC CGC TAC CAT GAC CAT GTT TTG
2	NAP1-B	TCT TTC GTA TTT ACC TGC GGA TCC AGT TAA TAT GGG TTG TGT
3	NAP1-C	ACA CAA CCC ATA TTA ACT GGA TCC GCA GGT AAA TAC GAA AGA
4	NAP1-D	TGC GGC CGC GAT AAG TGA TAA GAG AAT
5	NAP1-E	TTT ATC TCT TTG TAA CCA
6	NAP1-F	ACA CAA CCC ATA TTA ACT
7	NAP1-G	TCT TTC GTA TTT ACC TGC
8	NAP1-H	GAA GGT GAT GAA GAT GAA TAT
9	NAP1-I	CGC GGA TCC TGA TGG TTG TGA AAT TCG
10	NAP1-J	CGG ACT AGT TTA CTG TTG TTT ACA TTC
11	NAP1-K	CGG GGT ACC GGT TAC AGT GGA GAT TTT
12	NAP1-L	CCG CTC GAG CTG TTG TTT ACA TTC TGG
13	NAP1-M	GAT CAA GAA GAA ACT TAC ATT
14	NAP1-N	GAA TTC AAA CCA AAT GAT TTT
15	NAP1-O	AAC ACA AGA GTA TGT TAA TTT
16	NAP1-P	CGG GGT ACC CAA ATG GAT GTG GTA AAA CA
17	NAP1-Q	CCA TCG ATA TGA CTG AAC AAC CAA TCA
18	NAP1-R	TGC ACT GCA GTT ACT GTT GTT TAC ATT CTG
19	NAP1-S	TGC ACT GCA GCA GAT ACT GTA GAT AAA TTT
20	NAP1-T	CTG GAT AT ATT GAT AAT CAA TTA AAT CAA ATG
21	NAP1-U	CAT TTG ATT TAA TTG ATT ATC AAT ATA TCC AG
22	NAP1-V	CTA TAA CCA TTG AAA GAA CAA AGC AAA CTA GAA C
23	NAP1-W	GTT CTA GTT TGC TTT GTT CTT TCA ATG GTT ATA G
24	NAP1-X	TAG CAA ATA ATC CAG TAT TA

25	NAP1-Y	GGA GAT TTT GTA TAT GAT C
26	TRUN-1	CCG CTC GAG TCT TTC AAT GGT TAT AG
27	TRUN-2	CCC ATC GAT AGA AAA CAA AGA AAT AAA
28	TRUN-3	CCC ATC GAT TTC AGT CAT AGT TAA TAT GG
29	TRUN-4	TGC ACT GCA GTC TTT CAA TGG TTA TAG
30	TRUN-5	GGG TAC CTC GAA ACC TAA TGA TGA TG
31	TRUN-6	CCT CGA GAG TTA ATA TGG GTT GTG TT
32	MNAP1 -1	GGG GAT ATT GCT AAA GCC CCT GCG CCA CAG AAC GCT CCT GCT AGT
33	MNAP1 -2	GCT CCT GCT GCT GTC GCC AAC GCC TAT ATG AGA GCC AAA CCA CCG ACG
34	MNAP1 -3	ACG GTG TCC GCC ATT CAA GAA GCA AAC AAT GAA GAT GGT GCT GGT GCT GCT
35	MNAP1 -4	GAT GAA TAT GCT GAT GAA GAT GGT GAA GGT GAT GCT GAT GAT GAT
36	MNAP1 -5	AAG AAT GGG GAT ATT GAA AAA GCC CCT GAG CCA CAG AAC GAG CCT GCT AGT GTC ACC
37	MNAP1 -6	GAG CCT GCT GAA GTC GAG AAC GAG TAT ATG AGA GAG AAA CCA CCG ACG
38	MNAP1 -7	ACG GTG TCC GAG ATT CAA GAA GAG AAC AAT GAA GAT GGT GAG GGT GCT GCT
39	MNAP1 -8	CAG AAC GAG CCT GCT GAA GTC GAG AAC GAG TAT ATG AGA GAG AAA CCA CCG ACG GTG
40	MNAP1 -9	CCA CCG ACG GTG TCC GAG ATT CAA GAA GAG AAC AAT GAA GAT GGT GAG GGT GCT GCT GCT GCT
41	MNAP1 -10	CCA CCG ACG GTG TCC GAG ATT CAA GAA TCA AAC AAT GAA GAT GGT GAG GGT GCT GCT GCT GCT
42	MNAP1 -11	CCA CCG ACG GTG TCC GAG ATT CAA GAA GAG AAC AAT GAA GAT GGT ACT GGT GCT GCT GCT GCT
43	CDC3-1	GGG GGT ACC agg ttt aca att ctt gct a
44	CDC3-2	CCG CTC GAG ACG TAA AAA TCC TTT ACG A
45	CDC3-3	GGG GGT ACC atg gct gca ggt atg tat
46	CDC3-4	CCC ATC GAT ATG GCT GCT GGT ATG TAT
47	CDC3-5	TGC ACT GCA GGT TGA TTT GAT CTT GAC AG
48	CDC3-6	CGG GGT ACC GAG GAA TTA AAA GAA CAT AC
49	CDC3-7	CC ATC GAT GAG GAA TTA AAA GAA CAT AC
50	CDC3-8	TGC ACT GCA GCT AAC GTA AAA ATC CTT TAC
51	CDC3-9	TGC TCT AGA CAT CTT TAG TTG TAT GTT TC
52	CDC3-10	TGC TCT AGA GAG GAA TTA AAA GAA CAT AC
53	CDC3-11	CGC GGA TCC GCT GAT TTA TTT GCC AG
54	CDC3-12	ATG GCT GCA GTT GAT CAT GCT ACC ACA GGA GAA ATT GTT
55		

56	CDC3 MUT-1	GCT GCA GTT GAT CAT TCT GCC ACA GGA GAA ATT GTT CCA
57	CDC3 MUT-2	GCA GTT GAT CAT TCT ACC GCA GGA GAA ATT GTT CCA CAA
58	CDC3 MUT-3	CAA CCA GCT CCA CAA AAG GAA CGT AAA GGA TTT TTA CGT TAG
59	CDC3 MUT-4	CAA CCA GCT CCA CAA AAG GCT CGT AAA GGA TTT TTA
60	CDC3 MUT-5	CAA CCA GCT CCA CAA AAG GCT CGT AAA GGA TTT TTA CGT TAG

2.4.2 DNA recombination methods

DNA fragments were amplified from genomic DNA of *C. albicans* using high fidelity polymerase (Roche). Restriction enzymatic digestion was performed using the buffers provided by manufacturers. Klenow DNA polymerase (New England Biolabs) was used to generate an insert blunt fragment. Dephosphorylation of vectors was done using calf intestinal phosphatase (CIP) (NEB). T4 DNA ligase (Fermentas) was used for fragment ligation. DNA sequencing was performed with the Sequenase DNA sequencing kit (US Biochemical, USA).

2.4.3 *E. coli* transformation

Electroporation competent *E. coli* cells were prepared as followed:

1. 1:1000 dilution of a fresh saturated *E. coli* culture to LB medium.
2. Grow the cells at 37^{o}C at 200 rpm till OD_{550} reaches a reading from 0.6 to 0.8.
3. Spin down the cells in a centrifuge at 4000 rpm for 10 min and keep the cells ice-cold throughout the procedure.

4. Wash cells by resuspending them in ice cold 10% sterile glycerol equal to the original volume.
5. Spin down the cells again at 4000 rpm for 10 min. Repeat the washing twice.
6. Discard the supernatant and resuspend cells in 125µl of ice-cold 10% glycerol per 100 ml of original culture.
7. Quickly freeze the cells in 20µl aliquotes.

For transformation, 1-2µl of plasmid or ligation products was mixed into 20µl of competent cells and incubated on ice for 5 min. Electroporation was done by a Gene Pulser (BioRad) at 1.8KV, 200Ω resistance and 25µF capacity. Aliquots of cells were then spread onto plates containing ampicillin.

2.4.4 Plasmid purification and analysis

Small-scale plasmid purification from *E. coli* was carried out using QIAGEN Miniprep Kit. The procedures were as follows:

1. Harvest the cells by centrifugation from 2 ml over night culture.
2. Discard the supernatant and resuspend the cells in 250µl P1 solution.
3. Lyse the cells by adding 250µl P2 solution. Mix by gently inverting.
4. Add in 350µl N3 to neutralize the solution and mix by inverting.
5. Centrifuge at >13,000 rpm for 10 min. Transfer the supernant to a Miniprep column. Centrifuge at full speed and discard the flow-through.

6. Wash the column with 0.75ml buffer PE and centrifuge for 1 min. discard the flow-through. Centrifuge for another 1 min to ensure the removal of any residual buffer.
7. Place the column in a fresh 1.5ml tube. Add 50µl water to the column and stand for 1 min before centrifugation to elute the DNA.

Restriction digestion and sequencing were used to analyze the plasmids. 1-2µg of plamid DNA was digested with 1-2 units of the restriction enzyme in a 20µl reaction at 37^{o}C for 30 min. The digestion products were then analyzed by agarose gel electrophoresis. Sequencing was done to ensure the insertion of correct fragments. Standard sequencing PCR was carried out.

2.5 Gene disruption and expression

2.5.1 *C. albicans CDC3* shut off and phosphomutants

The shut down mutant was generated by Dr. Yap Wai Ho. To generate the *cdc3*△/P_{MET3}-*CDC3* strain, one copy of *CDC3* was deleted using the *URA3* flipper cassette (Morschhäuser et al., 1999), which was subsequently looped out, and the other copy was placed under control of the *MET3* promoter by a promoter replacement strategy (Care et al., 1999). A region containing the 5'-untranslated region from nt -650 to -1 was amplified from genomic DNA with *KpnI* and *BglII* sites added to the 5' and 3' ends, respectively. The fragment was then inserted into plasmid with HFM tag at the C terminal of *CDC3* gene. Site-directed mutagenesis was then carried out to generate a unique *SalI* site at nt -371 within the 5'-untranslated region. Site-directed mutagenesis

was the carried out to generate serine to alanine, threonine to alanine, serine to aspartate and threonine to aspartate individual mutations corresponding to amino acid positions 7, 8, 9, 41, 47, 263, 365 and 422 of cdc3 protein using Stratagene QuickChange Multi-site Directed Mutagenesis kit. Mutant strand synthesis reactions consisted of 2.5 µl 10x reaction buffer, 0.75 µl QuickSolution, 0.5 µl templet, 0.25 µl of each primer, 1 µl dNTP, 1 µl Quick Change Enzyme, topped up with dH_2O to 25 µl. The thermocycle reaction was similar to normal PCR except extension at 65 ^oC with the speed of 2 min/kb of template plasmid. After the reaction, the mixture was treated by 1 µl DpnI restriction enzyme for 1 hr at 37 ^oC to digest the parental ds-strand, and then transformed into *E. coli* competent cells. Plasmids extracted from ampicillin positive colonies were then subjected to sequencing.

The resultant plasmids with correct mutations were linearized with *SalI* and integrated separately into the genome of the *cdc3*△/P_{MET3}-*CDC3* strain, yielding *cdc3*△/P_{MET3}-*CDC3*/*cdc3*^{S7A}-*HFM*, *cdc3*△/P_{MET3}-*CDC3*/*cdc3*^{S7D}-*HFM*, *cdc3*△/P_{MET3}-*CDC3*/*cdc3*^{T8A}-*HFM*, *cdc3*△/P_{MET3}-*CDC3*/*cdc3*^{T8D}-*HFM*, *cdc3*△/P_{MET3}-*CDC3*/*cdc3*^{T9A}-*HFM*, *cdc3*△/P_{MET3}-*CDC3*/*cdc3*^{T9D}-*HFM*, *cdc3*△/P_{MET3}-*CDC3*/*cdc3*^{S41A}-*HFM*, *cdc3*△/P_{MET3}-*CDC3*/*cdc3*^{S41D}-*HFM*, *cdc3*△/P_{MET3}-*CDC3*/*cdc3*^{S47A}-*HFM*, *cdc3*△/P_{MET3}-*CDC3*/*cdc3*^{S47D}-*HFM*, *cdc3*△/P_{MET3}-*CDC3*/*cdc3*^{S236A}-*HFM*, *cdc3*△/P_{MET3}-*CDC3*/*cdc3*^{S236D}-*HFM*, *cdc3*△/P_{MET3}-*CDC3*/*cdc3*^{S365A}-*HFM*, *cdc3*△/P_{MET3}-*CDC3*/*cdc3*^{S365D}-*HFM*, *cdc3*△/P_{MET3}-*CDC3*/*cdc3*^{S422A}-*HFM* and *cdc3*△/P_{MET3}-*CDC3*/*cdc3*^{S422D}-*HFM*. Strain genotypes were verified by PCR or Southern blotting. Cdc3^{S422A} and Cdc3^{S422D} GFP tag were constructed by replacing the HFM with GFP, followed by site specific integration in the promoter site of *cdc3*△/P_{MET3}-*CDC*.

2.5.2 *CDC3* domain deletion

CDC3 C terminal extension (nt1003 to nt 1284) was amplified from genomic DNA and inserted after MAL2 promoter with GFP tag. The plasmid was then integrated at MAL2 promoter site in *cdc3*△/P_{MET3}-*CDC* strain. Mutations of S422 to Ala or Asp were done using the same strategy described in **Chapter 2.5.1**.

2.5.3 *C. albicans NAP1* gene disruption and domain deletion

Two alleles of a gene were deleted sequentially from *BWP17* (Enloe et al., 2000). Gene deletion cassettes consisted of 2 fragments corresponding to the 5'- and 3'-untraslated regions of the gene of interested *NAP1* flanking the marker gene *hisG-URA3-hisG*. The flanking fragments were amplified from genomic DNA and the restriction sites were added to the facilitate ligation. Transformants were selected on uridine drop out plates. Correct deletion of *NAP1* was verified by PCR. *URA3* marker in the 1st copy knockout was flipped out on a GMM plate with 5-FOA. Correct flipping was verified by PCR. The 2nd copy of NAP1 gene was deleted the exact same way except the 3'-untranslated region was brought forward 500 nt to facilitate the PCR checking. Proper deletions of both alleles were checked by PCR with primers NAP1-F and G. Thus, all three selection marker (*HIS1, ARG4* and *URA3*) were usable for subsequent genetic manipulation.

NAP1 gene was cut into 2 parts at amino acid position 287 in this study. *NAP1* was constructed by PCR amplification from genomic DNA using this pairs of oligonucleotides NAP1-P and L, NAP1-N using TRUN-4 and 5, NAP1-C from TRUN-3

and 5, TRUN-2 and NAP1-L. 900 nt of promoter region was included in both truncates to facilitate site specific integration.

NES deletion was carried out using primers NAP1-T and U. Deletion was confirmed by sequencing with primer NAP-X. Mutated *NAP1* was then integrated into *nap1Δ/Δ* at the promoter region. Expressions were checked by either western blot or microscopy.

2.5.3 *NAP1* mutagenesis

All non-phosphorylatable and phospho-mimic mutations of NAP1 were done by Stratagene QuickChange Multi-site Directed Mutagenesis kit. Promoter + full length wt *NAP1* was used as the template for mutagenesis. Properly mutated constructs were then transformed into *nap1Δ/Δ* at the promoter region. Expressions were checked by either western blot or microscopy. Mutations were further confirmed by genomic PCR of the ORF region followed by sequencing.

2.5.4 Chromosomal tagging at C terminus

Construction of plasmids pGFPutr, pMYCutr and pHFMutr were previously described (Sinha et al., 2007). To tag *CDC3*, a region of *CDC3* from nucleotide (nt) 155 to 1284, and a region of NAP1 from nt 768 to 1304 (the first nucleotide of the coding sequence is 1) were PCR-amplified from genomic DNA, with *KpnI* and *XhoI* sites added to the 5' and 3' ends respectively. The fragments were then inserted in frame with GFP-, Myc- or HFM-coding sequences in pGFPutr, pMYCutr and pHFMutr previously digested with *KpnI* and *XhoI*, yielding pCDC3-GFPutr, pCDC3-MYCutr and pCDC3-HFMutr,

respectively. These constructs were then linearized at a unique *BglII* site (nt 1117) in *CDC3* and *XcmI* site (nt 1069) in *NAP1* before being integrated into the genome.

2.6 Protein work

2.6.1 1D western blot analysis

Standard SDS-PAGE protocol (Sambrook et al., 1989) was carried out with the Mini-PROTEAN II electrophoresis system (BioRad, USA) in Tris-glycine running buffer (25 mM Tris, 250 mM glycine and 0.1% SDS). Proteins resolved on the gel were subsequently transferred onto PVDF membrane (Amersham, UK) using the Bio-Rad Wet Transfer System in transfer buffer (48mM Tris, 39mM glycine and 10% methanol).The membrane was blocked in 5% BSA for 1 hour. Primary anti-body incubation was normally carried out in room temperature for 1 hr or 4^{o}C overnight, followed by washing with PBST (PBS with 0.1% Tween-20). The membrane was incubated in secondary antibody for 50 min, followed by washing extensively. The protein bands were visualized by the Enhanced Chemi-Luminescence (ECL) system (Amersham, UK) and Fuji Medical X-Ray Film (Fuji, Japan).

2.6.2 2D western blot

First dimension isoelectric focusing (7cm strip) was done as described previously by Indrajit et al. (2007):

1. Into 10 µg of protein, add in 0.5µl TCEP and 0.6 µl IPTG buffer of corresponding Ph range. Top up with sample buffer to 125 µl.

2. Apply the solution evenly to the strip holder.

3. Remove the plastic protective cover on the gel strip and submerge in the sample solution applied to strip holder.

4. Cover the strip with 600 µl cover fluid.

5. Run at 20^{o}C at 50 µA/strip and set the program as 30 V for 13.5 hrs, 500 V for 45 min, 1000 V for 45 min, and 8000 V for 90 min.

Total run of first dimension took 16.5 hrs. Second dimension was done as follows:

1. Rinse the strip with Milli-Q water.

2. Equilibrate the strip in equilibration buffer containing 10 mg/ml DTT for 10 min with shaking.

3. Rinse with Milli-Q water.

4. Equilibrate the strip in equilibration buffer containing 25 mg/ml iodoacetamide for 10 min with shaking.

5. Trim strips on both sides and carefully insert it between glass plates till it is well layered on the gel.

6. Seal gel with 0.5% agarose in running buffer containing trace of bromophenol blue.

The mounting of gel apparatus and the separation of the proteins were similar to 1D SDS-PAGE described in **Chapter 2.6.1**.

2.6.3 Immunoprecipitation (IP)

500ml of total cell lysate was mixed with either anti-Myc, anti-HA or anti-GFP agarose beads (Santa Cruz, USA) with rotation for at least 2 hr at 4^{o}C. The beads were then washed with lysis buffer 3 times. The precipitated proteins were resolved on SDS-PAGE and detected by western blot as described in **Chapter 2.6.1**.

For co-immunoprecipitation, 10-15 ml overnight culture was refreshed into 100-200 ml fresh culture till OD_{595} reached 1.2-1.6. Cell pellets were harvested for beads-beating. Cell lysates were then incubated with the appropriate agarose beads overnight. The rest was handled the same way as IP.

2.6.4 Phosphorylation site mapping

For mapping the phosphorylation sites of Cdc3 and Nap1, 1L YPD culture was grown over night. Cells were harvested and lysed as described in **Chapter 2.3.4** and immuno-precipitated as described in **Chapter 2.6.3** for overnight. Proteins were then resolved on SDS-PAGE and the gel was stained with Coomassie Blue. The Cdc3 HA and Nap1 HA bands were excised for MALDI-TOF in University at Albany, Center for Functional Genomics (USA).

2.7 Centrifugal elutriation

Synchronized *C. albicans* G1 cells were obtained by centrifugal elutriation. 400-500ml overnight galactose minimal media culture with required amino acids was injected into the chamber of a Beckman JE5.0 rotor in the Avanti J-26XP Beckman Centrifuge (Beckman, USA). The flow rate of a MasterFlex L/S pump (MaterFlex, USA) was then increased at small increments. Small G1 cells were eluted out first. The size of the eluted

cells was carefully monitored by microscopy. The synchronous G1 cells were then released into YPD, or GMM, or YPD with 20% serum for growth at 30^{o}C or 37 ^{o}C. Aliquots of cells were collected for microscopy or western blot analysis.

2.8 Microscope studies

2.8.1 Fluorescence microscopy

The Leica DMR fluorescence microscope with a 100X objective lens and a Hamamatsu digital camemra interfaced with METAMORPH software (Universal Imaging) were used to capture and analyze the images. General cell morphology was captured using differential interference contrast optics (DIC). GFP and nuclear DAPI (Vector Labboratories, USA) staining were visualized by corresponding fluorescence wave lengths. For GFP localization, live cells without fixation were examined. Cell wall staining was done using Fluorescent Brightener 28 (Sigma, USA) to a final concentration of 6µl/ml culture. Images were then processed with Adobe Photoshop to adjust the level and contrast.

2.8.2 Confocal microscopy and fluorescence recovery after photo-bleaching (FRAP)

FRAP experiments were performed with a heating stage and objective heater system (Biotechs) maintained at 37 ˚C using the Zeiss LSM700 confocal microscope with a 100X oil-immersion objective. Briefly, cells expressing Cdc3 GFP were allowed to grow to the early log phase at 30 °C. Cells were harvested and resuspended in fresh media, and adhered to the surface of poly-lysine coated chambered slide (Lab-Tek). Excitation for image acquisition was set at 3% of the maximal laser intensity; whereas

bleaching of the septin ring was with 25 iterations of 100% laser intensity at 488 nm. Single-section images were then collected every 1 s for a total of 5 min. Fluorescence intensity was analyzed using NIH ImageJ. For each FRAP data set, three separate experiments were performed, typically including up to five cells investigated per strain. Normalized fluorescence intensity was obtained by subtracting the background (mean fluorescence intensity in the bleached region after bleach) and correcting for acquisition bleach (a control cell in the same field was used). The ratio between mean fluorescence intensity of the bleached region and the mean fluorescence of the whole cell was then expressed as a percentage and plotted against time.

Chapter 3 Phosphorylation of Cdc3 plays a critical role in regulating septin organization, stability and function

3.1 Introduction

Septins belong to a family of GTP-binding and filament-forming proteins (Faty et al., 2002; McMurray and Thorner, 2009a; Oh and Bi, 2010). They are evolutionarily conserved from fungi to humans and best known for their roles in cytokinesis (Estey et al., 2010; Finger, 2005; Longtine et al., 1998) Studies in recent years have revealed new conserved functions of septins. For example, many cell types assemble septin filaments underneath the plasma membrane to form diffusion barriers that divide cells into functionally distinct compartments (Caudron and Barral, 2009). Septin complexes also serve as scaffolds that recruit and organize protein components of related functions at a certain cellular location to perform specific functions (Kozubowski et al., 2005; Longtine et al., 2000).

Septin structure and function have been most extensively investigated in the budding yeast *Saccharomyces cerevisiae* (Sc). This model organism encodes 5 mitotic septins including Cdc3, Cdc10, Cdc11, Cdc12 and Sep7/Shs1 (Finger, 2005). At the beginning of the cell cycle, these septins assemble into a ring structure at the presumptive budding site that defines the future cell division plane (Caviston et al., 2003; Gladfelter et al., 2001; Iwase et al., 2006). The ring persists at the bud neck throughout the cell cycle until the time of cytokinesis when it splits into two rings followed by disassembly in the early stages of the next G1 phase (Tang and Reed, 2002; Longtine and Bi, 2003;). The dynamics of septins within the ring also changes with the progression of the cell cycle, being mobile at bud emergence and telophase and immobile during S, G2, and M phases

(Dobbelaere et al., 2003). Through its scaffold and diffusion-barrier functions, the septin ring plays crucial roles in morphogenesis, cell cycle progression, cytokinesis and cell separation (Longtine and Bi, 2003; McMurray and Thorner, 2009b; Oh and Bi, 2010; Weirich et al., 2008). These roles require the septin ring to be assembled and disassembled and its dynamics regulated precisely in a cell cycle dependent manner. However, the underlying molecular mechanisms of control remain poorly understood. Particularly, little is known about the molecular events that trigger septin ring assembly, disassembly and split. Several protein kinases have been reported to phosphorylate septins and influence their property and function. The cyclin-dependent kinase (CDK) Cdc28 phosphorylates Cdc3 at two consensus CDK phosphorylation sites near the C-terminal end in G1 to promote disassembly of the old ring inherited from the previous cell division (Tang and Reed, 2002). Cdc28 and/or another CDK Pho85 are thought to target Shs1 in G1, playing a role in later phases affecting bud morphogenesis and septin's association with the Nim1 kinase Gin4, a well known septin regulator (Egelhofer et al., 2008). Several studies reported that Gin4 and the p21-activated kinase (PAK) Cla4 regulate septin ring assembly, split and dynamics by targeting Cdc3, Cdc10 and Shs1 (Longtine et al., 1998; Mortensen et al., 2002; Dobbelaere et al., 2003; Versele and Thorner, 2004; Asano et al., 2006;). Rts1-dependent protein phosphatase 2A appears to be involved in Shs1 dephosphorylation to modulate septin ring dynamics in telophase **(**Dobbelaere et al., 2003), and the Cdc14 phosphatase of the mitotic exit network has been implicated in septin ring split (Bloom et al., 2010; Cid et al., 2001; Clemente-Blanco et al., 2006).

Candida albicans (Ca), a polymorphic fungus that can grow as yeast, pseudohyphae and hyphae (Berman and Sudbery, 2000; González-Novo et al., 2008), encodes homologues to all five *S. cerevisiae* mitotic septins. Like their *S. cerevisiae* counterparts, the *C. albicans* septins exhibit cell cycle dependent organizational and dynamic changes during yeast growth (Warenda and Konopka, 2002). However, during hyphal growth, the septin rings are not disassembled after cytokinesis; instead they persist at the septum through multiple cell cycles (González-Novo et al., 2008). Furthermore, Cdc10 molecules in the ring behave differently from other septins in dynamics during hyphal growth. These data indicate differential regulation of *C. albicans* septins in different growth forms. Interestingly, phosphorylation has also been found to play important roles in septin regulation. Sinha et al. (2007) reported that Cdc11 undergoes cell cycle dependent phosphorylation by at least two kinases Cdc28-Ccn1 and Gin4 during yeast growth. It is phosphorylated at S395 by Gin4 around the time of cytokinesis that primes it for further phosphorylation at S394 by Cdc28-Ccn1 before bud emergence in the next cell cycle. And after the G1/S transition Cdc11 becomes completely dephosphorylated until being phosphorylated again by Gin4 near the end of the cell cycle. In contrast, during hyphal growth both S394 and S395 are locked in phosphorylated state independent of cell cycle phases, which is achieved through coordinated actions of three kinases Gin4, Cdc28-Ccn1 and the hyphal-specific Cdc28-Hgc1 (Sinha et al., 2007). Blocking these phosphorylations causes defects in both yeast and hyphal cells. Cdc28-Hgc1 also regulates Sep7 phosphorylation and contributes to the inhibition of cell separation after cytokinesis (González-Novo et al., 2008). Taken together, current data from studies of both *S. cerevisiae* and *C. albicans* suggest that

timely phosphorylation and dephosphorylation of septins at specific stages appear to be a main mode of control underlying the cell cycle dependent regulation of septin organization and function (McMurray and Thorner, 2009).

Septins have the capacity to assemble into structures of different levels of complexity. In solution, purified septin monomers can assemble into symmetric heterooligomeric rods that, in turn, form higher-order structures such as filaments, rings, and gauze. Salt and lipids play important roles in determining the levels of septin structures both *in vitro* and *in vivo* (McMurray et al., 2011; Bertin et al., 2008; Bertin et al., 2010). Two types of interaction interfaces G and NC alternate to link the septin monomers in a rod. The G interface involves the GTP-binding domain of adjacent monomers, and the NC interface involves residues in the N- and C-terminal segments. Most septins have a variable C-terminal extension (CTE). The CTEs often contain a segment with coiled-coil-forming potential thought to mediate protein-protein interaction. The CTE is essential for *S. cerevisiae* Cdc3 and Cdc12 functions in vivo (Versele et al., 2004). The two septins associate through the G interface in septin rods and their CTEs form a coiled-coil structure (Bertin et al., 2008). Under low salt conditions the CTE coiled-coils projecting from one filament associate with those from a parallel filament, forming lateral bridges that cross-link the filaments into a higher order ‘rail-track’-like structure (Bertin et al., 2010). Thus, the CTEs of Cdc3 and Cdc12 play key roles in the assembly and stabilization of septin structures. The CTE of Cdc11 has also been shown to associate in a homotypic manner which mediates the end-to-end assembly of septin rods into long filaments and further into mesh-like structures (Bertin et al., 2010). It is thus tempting to speculate that the CTEs might be the points of control by protein

modifications to regulate septin organization. The reported phosphorylation of ScCdc3 and CaCdc11 by CDK in the CTE supports this hypothesis (Tang and Reed, 2002; Sinha et al., 2007).

To investigate the role of phosphorylation in regulating the septins, we have used 2D western blotting (Sinha et al., 2007) to examine the phosphorylation status of each septin during cell cycle progression. In this study, I report that Cdc3 is a phosphoprotein and exits in multiple phosphoisoforms. Its phosphorylation is regulated in a cell cycle dependent manner. The most phosphorylated isoforms were observed in early G1 cells followed by a period of dephosphorylation through the rest of G1 phase; and rephosphorylation occurs gradually from the START to the end of the cell cycle. Phospho-mapping of immunopurified Cdc11 by mass spectrometry identified phosphorylation on S422 near the C-terminus. Mutating S422 to the phosphomimetic D causes severe cytokinetic defects and elongation of cells as well as disorganization of septin structures. In contrast, the S422A mutation leads to a much weaker phenotype. Gin4 is involved in the phospho-regulation of Cdc3, but Cdc28, Cla4 and Cdc14 are not. The results suggest that controlling the phosphorylation status of S422 may play a crucial role in regulating the assembly or stability of septin rings.

3.2 Cdc3 is a phospho-protein

In *S. cerevisiae*, Cdc28 phosphorylates Cdc3 at a pair of SP sites near the C-terminal end, which is thought to initiate septin ring disassembly (Tang and Reed, 2002). The *C. albicans* Cdc3 sequence does not contain any consensus CDK phosphorylation site such as SP or TP in the CTE. Given the high evolutionary conservation and

essentiality of Cdc3 in the two organisms (Warenda and Konopka, 2002), I thought that in *C. albicans* either Cdc28 can phosphorylate Cdc3 at nonconsensus sites as is the case of Cdc11 phosphorylation (Sinha et al., 2007), or other kinases phosphorylate Cdc3. To begin to address this issue, I first wanted to determine whether CaCdc3 is a phosphoprotein. To detect Cdc3 phosphorylation, we used 2D western blotting which has the power to separate different phosphoisoforms as distinct spots according to their isoelectric points (Sinha et al., 2007). I tagged Cdc3 with GFP at the C-terminus in BWP17 cells. Proteins were extracted from exponential phase cells, resolved by 2D electrophoresis and analyzed by western blot using GFP antibodies. By this protocol, I consistently detected 10-11 spots of Cdc3-GFP in asynchronous cells (**Fig. 3.1A**). Treating the cell lysate with λ phosphatase eliminated all the isoforms closest to the acidic end of the gel and collapsed them into three spots near the basic end. This result demonstrates that the 7-8 spots closest to the acidic end of the gel are Cdc3 isoforms carrying different numbers of phosphorylated residues. The phosphatase-resistant spots may represent other types of modification that alters Cdc3's isoelectric point.

3.3 Cdc3 phosphorylation is cell cycle dependent

To determine when Cdc3 phosphorylation occurs during the cell cycle and whether it correlates with certain changes of septin behavior, I used centrifugal elutriation to prepare G1 cells to start synchronous cultures. Aliquots of cells were collected at timed intervals. The budding index of this culture shows that the cells start to bud at around 120 min and undergoes cytokinesis between 180 and 210 min (**Fig. 3.1B**). I also examined septin localization at each time point of sample collection (**Fig. 3.1C**). All newly prepared G1 cells had a septin ring at one pole which was clearly the old ring from the previous cell division. At 60 min, most cells did not show any clear septin localization, indicating that the old ring had disassembled. At 90 min, a small percentage of cells had assembled a septin patch or a new ring in the cortex of unbudded cells, and at 120 min a bright ring was present at the presumptive budding site in most cells. At 210 min, two rings were seen in many large budded cells indicating completion of cytokinesis. Next, I harvested cells at several time points coinciding with major changes of septin organization to examine Cdc3 phosphorylation status. The results of 2D western blotting are shown in **Fig. 3.1C**. Cdc3 in newly prepared G1 cells (0 min) exhibited the same 10-11 spots as those detected in the asynchronous exponential culture shown in Fig.3.1A above. Strikingly, at 60 min nearly all of the most phosphorylated isoforms disappeared, and only the few least phosphorylated ones were detected, indicating rapid dephosphorylation of Cdc3 during the early stages of G1 during which the old septin rings are disassembled. At 90, 120, 180 and 210 min, the number of hyperphosphorylated spots increased progressively with the pattern at 180 and 210 min being similar to that at 0 min. At 270 min when the culture was in the next G1 phase dephosphorylation was

detected again. The results demonstrate that Cdc3 undergoes cell cycle dependent phosphorylation and dephosphorylation. Phosphorylation occurs progressively from late G1 throughout most of the cell cycle and peaks near the end of the cell cycle. The hyperphosphorylated isoforms are inherited by new G1 cells but quickly dephospharylated in early G1 coincident with the old septin ring disassembly until rephosphorylation starts shortly before the assembly of a new septin ring.

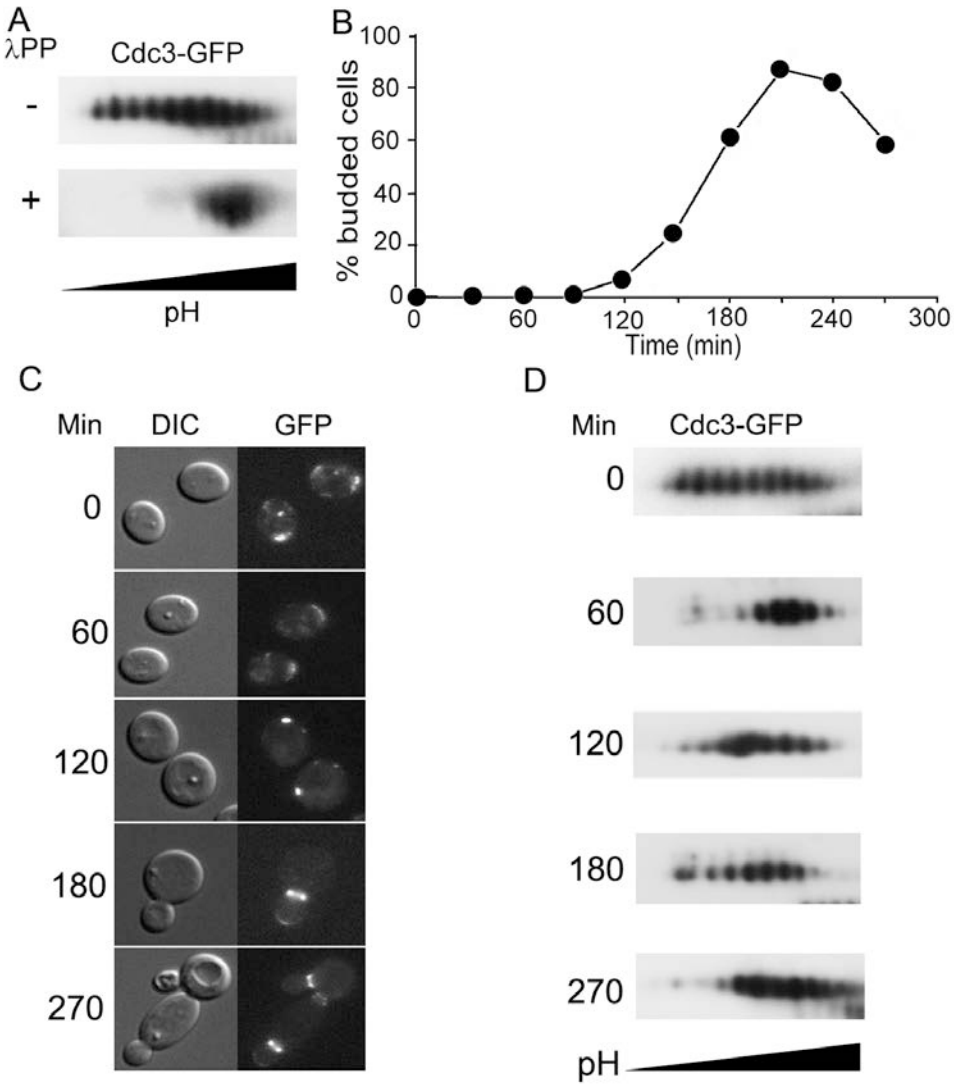

Figure 3.1 Cdc3 undergoes cell cycle dependent phosphorylation and dephosphprylation

(A) 2D WB of Cdc3 GFP in WT cells treated and untreated with λ phosphatase. Asynchronous cells were used. (B) Budding index of WT G1 cells recovered in GMM. (C) WT G1 cells with Cdc3-GFP were released in GMM at 30°C. Aliquots of cells were

collected at indicated time points for microscopy (C) and 2 D WB analysis (D). Blots in (D) were aligned by the position of protein markers.

3.4 Identification of phospho-residues in Cdc3

To map the phosphorylated residues in Cdc3, Cdc3 was tagged with a hemagglutinin (HA) epitope for immunoaffinity purification. The protein was purified from 1L of asynchronous culture and separated by SDS PAGE. After Coomassie Blue staining, the Cdc3 band was excised and processed for mass spectrometry (MS) analysis. The MS mapping was repeated three times and identified phosphorylation on S7, S41, S365 and S422 (**Fig. 3.2A**). S7 is located in the N-terminal extension (NTE), S41 in the GTP binding site, S365 in the C-terminal coiled coil domain and S422 near the C-terminal end. I then created a series of Cdc3 mutants, replacing each of the identified residues either with the nonphosphorylatable alanine (A) or the phosphomimetic aspartate (D). Since *CDC3* is essential (Warenda and Konopka, 2002), to examine the effect of these mutations I first created a strain (P_{Met3}-*CDC3*) in which one copy of *CDC3* was deleted and the other placed under the control of the *MET3* promoter. In glucose minimal medium (GMM), the strain grows normally. But when grown for >6 h in GMM supplemented with 0.5 mM each of methionine and cysteine (GMM+MC) to shut down the expression of *CDC*3, the cells exhibited severe cell elongation and cytokinetic failure, forming long branched filaments after 18 h (**Fig. 3.2B**). Methylene blue staining of the 18 h cells revealed the presence of many dead cells, consistent with the essentiality of the gene (**Fig. 3.2B**). To examine the effect of Cdc3 depletion on septin structures, I tagged Cdc10, Cdc11 and Cdc3 with GFP and found complete mislocalization of all the three

septins with Cdc10 and Cdc11 evenly distributed in the cytoplasm and Cdc12 forming large random aggregates (**Fig. 3.2C**). Furthermore, many elongated cells contained multiple nuclei, consistent with cytokinesis defects (**Fig. 3.2D**). The delayed appearance of the phenotype is most likely due to the high stability of septins such that only after several generations in the repressive condition would the amount of wild-type Cdc3 molecules be reduced to a level that can no longer carry out its functions. The results show that the shut-off of *CDC3* was rather complete, thus providing a proper background for testing the functions of the various *CDC3* mutant alleles.

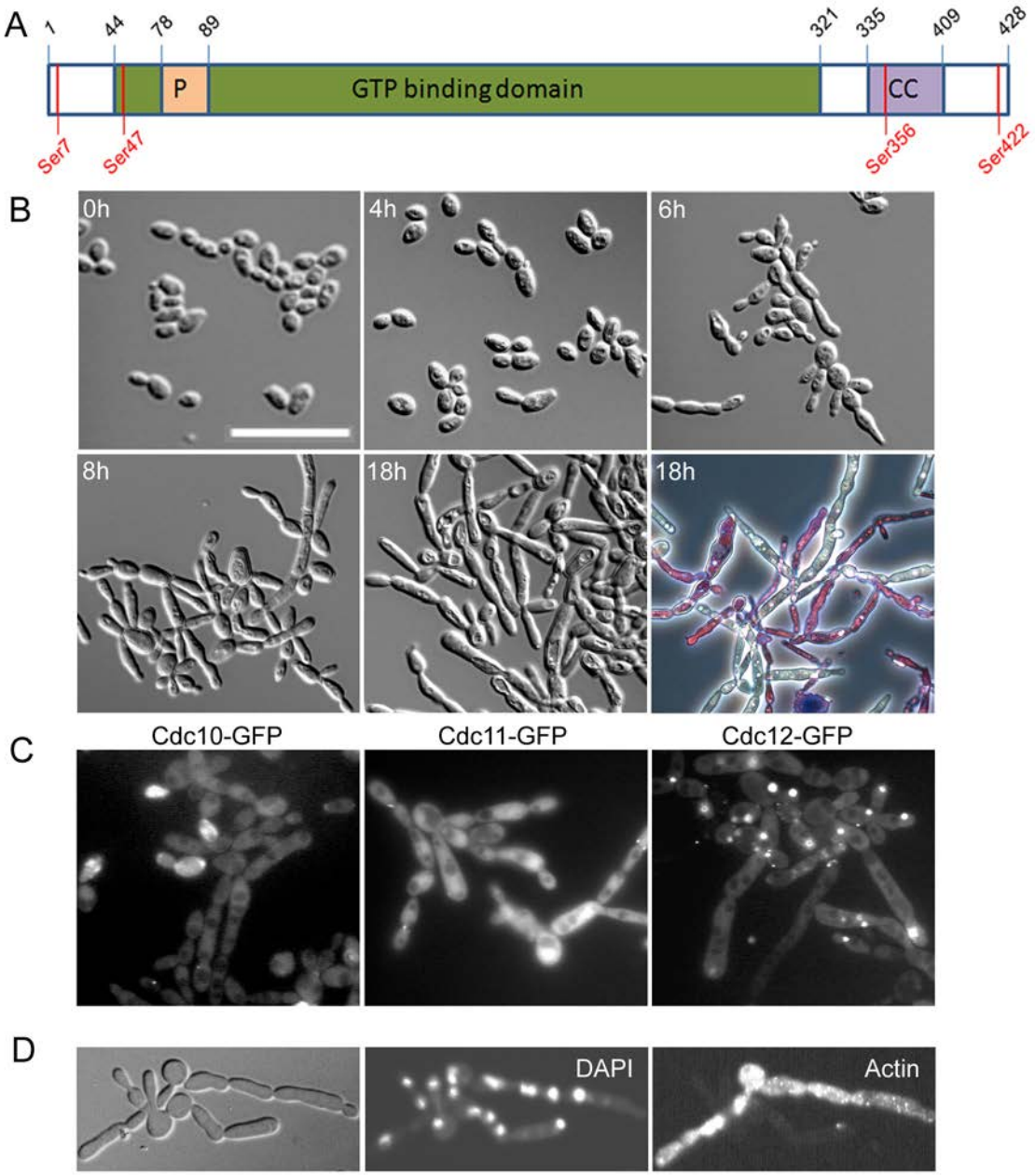

Figure 3.2 Cdc3 is essential for cell growth and septin function

(A) Domain structure of Cdc3. Residues revealed by MS phospho-mapping are in red. P = poly basic domain; CC = coiled coil domain. (B) 0.5 mM Met+Cys were added to the culture. Aliquots of cells were collected at indicated time points for microscopy.

Methylene blue was used to stain the cells after 18 hr shutoff of *CDC3*. Cells stained purple are dead. Bar = 10 μm. Scale bar is representative for all panels. (C) GFP tagged Cdc10, Cdc11 and Cdc12 in overnight *CDC3* shutoff cells. (D) DAPI staining of the nucleus and rhodamine-phalloidin of the F-actin in overnight *CDC3* shutoff cells.

Next, I integrated a *CDC3* mutant allele at the native *CDC3* promoter region in the P_{MET3}-*CDC3* strain and evaluated the effect of each of the mutations by growing the strains in GMM+MC. Under yeast growth conditions, mutating S7, S41 and S365 to either A or D all caused a similar degree of moderate morphological defects with 10-15% of the cells showing elongated buds or necks (**Fig. 3.3A**). In contrast, the S422A and S422D mutants exhibited dramatically different defects. While the S422D mutation caused severe morphological and cytokinetic abnormalities comparable to the depletion of Cdc3, the effect of the S422A substitution was much weaker. After overnight shutoff of the wild-type *CDC3*, nearly all S422D cells were highly elongated and failed in cytokinesis, but only ~20% of the S422A cells were elongated and normal yeast cells were still present in the culture indicating completion of cytokinesis (**Fig. 3.3A**). When the mutants were grown under hyphal-induction conditions, >50% of the S7A cells grew multiple germ tubes resembling the septin $cdc11^{S395A}$ mutant (Sinha et al., 2007) (**Fig. 3.3B**). In comparison, ~20% of the S7D cells grew more than one germ tube, suggesting that phosphorylation at S7 may have a role in hyphal development. The S422D mutant completely lost its hyphal growth ability after overnight growth in media that turned off the wild-type *CDC3* just like the Cdc3-depleted cells (**Fig. 3.3B**). In contrast, in spite of the morphological and cytokinetic defects the S442A cells exhibited largely normal

hyphal growth, again demonstrating differential effects between the A and D mutations of S422 (**Fig. 3.3B**). Together, the data strongly suggest that S422 is of great importance for the function of Cdc3 and is likely a critical site where phosphoregulation of the septins occurs. This hypothesis prompted me to focus this study on the S422 mutations.

Another interesting observation of the *cdc3* mutants is that the protein levels of $Cdc3^{S7A}$ and $Cdc3^{S422D}$ are significantly lower than WT and other Ser site mutations. Is it possible that the phenotypes observed in the $cdc3^{S422D}$ mutant are due to the lowered expression of the mutated protein but not the mutation itself? This scenario is unlikely because $Cdc3^{S7A}$ and $Cdc3^{S422D}$ showed a comparable level of protein expression, yet cells expressing $Cdc3^{S7A}$ as the only source of Cdc3 exhibited relatively normal morphology. Therefore, it is highly likely that S7A and S422D mutations reduce the stability of the protein but exert differential effects on cell morphogenesis.

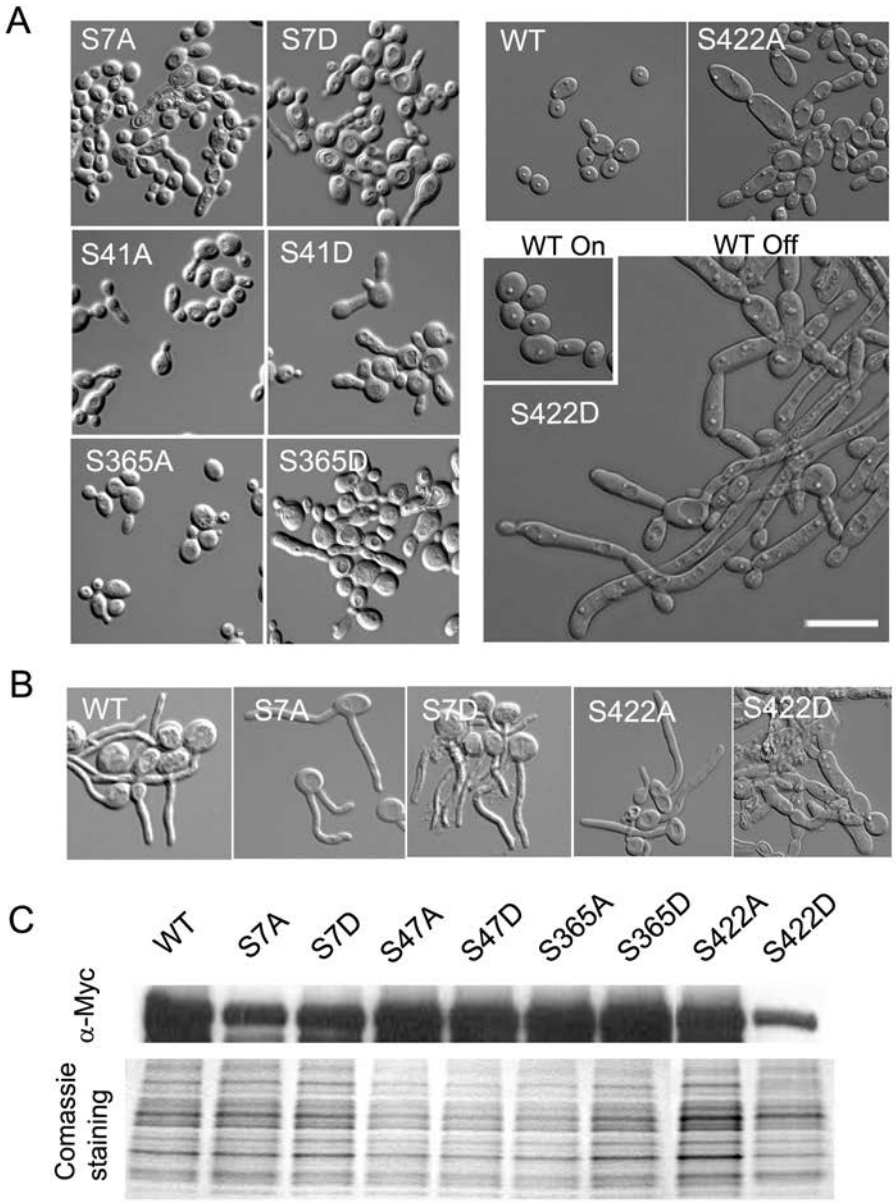

Figure3.3 Morphology and protein stability of Cdc3 phospho-mutants

(A) Cells were grown in GMM with 0.5 mM Met+Cys at 30°C for overnight. Bar = 10µm. Scale bar is representative for all panels. (B) Cells from the overnight culture were grown in GMM+20% serum for 90 min. (C) Myc tagged Cdc3, Cdc^{S7A}, Cdc^{S7D}, Cdc^{S47A}, Cdc^{S47D}, Cdc^{S365A}, Cdc^{S365D}, Cdc^{S422A} and Cdc^{S422D} were compared. Comassie blue

stained gel of the same total lysates was used as loading control.

3.5 Cdc3^{S422D} does not localize to the bud neck and fails to associate with other septins

Next, I determined whether Cdc3^{S422D} and Cdc3^{S422A} can still localize to the bud neck and associate with other septins in the absence of WT Cdc3. GFP-tagging revealed that both mutant versions of Cdc3 localized and behaved normally in the presence of WT Cdc3. After switching off wild-type Cdc3 overnight, Cdc3^{S422A} exhibited essentially normal localization at the presumptive budding site and septum, but also formed strong cortical patches and circles. In stark contrast, Cdc3^{S422D} showed complete mislocalization, and no signal could be observed at the neck region (**Fig. 3.4 A**).

I used 2D WB to check the phosphorylation status of Cdc3^{S422A}. Two spots on the most phosphorylated end were missing and 3 were significantly weakened, while 3 least phosphorylated spots were enhanced (**Fig. 3.4B**). This result is consistent with S422 being a site of phosphorylation and also suggests that phosphorylation of S422 may be required for further phosphorylation of the protein at other sites.

In *S. cerevisiae*, the CTE of Cdc3 is known to be essential for stabilizing septin octamers and higher-order filaments by forming a coiled coil bundle with the CTE of Cdc12. Although how the different septin monomers are organized in *C. albicans* have not been determined, we hypothesized that the CTE of Cdc3 may play a similar role which may be regulated by phosphorylation of S422. To test this hypothesis, I tagged Cdc10, Cdc11 and Cdc12 with GFP in the P_{MET3}-*CDC3 cdc3*^{S422A}-*Myc* and P_{MET3}-*CDC3 cdc3*^{S422D}-*Myc* strains as well as in a *CDC3-Myc* strain. After shutting off the WT *CDC3*,

I first immunoprecipitated Cdc3 and then probed the other septins with GFP antibody in western blotting. A strain expressing Cdc3-Myc without other tagged septins was included as negative control. The coimmunoprecipitation (co-IP) results showed that $Cdc3^{S422A}$ exhibited similar levels of association with Cdc10, Cdc11 and Cdc12 as the wild-type Cdc3 (**Fig. 3.4C**). In contrast, $Cdc3^{S422D}$ pulled down much less Cdc11 than the wild-type Cdc3 and $Cdc3^{S422A}$ although its association with Cdc10 and Cdc12 was unaffected (**Fig. 3.4C**). Thus, the data indicate that the S422D mutation has a strong effect on the integrity of the septin complex, consistent with a role of the CTE of Cdc3 in determining the stability of the septin filaments. However, we do not yet know whether the Cdc3 CTE directly associates with Cdc11 or the S422D mutation causes conformational changes of the septin oligomers which releases the Cdc11 molecules. If the *C. albican*s septin monomers are organized in the same order as in the *S. cerevisiae* septin octomers Cdc11–Cdc12–Cdc3–Cdc10–Cdc10–Cdc3–Cdc12–Cdc11, CaCdc3 is not expected to directly interact with Cdc11. In *S. cerevisiae*, the CTE of Cdc11 mediates end-to-end linkage of the octomeric septin rods and inter-filament interactions and thus plays an important role in assembling septin rods into higher-order structures (see **Fig. 1.5**). If Cdc11 has a similar role in *C. albicans*, the strong effect of the S422D mutation on Cdc3's association with Cdc11 is consistent with the severe septin disorganization in the $cdc3^{S422D}$ mutant (**Chapter 3.6**).

3.6 The S422D mutation causes premature disassembly of septin rings

In light of the weakened interaction between $Cdc3^{S422D}$ and Cdc11, I wondered whether the localization of Cdc11 and other septin components was affected. GFP tagged

Cdc11, Cdc12 and Gin4 were examined in both *cdc3*^{S422A} and *cdc3*^{S422D} mutants before and after shutting off the WT *CDC3*. In *cdc3*^{S422A} mutants, all Cdc11, Cdc12 and Gin4 could localize to the neck in yeast cells (**Fig. 3.4D**). Cdc12 also exhibited some cortical signals in both yeast like and pseudohyphal cells. In *cdc3*^{S422D} mutants, both Cdc12 and Gin4 could be seen as a band at the mother daughter neck of some cells and a diffused band near the tip of some filaments (**Fig. 3.4E**). In comparison, when I examined Cdc11-GFP localization in the *cdc3*^{S422D} background, I only saw occasional assembly of Cdc11 rings at the base of small buds that was emerging from the elongated cells (**Fig. 3.4D**), suggesting that septin rings can form when buds initially emerge but are quickly disassembled.

To confirm the transient localization of Cdc11 to the neck, I monitored septin organization in emerging buds using time-lapse confocal microscopy. Cells were first grown for 8 hours in GMM+MC before time-lapse observation. The cells were elongated and formed branched filaments confirming that the shut-off of WT *CDC3* was complete. Images were taken every 15 min for several hours. We managed to capture several emerging buds and **Figure 3.4F** shows a representative one. Cdc11-GFP first localized to the presumptive budding site and then formed a ring at the bud neck. However, the ring disappeared quickly after 30 min as the bud elongated. In comparison, in wild-type cells the interval between the initial localization of septins to the presumptive budding site and the disassembly of the ring is 90-100 min under the same culture condition (not shown). The results indicate that septin rings can be assembled in cells expressing Cdc3^{S422D} as the sole source of Cdc3, but such rings are not stable leading to premature disassembly. I also examined Cdc12 localization under the same conditions. Interestingly, Cdc12 was

able to form a ring at the bud neck which persisted much longer than Cdc11 (**Fig. 3.4E**). However, the Cdc12 ring was broader than a normal ring, and often incomplete and appeared as a set of bars (**Fig. 3.4F**). This defective ring was not disassembled after cytokinesis, but moved up to near the tip of the daughter cell. Together, the results suggest that the S422D mutation of Cdc3 causes early dissociation of Cdc11 from the ring leaving behind a disorganized and unstable septin structure at the neck.

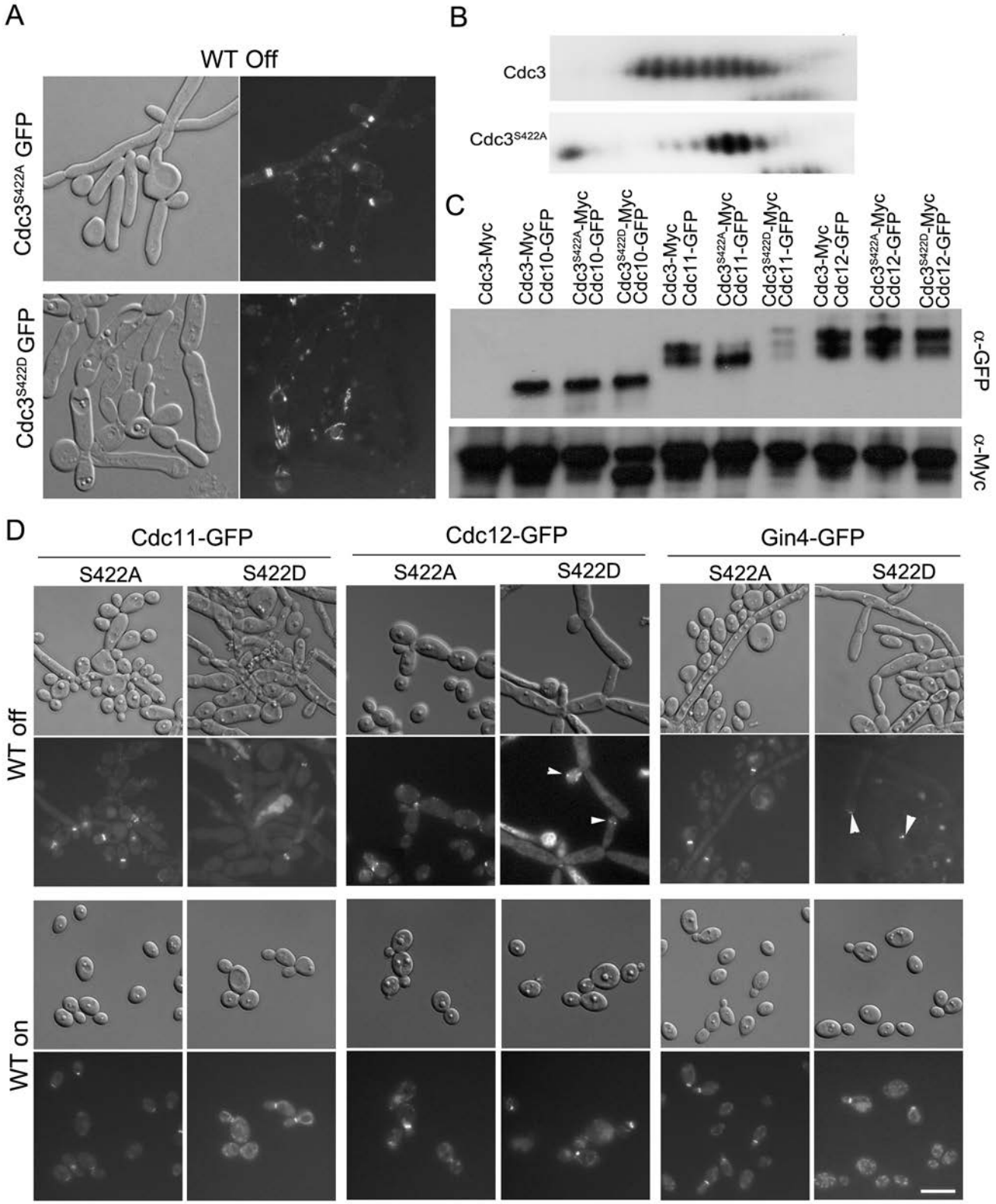
A
WT Off
Cdc3S422A GFP
Cdc3S422D GFP
B
Cdc3
Cdc3S422A
C
Cdc3-Myc
Cdc3-Myc Cdc10-GFP
Cdc3S422A-Myc Cdc10-GFP
Cdc3S422D-Myc Cdc10-GFP
Cdc3-Myc Cdc11-GFP
Cdc3S422A-Myc Cdc11-GFP
Cdc3S422D-Myc Cdc11-GFP
Cdc3-Myc Cdc12-GFP
Cdc3S422A-Myc Cdc12-GFP
Cdc3S422D-Myc Cdc12-GFP
α-GFP
α-Myc
D
Cdc11-GFP
Cdc12-GFP
Gin4-GFP
S422A
S422D
WT off
WT on

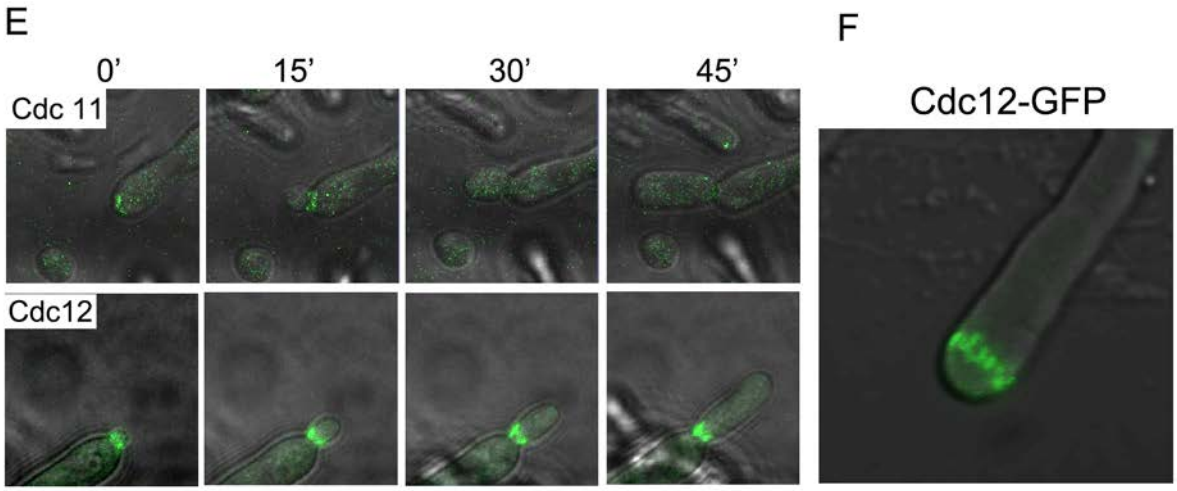

Figure 3.4 Cdc3^{S422D} cannot localize to the neck and affects interaction with Cdc11

(A) *cdc3*^{S422A} and *cdc3*^{S422D} mutants were grown in GMM with 0.5 mM Met+Cys at 30°C overnight to shut off of WT *CDC3*. (B) G1 cells of *cdc3*^{S422A} mutants were obtained for the 2D WB. (C) Cells were incubated in the shutoff media (+MC) overnight and diluted into fresh media (+MC) 10 times the original volume. More *cdc3*^{S422D} cells were used because of its lower protein level. WT Cdc3, Cdc3^{S422A} and Cdc3^{S422D} were immunoprecipitated with anti-Myc conjugated beads, and probed with anti-GFP antibody to detect other septins in western blotting. (D) GFP-tagged Cdc11, Cdc12 and Gin4 in *cdc3*^{S422A} and *cdc3*^{S422D} mutant background were cultures in the shutoff media overnight. Localizations of these proteins were examined before and after shutting off WT Cdc3. Arrowheads in the Cdc12 image indicate misorganized rings (a high resolution image is shown in F). Arrowheads in the Gin4 image indicate the tip and neck localization of Gin4. Bar = 10 μm. (E) *cdc3*^{S422D} cells with Cdc11-GFP or Cdc12-GFP were cultured in the shutoff media for 8 hours before live cell imaging. A z-stack of 15 images were taken at each of the indicated time points with minimum pinhole size to avoid photobleaching. (F)

Confocal images of Cdc12-GFP at the tip of elongated daughter cell in *cdc3*^{S422D} mutant. ~30% of filament tips showed this Cdc12 localization and organization.

3.7 S422 is dephosphorylated during the assembly of the new septin ring

Since Cdc3 undergoes cell cycle regulated phosphorylation and S422 plays an important role in septin organization, the next question I asked is whether the phosphorylation of S422 was also cell cycle dependent. To answer this question, polyclonal antibodies were commercially prepared (Genemed Synthesis Inc., USA) to recognize phosphorylated S422 within a 15 amino-acid peptide. I first performed western blotting to assess the specificity of the antibody. The antibody strongly reacted with WT Cdc3 and the reaction was significantly reduced after pretreatment of the sample with λ phosphatase; and the antibody also exhibited weakened reaction with Cdc3^{S422A} (**Fig. 3.5A**). The Cdc3 proteins had a C-terminal Myc tag and anti-Myc western blotting was used to confirm equal loading of proteins (**Fig. 3.5A**). The results indicate the polyclonal antibody has specificity for phosphorylated S422 although it can also react weakly with unphosphorylated Cdc3.

Using this antibody as a probe, I next investigated the stages in the cell cycle that S422 is phosphorylated. I constructed a strain with one copy of *CDC3* tagged with Myc at the C-terminus. I first pulled down the septin complex using an anti-Myc antibody and then probed the Cdc3 using the phospho-specific antibody in western blotting. Cdc3-Myc was also probed for loading control. The degree of phosphorylation was compared by calculating the ratio of signals detected by anti-phospho-S422 antibody over that by the anti-Myc antibody. Freshly elutriated G1 cells showed strong phosphorylation. This is in

agreement with strong Cdc3 phosphorylation revealed by 2D WB at the same time point (**Fig. 3.1D**) when Cdc3 showed highest number of phospho-isoforms. During the first 60 min, when the old septin ring is undergoing disassembly, phosphorylation at S422 was largely unaffected. At around 120 min, when the new septin ring is assembled, there was a sharp drop in S422 phosphorylation, indicating that dephosphorylation of the residue took place around this time. The phosphorylation was gradually restored as the cell cycle progressed. Together, I have shown that S422 is a critical amino acid in Cdc3 function, and its phosphorylation and dephosphorylation are temporally controlled.

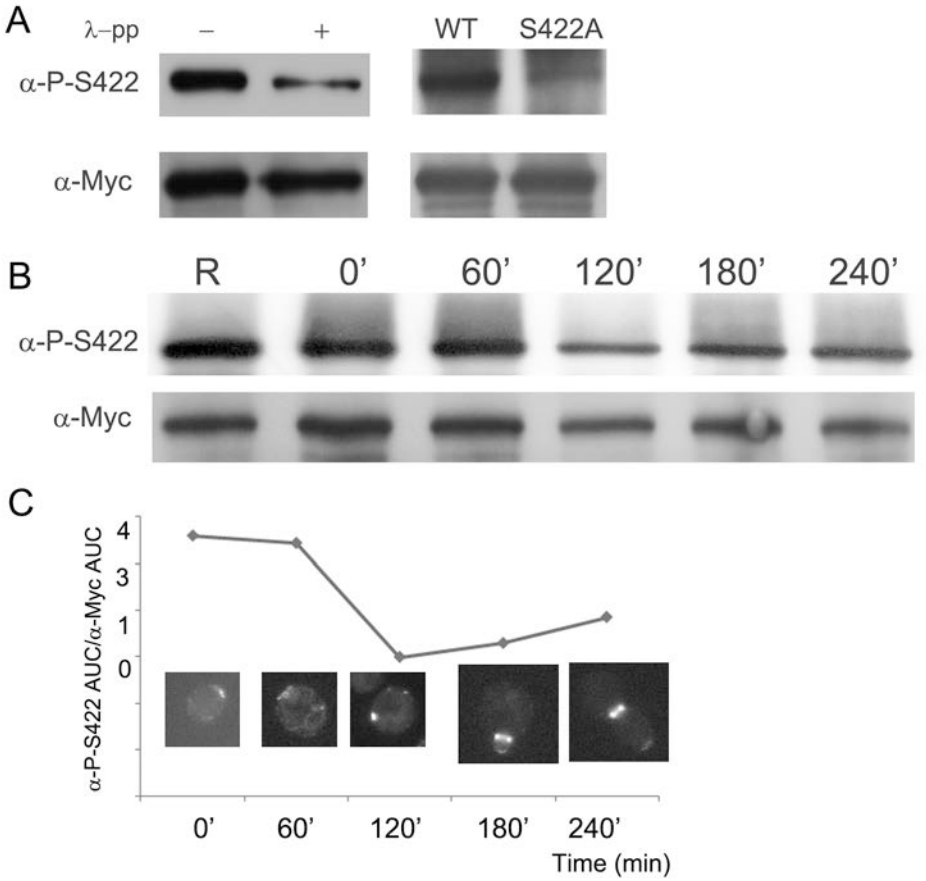

Figure 3.5 S422 is dephosphorylated during the assembly of new septin ring

(A) Cdc3-Myc and Cdc3^{S422A}-Myc from asynchronous cultures were immunoprecipitated. The blot was first probed with anti-phosphor-Ser422 antibody, followed by stripping and reprobing with anti-Myc antibody. (B) Cdc3-Myc was immunoprecipitated by anti-Myc-antibody conjugated beads. Untagged Cdc3 in the precipitate was detected by the anti-phosphor-S422 antibody. Cdc3-Myc also serves as a loading control between samples. (C) The autorad was scanned to determine the intensity of each band. Relative intensity was calculated by the ratio of the area under the curve (AUC) detected by the anti-phosphor-S422 antibody over that detected by the anti-Myc antibody. Cell images corresponding to the time points for sample collection are shown.

3.8 Gin4 but not Cdc28 is involved in the phosphorylation of Cdc3

Since my results above have shown that phospho-regulation of Cdc3 has high physiological importance, I set out to look for the kinases and phosphatases responsible for the regulation. One obvious candidate is Cdc28, which is known to phosphorylate Cdc3 in the budding yeast (Tang and Reed, 2002). To test whether it was the same case in *C. albicans*, I tagged Cdc3 with GFP in a *cdc28as* mutant and obtained G1 cells. The G1 cells were first grown in GMM at 30°C for 1 or 2 hours and then treated with the Cdc28as-specific inhibitor 1NM-PP1 for 1 hour. Upon addition of 1NM-PP1, the kinase activity of Cdc28 is blocked (Bishop et al., 2000). However, significant reduction of Cdc3 phosphorylation was not observed at either time point compared with mock-treated samples (**Fig. 3.6A**). To show that 1NM PP1, at the concentration used, can effectively inhibit Cdc28as, I included Gin4 as control (unpublished data in Dr. Yue Wang's lab has shown that Gin4 contains 9 perfect consensus sites for Cdk phosphorylation and is a substrate of Clb2-Cdc28 both in vivo and in vitro). I found that 1NM PP1 abolished Gin4 phosphorylation. Thus, the data indicate that Cdc28 does not have a significant role in Cdc3 phosphorylation. Another candidate is Cla4, a PAK kinase shown to phosphorylate Cdc3, Cdc10 and Cdc11 in *S. cerevisiae* (Versele and Thorner, 2004). Cdc3 from asynchronous cultures of WT and *cla4*Δ mutants were compared and no obvious difference was observed in the degree of phosphorylation (**Fig. 3.6B**). Since Gin4 associates with septin complex tightly and phosphorylates Cdc11 (Sinha et al., 2007) and Sep7 (Dobbelaere et al., 2003), I next tested whether it is involved in Cdc3 phosphorylation too. 2D WB of an asynchronous culture revealed the loss of a few spots in kinase inactive mutant $gin4^{K57A}$ (data not shown). To examine more closely, $gin4^{K57A}$

G1 cells were prepared and phosphorylation of Cdc3 was profiled at different stages of the cell cycle. A clear reduction in the number of phosphorylated spots was observed at 0 hr (**Fig. 3.6C**) compared to the 11-spot-pattern in WT (**Fig. 3.1D**). The dephosphorylation observed in WT cells happened in the *gin4*^{K57A} mutant, but in a slightly different pattern. The signal of the two least phosphorylated spots were enhanced while one spot at the phosphorylated side remained. Interestingly, as the cell cycle progressed, rephosphorylation of Cdc3 occurred but was not complete, indicating that Gin4 is involved in Cdc3 phosphorylation. However, the observation that Cdc3 did not show any aberrant localization in *gin4*^{K57A} mutants suggests that phosphorylation of Cdc3 by Gin4 may not be relevant in Cdc3 localization. The attempt to search for the phosphatases did not show any conclusive results. Cdc3 in both *cdc14*Δ and *rts1*Δ showed a normal dephosphorylation 1 hr after recovery from elutriation (data not shown), while inhibition of Protein Phosphatases 1 and 2 by calyculin A blocked the dephosphorylation but also arrested the cell cycle.

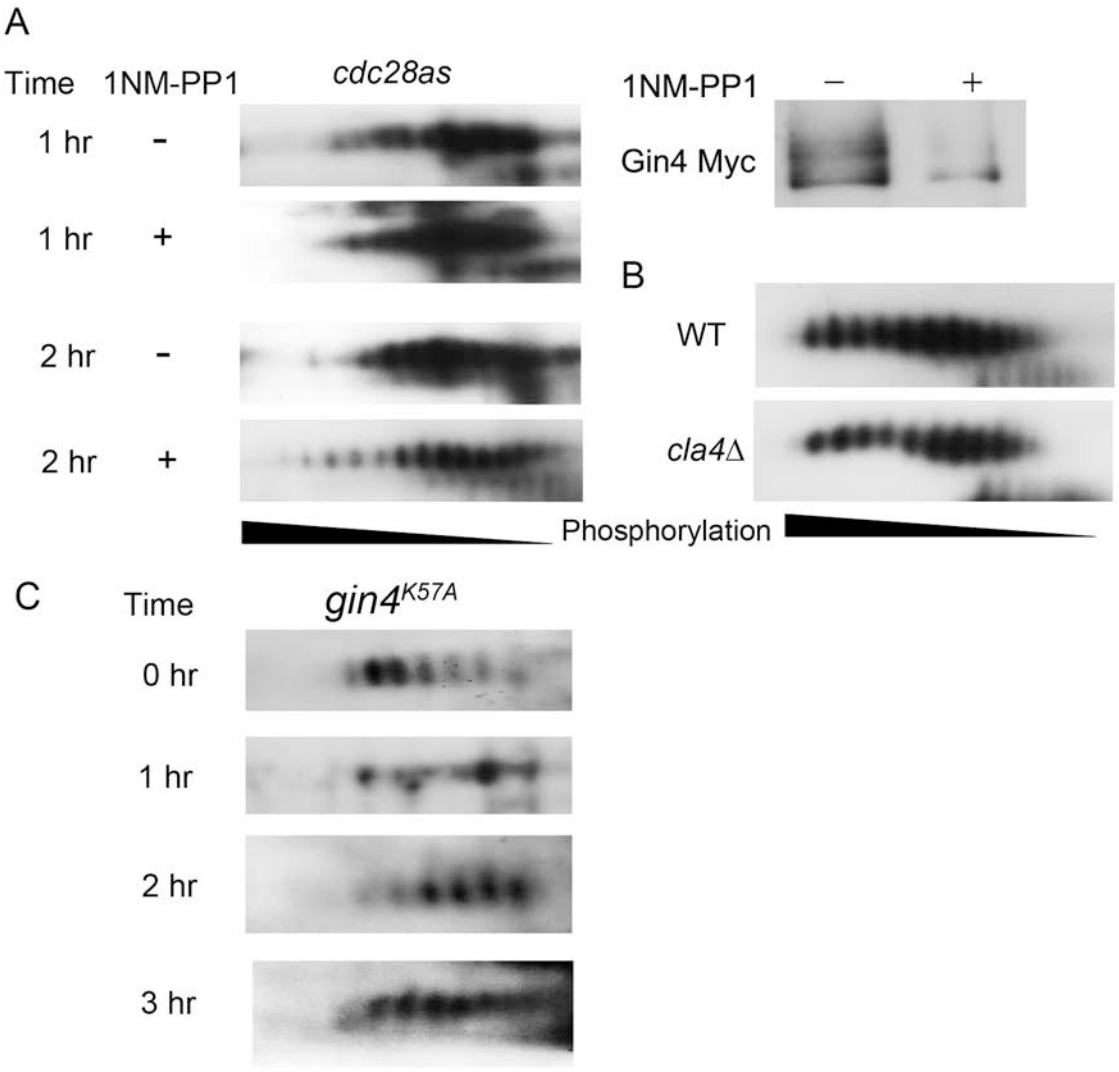

Figure 3.6 Gin4 but not Cdc28 is involved in Cdc3 phosphorylation

(A) G1 cells of *cdc28as* were obtained by centrifugal elutriation. After recovering in GMM at 30°C for 1 or 2 hrs, the cells were treated with 25 μM concentration of 1NM-PP1 for 1 hr. Cdc3-GFP was analyzed by 2D WB. WT cells with Myc-Gin4 were induced for hyphae for 120 min in GMM+20% serum with or without 1NM-PP1. Gin4 was immunoprecipitated with anti-Myc antibody-conjugated beads and detected by anti-Myc antibody. (B) Asynchronous cultures of WT and *cla4*Δ cells with Cdc3-GFP were

used for the 2D analysis. (C) G1 cells of *gin4*^{K57A} with Cdc3-GFP were obtained by centrifugal elutriation and recovered in GMM medium at 30°C. Aliquots of cells were harvested at the indicated time points and subjected to 2D WB analysis.

3.9 Discussion

In this project, I found that the *C. albicans* septin Cdc3 undergoes cell cycle dependent phosphorylation and that phosphorylation at a single amino acid S422 plays a critical role in determining septin organization and function. Cdc3 exhibits the highest level of phosphorylation in early G1 cells, followed by a period of dephosphorylation. After the cells traverse the START, Cdc3 phosphorylation increases gradually through the rest of the cell cycle and peaks around the time of cytokinesis. Phospho-mapping by mass spectrometry identified phosphorylation on several residues, and subsequent mutational studies indicated that phosphorylation on S422 may play a key role in regulating septin organization and stability. The phosphomimetic S422D mutation causes gross disorganization of septin structures, severe cytokinetic defects, dramatic cell elongation, and inability of Cdc3 to localize to the bud neck. The nonphosphorylatable S422A mutation causes a much weaker phenotype, and Cdc3^{S422A} can localize to the bud neck although it also forms random cortical patches and circles. Coimmunoprecipitation experiments demonstrate that the S422D mutation greatly weakens Cdc11's association with the septin complex and causes premature dissociation of Cdc11 from the ring. I found that the septin-associated kinase Gin4 is involved in the phosphorylation of Cdc3, but it remains to be determined whether it includes S422. Using the analog-sensitive *cdc28as* mutant did not reveal any significant difference in Cdc3 phosphorylation

between 1NM PP1-treated and untreated cells, indicating that Cdc28 is not involved. Interestingly, mutating S422 of Cdc3 to alanine causes disappearance of multiple phosphoisoforms, suggesting that phosphorylation of S422 may facilitate further phosphorylation at other sites. Thus, S422 appears to be a major determinant of the overall phosphorylation level of Cdc3. Together, my findings strongly support the idea that S422 serves as a critical site of control that regulates septin assembly/disassembly, organization and stability in a cell cycle dependent manner.

Based on my findings above, I propose the following model **(Fig. 3.7**) to explain how Cdc3 phosphorylation regulates the septin structures throughout the cell cycle. Cdc3 phosphorylation and dephosphorylation, in which S422 is a key determinant, is temporally controlled during the cell cycle: it is phosphorylated in early G1, dephosphorylated in late G1 and rephosphorylated progressively throughout S, G2 and M phases until the time of cytokinesis when most Cdc3 molecules are phosphorylated. Cdc3 phosphorylation causes disassembly of the long, cross-connected septin filaments in the old septin ring into short oligomers in early G1; and at the same time it also prevents premature assembly of septin oligomers into new rings. When cells approach the START, cell cycle signals trigger a rapid dephosphorylation of Cdc3, which removes the hindrance for septin oligomers to assemble into long, cross-connected filaments, thus forming a new ring at the presumptive bud site. After the cells have entered the cell cycle, rephosphorylation of Cdc3 occurs in a progressive manner and reaches the highest level near the end of M phase. The slow and progressive rephosphorylation of Cdc3 may be important for maintaining the stability and integrity of the septin structure during the cell cycle. Only when the overall phosphorylation level of Cdc3 rises above a threshold level,

the septin structure will be significantly destabilized thus initiating the process of disassembly. The instability could be the result of weakened inter-oligomer or inter-filament associations mediated by Cdc3 itself or Cdc11 (**Fig. 3.4C**) or both. In *S. cerevisiae*, Cdc11 mediates end-to-end association of septin octamers and the CTE of Cdc3 forms a coiled-coil bundle cross-linking parallel septin filaments (Bertin et al., 2008. See more discussion below). This model is also supported by my findings that $Cdc3^{S422D}$, in the absence of WT Cdc3, cannot localize to the bud neck, while $Cdc3^{S422A}$ experiences defects in disassembly (**Fig. 3.4A**). In the presence of WT Cdc3, $Cdc3^{S422D}$ can be incorporated into the septin ring and the septin structures appear normal throughout the cell cycle. This is likely due to the presence of WT Cdc3 and $Cdc3^{S422D}$ molecules in the same oligomers which allows the incorporation of $Cdc3^{S422D}$ into the septin ring. It also supports my hypothesis that only when Cdc3 phosphorylation rises over a threshold level, the stability of septin structures will be significantly reduced.

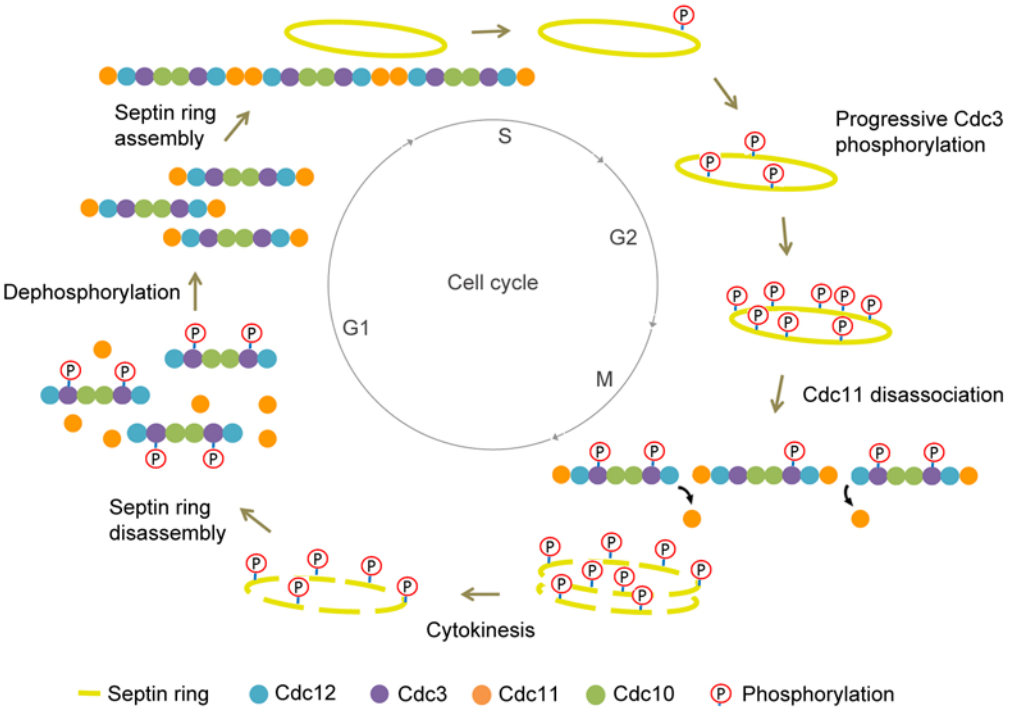

Figure 3.7 Working model for the dephosphorylation/phosphorylation of Cdc3 Ser422 in controlling septin ring assembly/disassembly and stability.

See the text for explanation.

In *S. cerevisiae*, the sequence of septin subunits in an octamer is found to be Cdc11–Cdc12–Cdc3–Cdc10–Cdc10–Cdc3–Cdc12–Cdc11 (Bertin et al., 2008). According to this model, Cdc3 does not interact with Cdc11 directly. It is possible that the phosphorylation at S422 causes conformational changes in Cdc12 that weakens the affinity between Cdc11 and Cdc12. Since $Cdc3^{S422D}$ cannot be integrated into the septin ring in the absence of WT Cdc3, in order to survive, the cell may be 'forced' to assemble septin filaments without Cdc3. The G face of Cdc12, which originally interacts with Cdc11, is switched to interact with Cdc10 to form a hexamer. Therefore, the affinity of

Cdc11 to this filament is greatly decreased, and Cdc11 dissociates from the ring rapidly after bud emergence.

In *S. cerevisiae*, G1 cyclin/Cdk1 kinases phosphorylate Cdc3 at S503 and S509 near the C-terminal end to facilitate the disassembly of the old septin ring (Tang and Reed, 2002). This mechanism seems to be conserved in *C. albicans* although a different kinase may be involved. CaCdc3 phosphorylation is at the peak level in early G1 cells which coincides the disassembly of the old ring. And in many S422A cells cortical septin circles and patches were observed in addition to the septin ring at the bud neck, suggesting defects in the disassembly of septin structures. Different from the budding yeast, CaCdc28 does not seem to be involved in the phosphorylation of Cdc3. Despite this distinction, phosphorylation of serine residues near the C-terminal end is required for the disassembly of old septin rings in both organisms.

Chapter 4 *C. albicans* Nap1 plays a role in polarized growth and septin ring organization

4.1 Introduction

C. albicans is polymorphic, capable of switching between yeast, pseudohyphal and hyphal forms of growth in response to environmental stimuli (Berman and Sudbery, 2002). Several pathways have been identified that mediate the yeast-to-hyphal growth transition, among which the mitogen-activated protein kinase (MAPK) cascade and the cAMP/protein kinase A (PKA) pathway play a key role (Liu et al, 1994; Lo et al, 1997; Liu, 2001). These two pathways activate two transcription factors, Cph1 and Efg1 respectively (Lo et al, 1997; Stoldt et al., 1997). They subsequently switch on the expression of hypha-specific genes (HSGs) responsible for diverse virulence traits (Stoldt et al., 1997; Liu, 2001; Berman and Sudbery, 2002). The only known HSG that is essential for hyphal growth is *HGC1*, which encodes a G1 cyclin (Zheng et al., 2004) and forms a functional complex with the cyclin-dependent kinase (CDK) Cdc28. One early molecular event crucial for hyphal growth is the phosphorylation of the septin Cdc11, which involves three protein kinases sequentially: the septin-associated kinase Gin4, the G1 cyclin–CDK complex Ccn1-Cdc28, and Hgc1–Cdc28 (Sinha et al., 2007). As the first kinase required, Gin4, a Nim1 kinase promoting mitosis, plays an essential role; however it remains unclear how Gin4 is regulated for Cdc11 phosphorylation.

Nucleosome assembly protein 1 (Nap1) was first identified in mammalian cells as a protein involved in nucleosome assembly (Ishimi et al., 1983). It is highly conserved among eukaryotes and has been implicated to have a variety of seemingly unrelated

cellular functions with many interacting partners. Studies in *S. cerevisiae* have shown that Nap1 interacts specifically with the B type cyclin Clb2 in cytoplasm to control proper mitotic progression (Kellogg and Murray, 1995; Miyaji-Yamaguchi et al., 2003), and the functional localization of Nap1 to the nucleus is regulated by the phosphorylation of casein kinase 2 (Calvert et al., 2008). It was later uncovered that Nap1, together with Clb2-Cdk1 and Gin4 are in the septin complex (Altman and Kellogg, 1997; Longtine et al., 2000; Okuzaki et al., 1997). Gin4 kinase activity is activated by hyperphosphorylation, which is dependent on Nap1 and Clb2-Cdk1. In addition, the bud neck localization of Gin4 is lost in the absence of *NAP1*. Thus, it is highly likely that Nap1 acts upstream of Gin4. However, Nap1 was later shown to affect septin organization in the budding yeast. In the absence of *NAP1*, instead of forming a clear band structure at the neck, the septin complex is either "fuzzy" or forms parallel bars at the neck (Longtine et al., 2000). Therefore, it is also possible that Nap1 and Gin4 act on septins in separate pathways, and that the efficient recruitment of Gin4 to the neck is impaired by the misorganized septin complex. This hypothesis is supported by the observation that the defects in the *nap1*Δ *gin4*Δ double mutant, including cell elongation and septin complex misorganization, are more severe than in the *nap1*Δ and *gin4*Δ single mutants (Longtine et al., 2000).

In *C. albicans*, cells deleted for *GIN4* exhibit severe cell elongation and failure to form the septin ring and complete cytokinesis (Wightman et al., 2004); and these defects are much stronger than those observed in *S. cerevisiae gin4*Δ mutants, which have weak effects on cell morphology and septin organization and function (Longtine et al., 2000). Therefore, using *C. albicans* as a model seems to have an advantage in revealing Nap1

functions especially in the aspect of how it interacts with and influences the function and organization of the Gin4-septin complex.

In this chapter, I report that deletion of *C. albicans NAP1* leads to constitutive filamentous growth and defective septin organization. In *nap1*Δ cells, Cdc3 forms random spots or partial rings in the cell cortex and experiences impairment of phosphorylation. Fluorescence recovery after photo-bleaching (FRAP) analysis of Cdc3-GFP uncovers more frequent exchange between the cytoplasm and septin collar in *nap1*Δ cells than in WT cells. Double deletion of *NAP1* and the septin gene *CDC10* results in exacerbated temperature sensitivity, defective septin ring formation and scattered Cdc3 localization. Phospho-mapping by mass spectrometry identified phosphorylation on 10 Thr/Ser residues in the N-terminal region of Nap1. Mutation of these 10 residues to non-phosphorylatable Ala results in pseudohyphal growth and affects Nap1's neck localization. Conversely, mutation of these 10 residues to phospho-mimetic Glu does not affect cell morphology, but causes random deposition of Cdc3. My findings unveil the involvement of Nap1 in septin organization and Cdc3 phosphorylation control.

4.2 *C. albicans NAP1*

Using *S. cerevisiae* Nap1 sequence to BLAST-search the *Candida* genome database revealed the highest identity of 49% to *C. albicans* protein encoded by Orf19.7501 (**Fig. 4.1**). This protein had been annotated as Nap1 in the database, although its function has not been characterized. CaNap1 contains 435 aa, which is slightly longer than ScNap1 (417 aa).

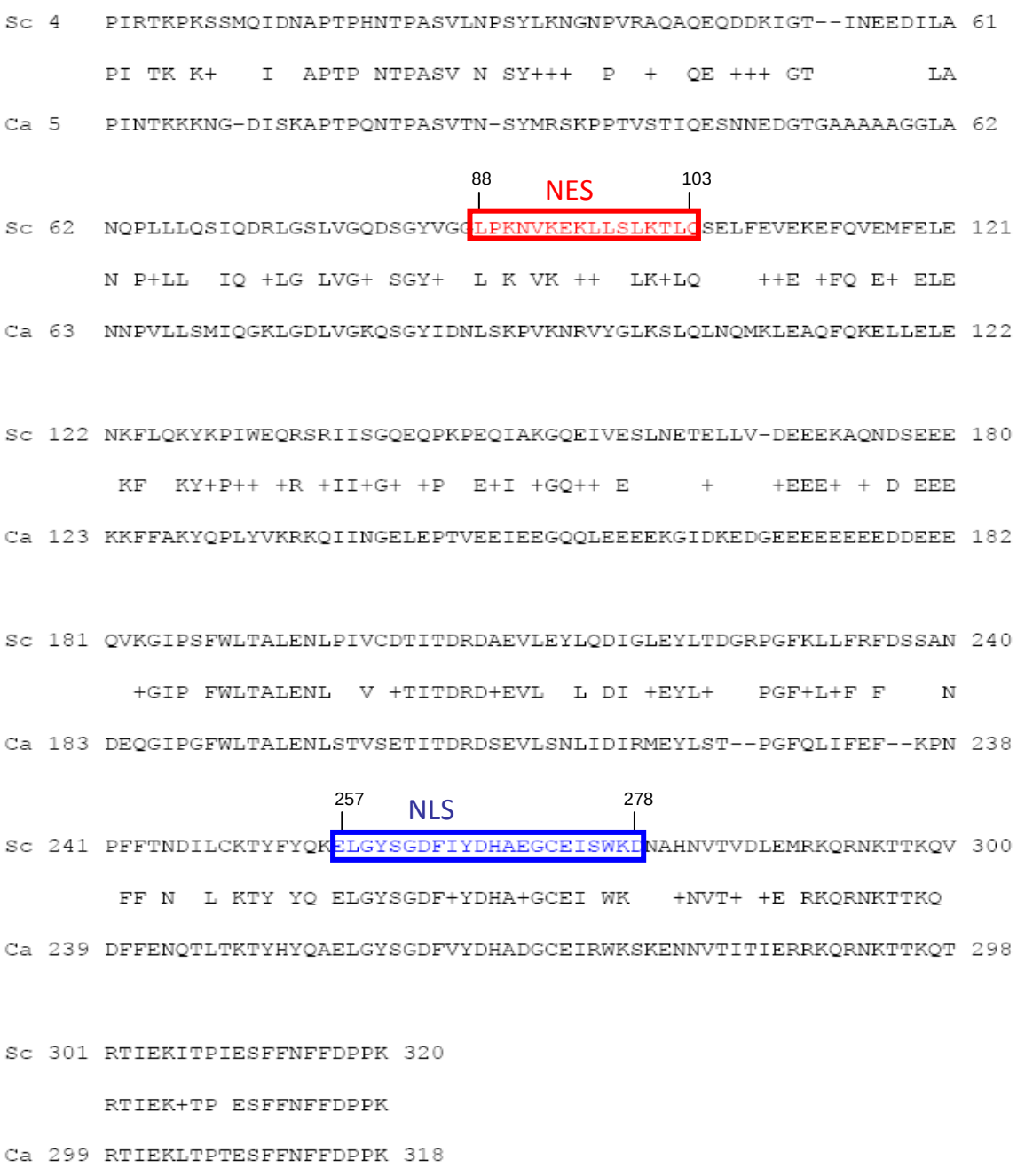

Figure 4.1 Sequence alignment of ScNap1 and CaNap1. Amino acid sequences of ScNap1 and CaNap1 are aligned. The red box indicates the nuclear export signal (NES) and the blue box the nuclear localization signal (NLS) previously identified in ScNap1 (Li et al., 1999). Only the homologous regions are shown.

4.3 Characterization of *C. albicans* Nap1 and its role in septin ring organization

4.3.1 *NAP1* deletion causes filamentous and invasive growth

To study its cellular functions, the two copies of *NAP1* were deleted using a recyclable *URA* blaster cassette (Fonzi and Irwin, 1993). This was constructed by first replacing one copy of *NAP1* with the *hisG-URA3-hisG* cassette flanked by DNA fragments from *NAP1* promoter and terminator regions respectively (**Fig. 4.2A**). The Ura+ prototrophs were then counter-selected on 5-FOA plates to identify isolates which had lost the *URA3* marker through recombination between the *hisG* repeats. The second copy was replaced with the same cassette except that the 3′ end of the *hisG-URA3-hisG* cassette is flanked by fragment IJ instead of CD (**Fig. 4.2A**). Oligonucleotide primers right before the start codon and after the stop codon were used to verify correct deletion of both copies of *NAP1*. PCR analysis of the first and second copy deletions generated 1.2 and 1.7-kb DNA fragments respectively, whereas analysis of the WT control produced a 1.3-kb band matching the size of the *NAP1* gene (**Fig. 4.2B**). All PCR products were purified and sequenced to confirm their identity. Since the *URA3* selectable marker was looped out for both copies, the *nap1*Δ mutant retains all three auxotrophic markers *HIS1*, *URA3* and *ARG4* to facilitate further genetic manipulations. The *nap1*Δ::*NAP1* reintegrant strain and a series of strains expressing truncated or mutated versions of Nap1 tagged with GFP, Myc or HA were constructed by site-specific integration at the *NAP1* promoter region (**Fig. 4.2C**). Various *NAP1* tagging in the WT was done by site-specific integration in the C-terminal region (**Fig. 4.2D**). Proper

expression of tagged Nap1 proteins was confirmed by Western blot analysis (images are shown in relevant figures).

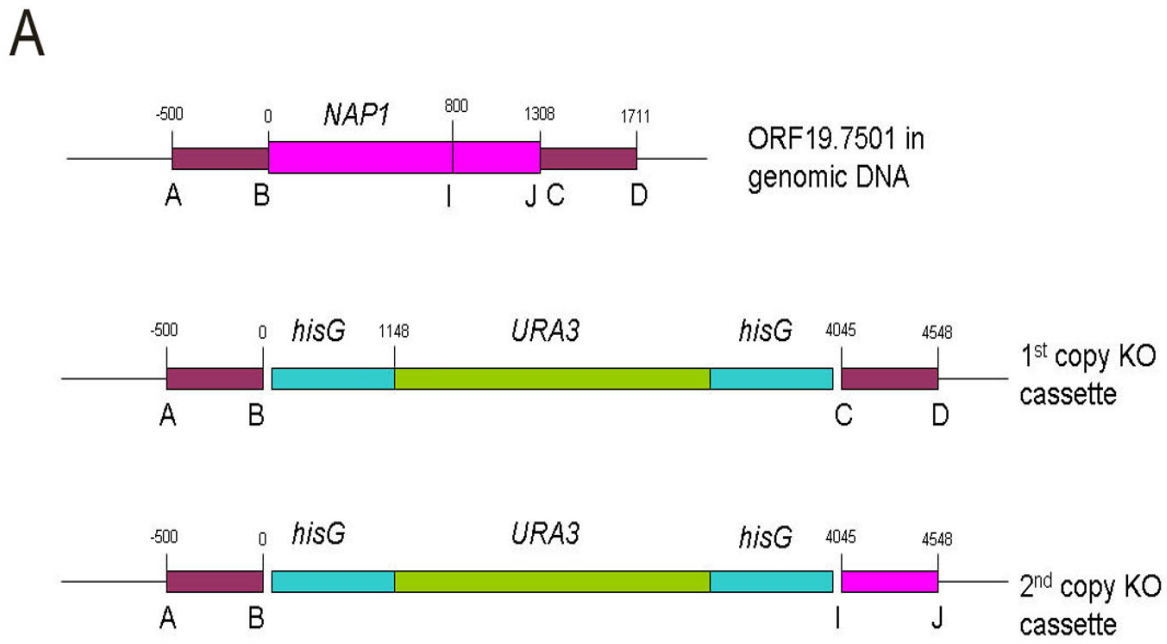

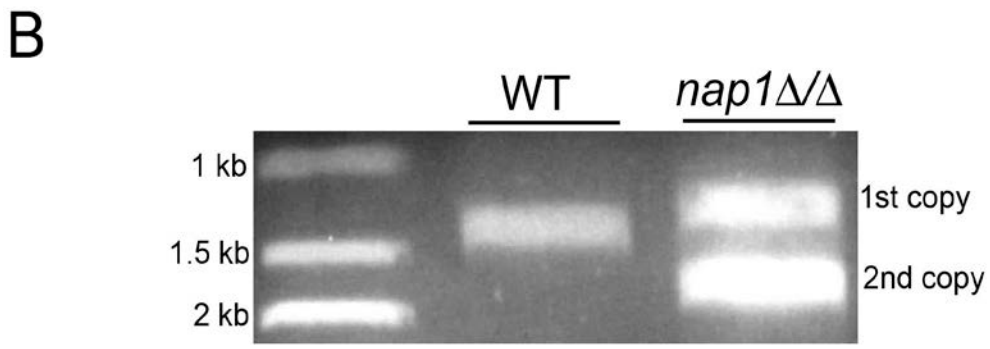

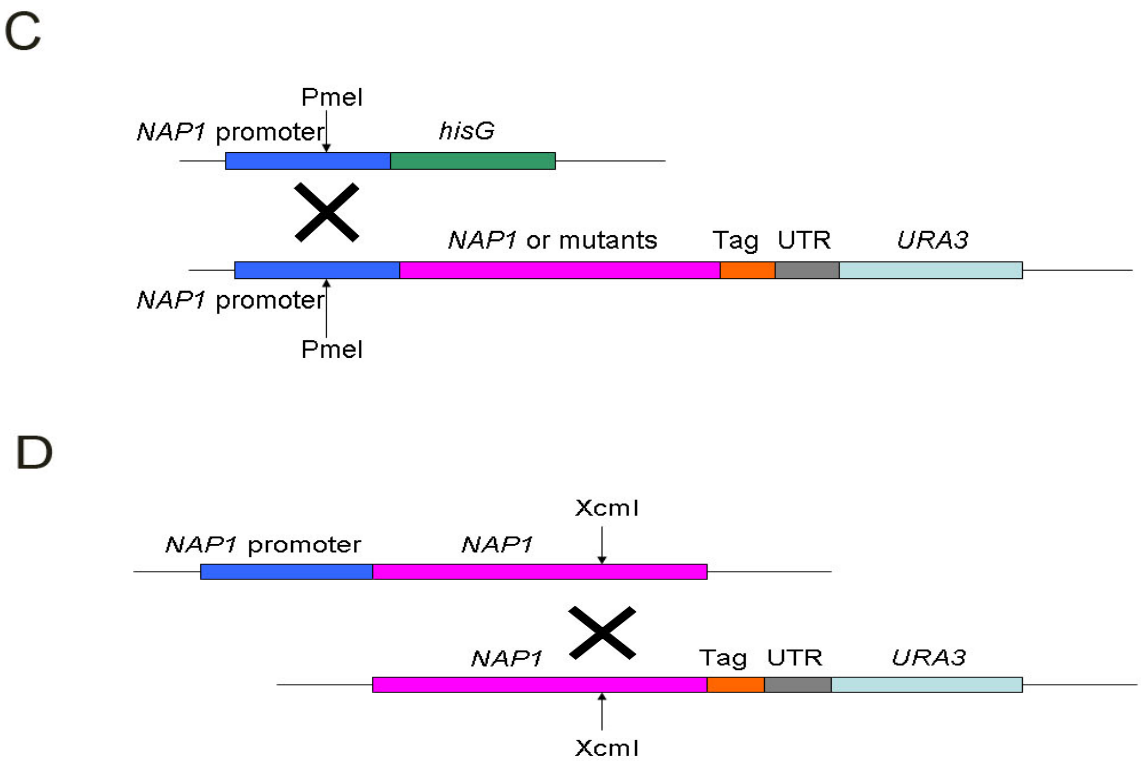

Figure 4.2 Chromosomal deletion of *NAP1*, re-integration and C terminal tagging

(A) Schematic description of the *NAP1* knock-out cassettes. The nucleotide immediately before the start codon ATG is designated as 0. The *hisG* fragments flanking *URA3* are of the same sequence to enable recombination. (B) PCR verification of *NAP1* chromosomal deletion. Primers F and G were used (Table 2.4.1). (C) Schematic representation of site-directed integration at the *NAP1* promoter region, using the restriction site PmeI. (D) Schematic representation of the method to tag *NAP1* at the C terminal region. The restriction site used for integration is XcmI.

While the heterozygous *NAP1/nap1*Δ mutant showed a normal growth rate and morphology, the homozygous *nap1*Δ mutant exhibited strong filamentous growth on YPD plates at 30°C (**Fig. 4.3B**), conditions where wild-type cells grew exclusively as yeasts. On plates, long thin filaments emanated from the edge of colonies in contrast to the smooth edge of the WT colonies (**Fig. 4.3A**). Unlike the WT colonies which could be easily washed off the agar surface, the filaments of the *nap1*Δ colonies penetrated into the agar (**Fig. 4.3A**). Filaments also formed in liquid medium (**Fig. 4.3C** *nap1*Δ 30°C), and the filaments are pseudohyphae because of clear constrictions at the septa.

To confirm that the *NAP1* deletion is indeed responsible for the morphological defects observed above, the complete coding sequence of *NAP1* carrying a Myc tag at the C-terminus was integrated into the *NAP1* promoter region of the *nap1*Δ mutant. Western blot analysis confirmed that the Nap1 protein was expressed to the WT level in the reintegrant (**Fig. 4.3D**). This reintegrant strain was found to be indistinguishable from the WT in phenotype (**Fig. 4.3E**).

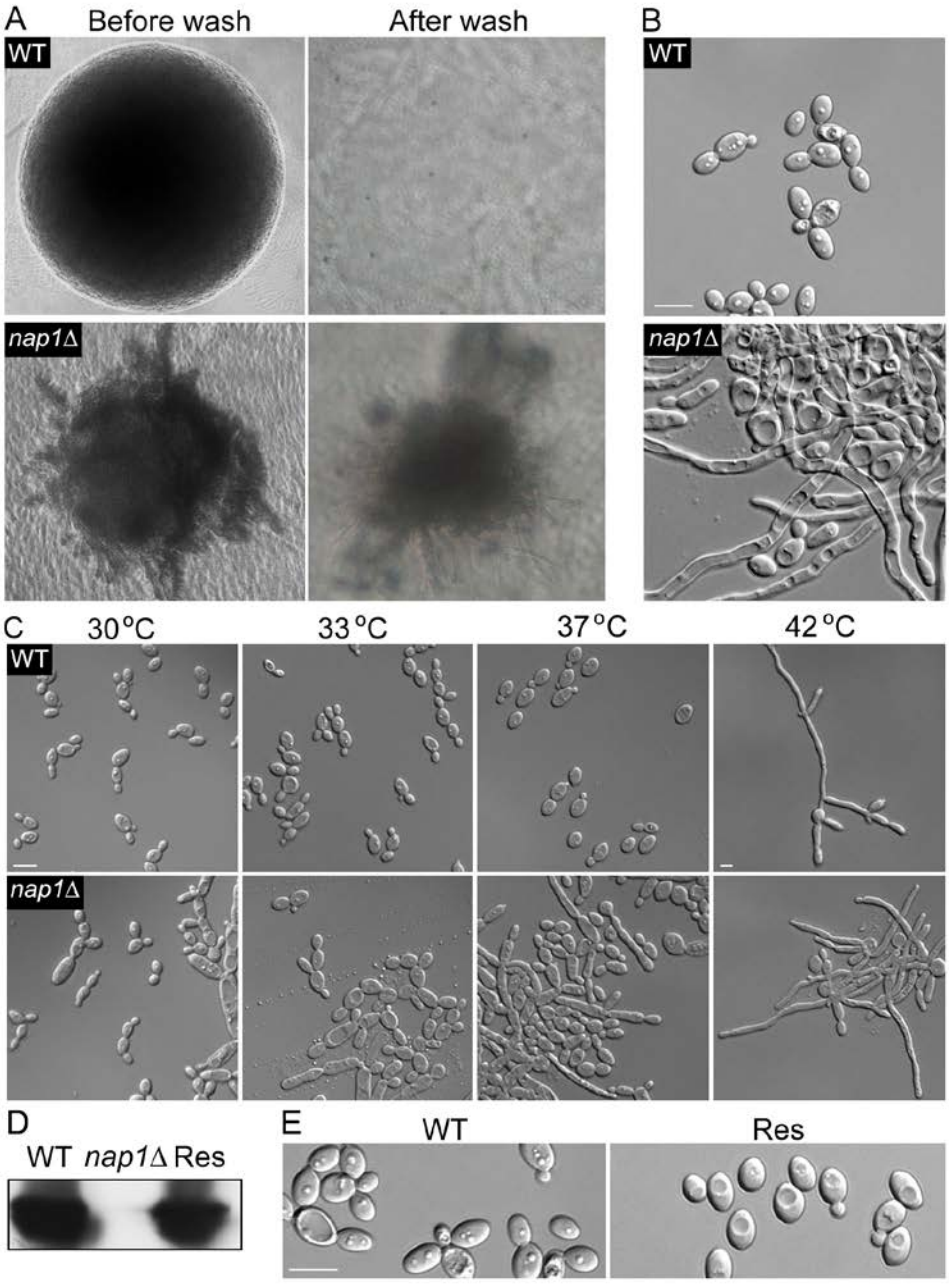

Figure 4.3 Filamentous and invasive growth of *nap1*Δ cells

(A) WT and *nap1*Δ cells were grown on YPD plates at 30°C for 2 days. Images of the same colonies before and after wash with water are shown. (B) WT and *nap1*Δ cells were grown in liquid YPD to log phase at 30°C. (C) WT and *nap1*Δ cells were grown in liquid

YPD at the indicated temperatures overnight. (D) Western blot analysis showed comparable levels of Nap1 in the rescued (reintegration of a copy of *NAP1*) and WT strains. Equal amounts of total protein was loaded for each lane. Anti-Myc antibody was used in western blotting. (E) The rescued strain exhibited a normal morphology. The cells were grown in YPD at 30°C. Bar = 10μm.

I next examined how higher temperatures would affect the morphological defects of the *nap1*Δ mutant. Cells were grown in liquid YPD at 30, 33, 37 and 42°C for 12 h. At 42°C, both WT and *nap1*Δ cells grew in extremely long filamentous form, which is most likely true hyphal growth which normally happens at temperatures above 42°C. At the temperatures lower than 42°C, WT cells underwent normal yeast growth. In contrast, the *nap1*Δ mutant exhibited an increase in the percentage of elongated cells with the elevation of temperature (**Fig. 4.3C**). At 30°C, ~50% of *nap1*Δ cells showed an elongated morphology with <30% growing into long filaments. When grown at 37°C, over 90% of the cells were elongated with more cells forming pseudohyphae. Cells at 33°C were intermediate of those grown at 30°C and 37°C in terms of the percentage of elongated cells and degree of filamentous growth.

To better understand the morphological defects, I obtained synchronous G1 yeast cells by centrifugal elutriation and then released them into YPD liquid media for growth at 30 and 37°C. WT cells started budding at ~120-150 min at both temperatures (**Fig. 4.4A**). Intriguingly, at 37°C, *nap1*Δ cells started to form germ-tube like protrusions at ~60 min (**Fig. 4.4A**) which continued to grow until ~240 min when the newly formed apical cells started to swell (**Fig.4.4A**). Afterwards, the cells gradually grew into chains

of mostly elongated cells with constrictions at the septum. The results suggest that the *nap1*Δ mutant may have become more sensitive to hyphal-induction signals such as temperature but is unable to maintain it beyond the germ-tube stage. In comparison, WT and mutant cells budded at about the same time at 30°C (**Fig. 4.4B**), although the *nap1*Δ mutant grew elongated daughter cells and had cytokinetic defects which were not seen in WT cells.

Both WT and *nap1*Δ G1 cells were then examined for the ability of hyphal growth. Hyphal induction was done in media containing 20% serum at 37°C. The *nap1*Δ mutant produced germ-tubes indistinguishable from the WT in morphology. However, germ tubes emerged significantly earlier in *nap1*Δ cells than in WT cells. At 30 min, when WT cells only showed a slight protrusion, the germ tubes of *nap1*Δ cells were at least 2 μm in length (**Fig. 4.4C**).

In summary, *NAP1* deletion resulted in strong pseudohyphal growth of *C. albicans* under non-inducing conditions and invasive growth into solid media. The severity of the mutant phenotype increases with the elevation of temperature. At 37°C and in the absence of serum, while WT underwent normal yeast growth, *nap1*Δ G1 cells formed germ-tube like protrusions. The mutant cells also produced germ tubes earlier than WT cells when induced with serum at 37°C. The data show that *nap1*Δ cells are more sensitive to hyphal induction signals, suggesting a role for Nap1 in repressing germ-tube formation in *C. albicans*.

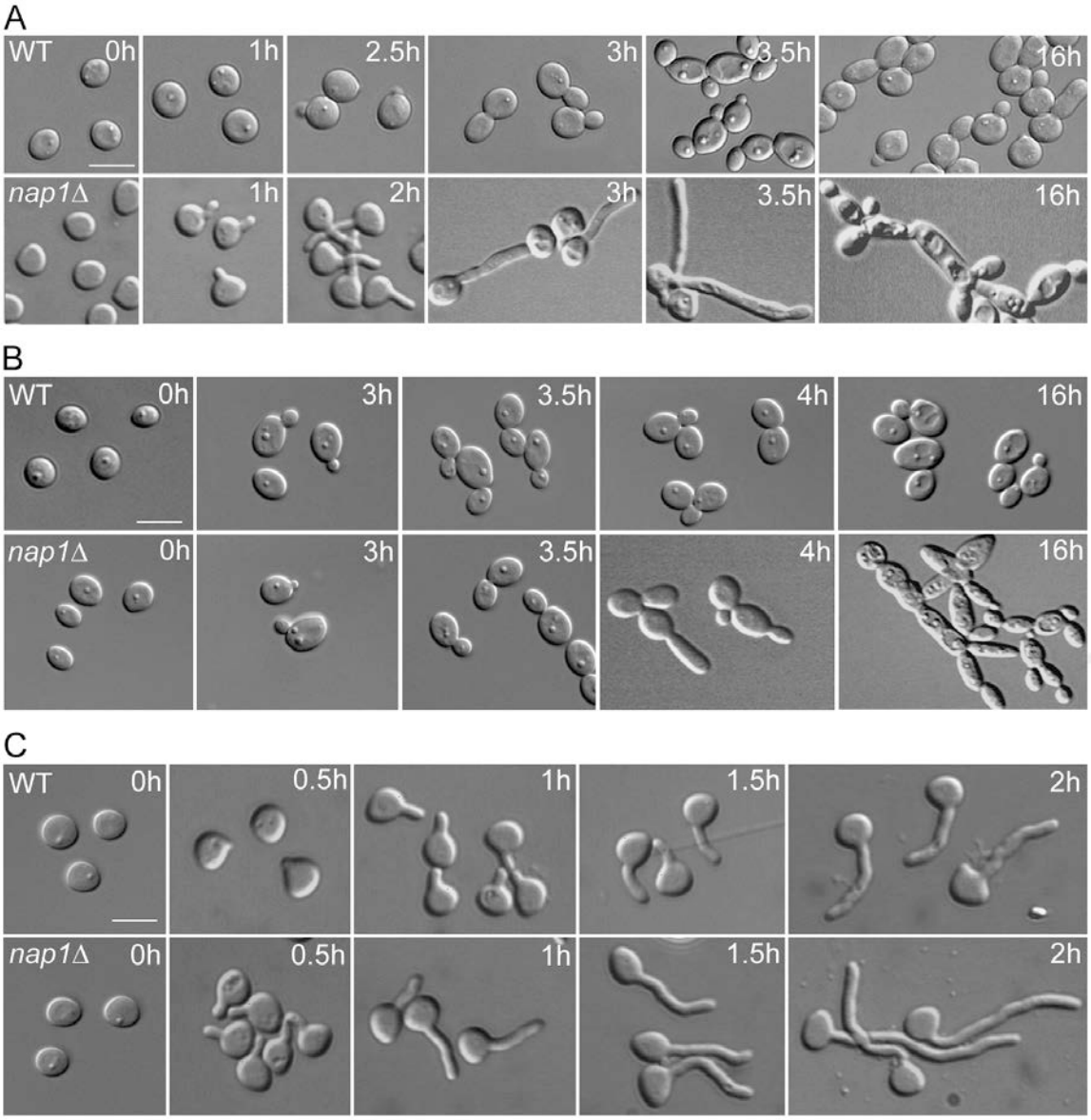

Figure 4.4 *nap1*Δ cells exhibited growth defects

Elutriated WT and *nap1*Δ G1 cells were released into liquid YPD for growth at (A) 37°C and (B) 30°C. Cells were collected at the indicated time points. (C) WT and *nap1*Δ G1 cells were induced in YPD containing 20% serum at 37°C. Bars = 10 μm.

4.3.2 Nap1 colocalizes with septins

It has been well established that 5 septins, Cdc3, Cdc10, Cdc11, Cdc12 and Sep7, form a cortical ring that defines the site for bud growth in early G1 phase (Warenda and Konopka, 2002). The septin ring resides at the mother-daughter neck throughout the cell cycle until the time of cytokinesis when it splits into two rings which disassemble during early G1 of the next cell cycle. Upon hyphal induction, septins first form a small cortical patch marking the site of germ tube emergence; and with the growth of the germ tube a fraction of septins localize persistently at the growing tip and another fraction forms a diffuse band that encircles the base of the germ tube. The basal band later disassembles. Upon entering the cell cycle, a septin ring is formed within the germ tube marking the site for future cytokinesis. This septin ring also splits into two rings at the time of cytokinesis which are however not disassembled like during the yeast growth (Asleson et al., 2001; Warenda and Konopka, 2002). To determine whether Nap1 colocalizes with septins, Nap1 was tagged with GFP at the C terminus by site-specific integration described in **Figure 4.2D**. I started the culture from G1 cells in GMM medium at 30°C or in GMM with 20% serum at 37°C, and collected cells at timed intervals for examination by fluorescence microscopy (**Fig. 4.5A**). In newly prepared small G1 cells, Nap1-GFP was seen as a faint cortical bar at one end of the cells, which is most likely the side view of a ring reminiscent of the old septin rings from the previous cell cycle as described in **Chapter 3**. With the growth of the G1 cells, the old ring gradually disappeared in ~60 min. At ~90 min, Nap1-GFP was found to form a new ring at the cortical site from which the bud later emerged. Like septins, the Nap1-GFP ring localized at the mother-daughter neck and split into two rings around the time of cytokinesis before

gradually disappearing in G1 of the next cell cycle (**Fig. 4.5A**). Slightly different from the septins, some Nap1 molecules remained at the bud tip forming a faint cap through most of the cell cycle. Upon serum induction, Nap1-GFP localized strongly to the tip of the germ tube and later faintly to the base of the germ tube (**Fig. 4.5A**). Together, the results show that the behavior and localization of Nap1-GFP are very similar to those of the septins, indicating their colocalization. Effort to Tag a septin and Nap1 with different fluorescent proteins were not successful because the signal of RFG or mCherry was extremely weak in *C. albicans*. However, I was able to detect coimmunoprecipitation of Nap1 with septins, consistent with their colocalization **(**see **Fig.4.6A)**.

In *Saccharomyces cerevisiae*, Nap1 has been shown to possess a nuclear export signal (NES) (**Fig. 4.1**) that facilitates nucleocytoplasmic shuttling of the protein. Deletion of the NES sequence sequesters the protein in the nucleus and results in Clb2-dependent mitotic delay (Miyaji-Yamaguchi et al., 2003). Since no nuclear localization of Nap1-GFP was observed throughout the cell cycle, next I examined whether there is any role of a putative nuclear localization signal (NLS) and nuclear export signal (NES) in *C. albicans* by creating NLSΔ and export deficient mutants. After deleting the putative NLS, the mutated Nap1 could largely rescue the phenotypes observed in *nap1*Δ cells (**Fig. 4.5B**). A moderate increase in the cytoplasmic localization for $Nap1^{NLS\Delta}$-GFP was observed compared to WT Nap1-GFP. The export deficient strain was constructed by mutating Leu98 and Leu102 to Ser in the NES. After integrating the mutant version of *NAP1* back to *nap1*Δ cells, filamentous growth was almost completely rescued and mutated Nap1 localized clearly to the neck region (**Fig. 4.5B**). Less than 20% cells showed enhanced nuclear fluorescence, suggesting that NES has little effect in

determining the Nap1 localization. Together, the data support the idea that in *C. albicans* the localization of Nap1 to the nucleus is very weak or transient and that the defects caused by *NAP1* deletion have little to do with its nuclear function.

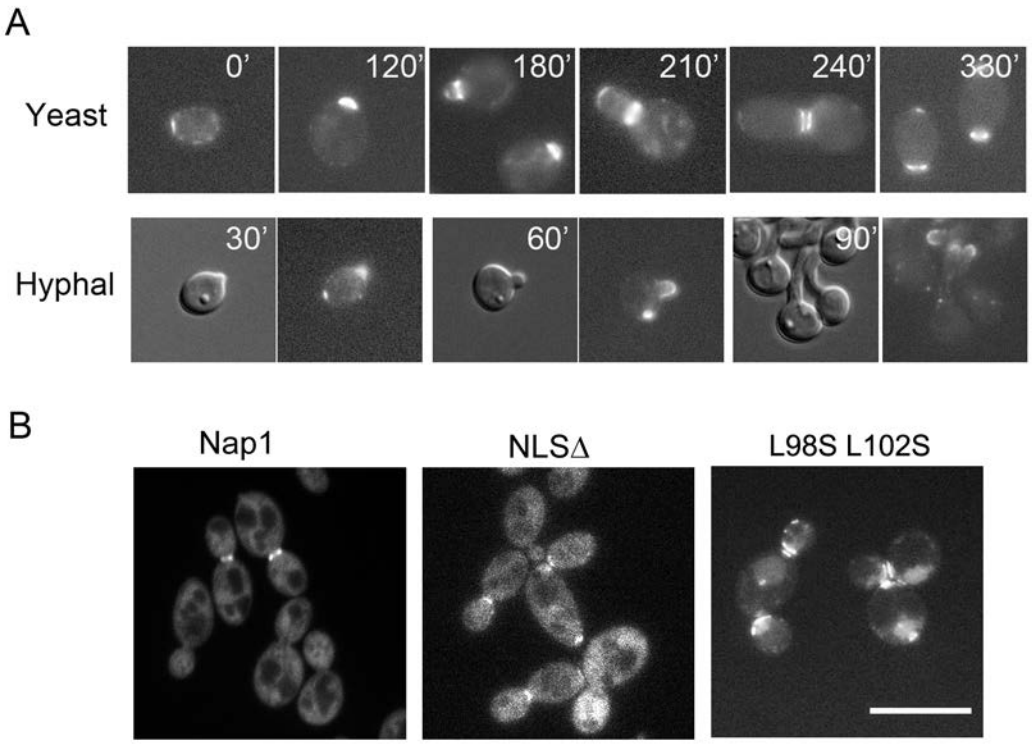

Figure 4.5 Nap1-GFP subcellular localization in yeast and hyphal cells

(A) Elutriated G1 cells expressing Nap1-GFP were released to GMM at 30°C and GMM containing 20% serum at 37°C. (B) Nap1 with NLSΔ and export deficiency could still localize to the bud neck. Cells were grown to the same OD. Bar = 10 μm.

4.3.3 Physical interaction of Nap1 with the septin complex

To confirm the physical association of Nap1 with the septins and the septin-associated kinase Gin4, co-immunoprecipitation was performed as described in **Chapter 2.6.3**. Strains were constructed coexpressing HA-tagged Nap1 with Myc-tagged Gin4 or HFM (His-Flag-Myc)-tagged Cdc3. A strain expressing Nap1-HA alone was used as a negative control. Overnight cultures were reinoculated into fresh media and grown to log phase. Nap1 was pulled down with anti-HA beads and the precipitation products were probed with anti-Myc antibodies in western blotting. **Figure 4.6A** shows that Nap1 physically associates with both Gin4 and Cdc3. This is consistent with the colocalization of Nap1 with the septins. Thus, like in *S. cerevisiae*, Nap1 interacts with the septin complex in *C. albicans*.

4.3.4 Nap1 subcellular localization depends on septins and the septin-associated kinase Gin4

Next I wanted to determine whether Nap1 localization depends on septins. Previous studies have shown that while the septin genes *CDC3* and *CDC12* are essential, *cdc10*Δ and *cdc11*Δ mutants are viable but display a diffuse and unstable septin ring at higher temperatures (Warenda and Konopka, 2002). Numerous studies in *S. cerevisiae* and *C. albicans* have demonstrated the importance of Gin4 in septin assembly and organization (Bouquin et al., 2000; Carroll et al., 1998; Dobbelaere et al., 2003; Longtine et al., 1998; Longtine et al., 2000; Mortensen et al., 2002; Wightman et al., 2004). Therefore, Nap1-GFP localization was examined in the *cdc10* Δ and *cdc11*Δ mutants and in a strain that allows the shutdown of *GIN4*. Western blotting showed that the Nap1-

GFP level in the three mutants was comparable to that in WT cells. However, Nap1 exhibited complete mislocalization in all three mutants (**Fig. 4.6B**), indicating that Nap1's subcellular localization depends on the integrity of the septin complex.

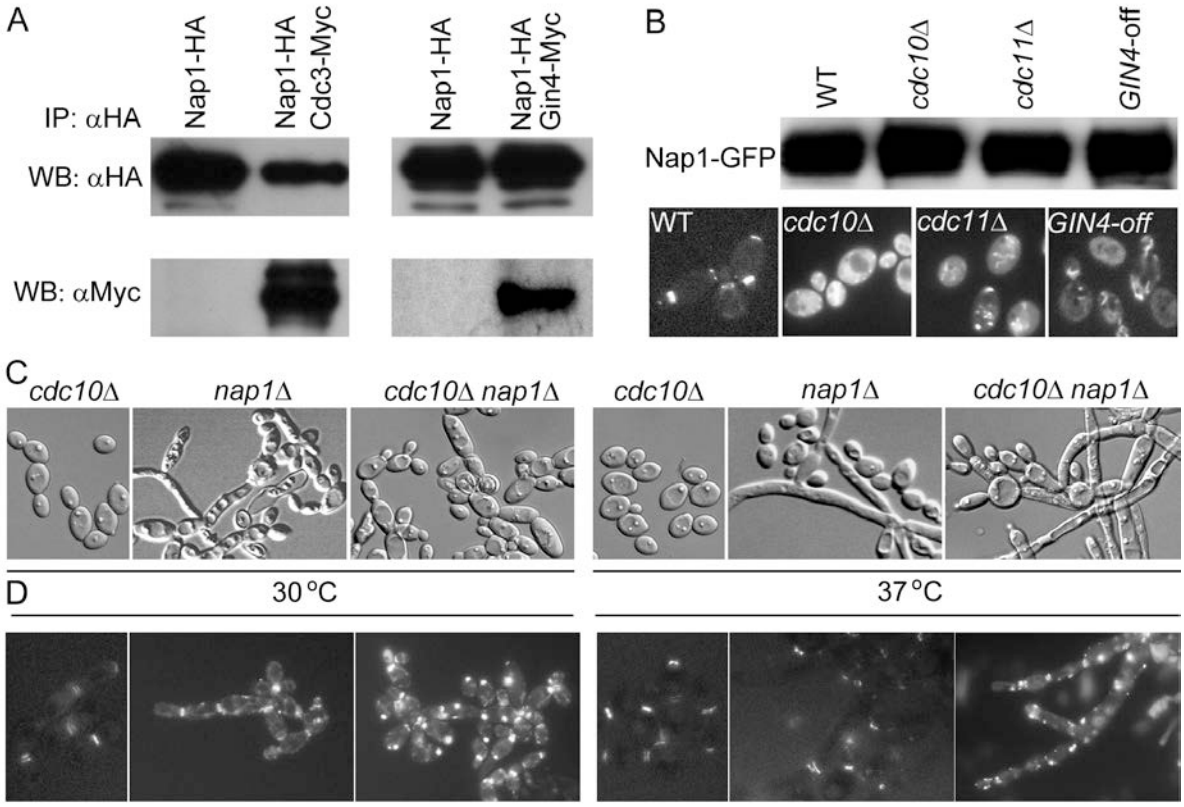

Figure 4.6 Nap1 interacts with septins both physically and genetically

(A) Nap1 was pulled down with anti-HA antibody-conjugated beads. Cdc3 and Gin4 were detected with anti-Myc antibody in western blot analysis. (B) Nap1-GFP localization was lost in *cdc10*Δ, *cdc11*Δ and *GIN4*-shutoff strains. For WB analysis, same amount of protein lysates were loaded from each strain. (C) *cdc10*Δ, *nap1*Δ and *cdc10*Δ *nap1*Δ cells were grown in YPD at the indicated temperatures to the same OD and

morphologies were examined. (D) Cdc3 was tagged with GFP at the C terminus in *cdc10*Δ, *nap1*Δ and *cdc10*Δ *nap1*Δ cells. After overnight culturing at the indicated temperatures, Cdc3-GFP localization was examined.

4.3.5 Genetic interaction between *NAP1* and *CDC10*

To gain more evidence that Nap1 functions through interactions with the septins, I next examined the genetic interaction between *NAP1* and the septin gene *CDC10*. *CDC10* is nonessential and its deletion only causes weak morphological defects and minor perturbations to the septin ring at 30°C (Warenda and Konopka, 2002). I constructed a *cdc10*Δ *nap1*Δ double mutant and found that, at 37°C, although some separate yeast cells were present in the culture, many cells became highly elongated, forming intertwining filaments that easily formed precipitates in liquid media (**Fig. 4.6C**). At 30°C, 50% of the cells grew in the pseudohyphal form, with some exhibiting a wide bud neck with a poorly defined mother-daughter junction (**Fig. 4.6C**).

To examine the septin structures, I tagged Cdc3 with GFP in the *cdc10*Δ *nap1*Δ mutant. Similar to the *nap1*Δ cells (see **Fig. 4.7A**), at both 30 and 37°C, Cdc3-GFP was found to be severely mislocalized, forming a range of random abnormal structures in the cortex not seen in the *cdc10*Δ mutants, including dots, patches, filaments and rings (**Fig. 4.6D**). At 37°C, while Cdc3-GFP could localize to the neck region of *nap1*Δ mutants, only a small percentage of *cdc10*Δ *nap1*Δ cells showed a septal GFP signal.

Taken together, the results clearly demonstrate that the *cdc10*Δ *nap1*Δ mutant has a range of defects that are either stronger than those or do not exist in either one of the

single-gene mutants. This genetic interaction indicates that Nap1 and septins are involved in the same cellular processes through parallel pathways.

4.3.6 Deleting *NAP1* causes severe defects in septin localization and organization

The data above have shown that Nap1 associates with the septin complex. Next, I wanted to investigate the role of Nap1 in septin localization, organization and dynamics. To this end, I tagged Cdc3 with GFP at the C-terminus in the *nap1*Δ mutant. In asynchronous cultures, although Cdc3 was seen to localize to the bud neck and split at the time of cytokinesis in some cells, it also localized as numerous small patches or short bars randomly distributed throughout the entire cortex in many cells (**Fig. 4.7A**). To investigate Cdc3 mislocalization in more detail, I examined Cdc3 localization in synchronized yeast cultures. In newly prepared early G1 cells, Cdc3-GFP appeared as a cortical ring in both WT and *nap1*Δ strains. These rings are the old septin rings from the previous cell division which disassembled within 60 min. When the cells were approaching the time of budding, random small cortical septin patches started to appear in both WT and *nap1*Δ cells (see **Fig. 4.7B,** 2h). However, the percentage of cells with 2 or more such patches was ~50% in the *nap1*Δ mutant compared with ~10% in the WT (n = 50). Suspecting that these random septin patches might behave differently in *nap1*Δ cells than in WT cells, I performed time-lapse microscopy on living cells, taking images at 2-5 min intervals and with 8 Z-stack sections at each time point. I found that the random septin patches moved rapidly in the cortex in G1 and completely disappeared at the time of the septin ring formation in all WT cells. In contrast, many septin patches persisted throughout the entire cell cycle in *nap1*Δ cells (**Fig.4.7C**). New cortical septin patches were also formed in later stages of the cell cycle in *nap1*Δ cells but never seen in

WT cells (**Fig.4.7D** arrows), and this happened only in the mother cell (**Fig.4.7A** arrows indicate daughter cells). The results suggest that Nap1 plays an important role in the temporal and spatial control of assembly and disassembly of septin structures during the cell cycle. Although assembly of random cortical septin patches also occurs in WT cells during G1, it is evident that mechanisms exist to disassemble them once the septin ring is formed at the presumptive budding site.

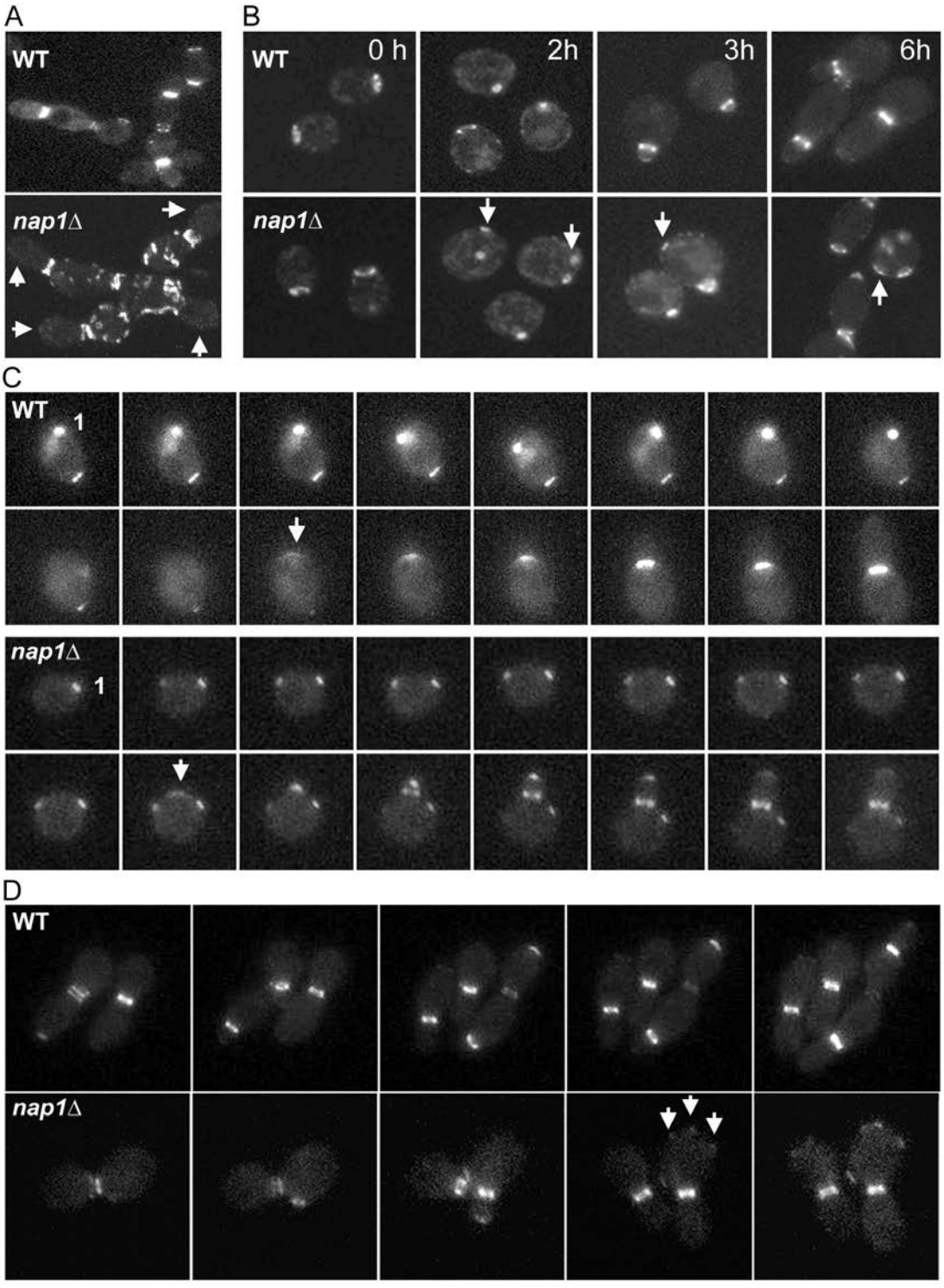

Figure 4.7 Cdc3 GFP localization in *nap1*Δ mutants

(A) Cdc3-GFP formed random patches in *nap1*Δ mother cells only. Arrows indicate daughter cells. (B) Time-course microscopic examination of elutriated G1 cells of WT and *nap1*Δ at 30°C. Arrowheads indicate mislocalization of Cdc3. (C) Time-lapse microscopic images of a single G1 cell of WT and *nap1*Δ at 30°C. (D) Time-lapse microscopic images of budding cells of WT and *nap1*Δ. Arrows indicate the formation of random cortical patches.

I next investigated whether the deletion of *NAP1* affects the dynamics of the septin ring. The 5 stages of dynamics of yeast septin complexes have been discussed in **Chapter 1**. In *C. albicans*, septin ring dynamics has been reported to be consistent with that in the budding yeast (González-Novo et al., 2008). Mainly, cells with a small bud or split rings showed no recovery of Cdc3-GFP after photo-bleaching, whereas in unbudded cells or cells with a single ring or cells undergoing ring splitting the septin complexes are more dynamic than in other stages (Dobbelaere et al., 2003). Here, I collected both WT and *nap1*Δ cells with a single Cdc3-GFP ring to compare the full-ring fluorescence recovery after photo bleaching (FRAP).

Fluorescence scanning was done every 60 seconds for a period of 300 seconds after bleaching. After analyzing the fluorescence intensity with the program ImageJ, a clear difference in Cdc3-GFP recovery rate was seen between the WT and *nap1*Δ mutants. **Figure 4.8** shows that Cdc3-GFP in WT cells achieved only 20% and 22% recovery of fluorescence at 50 and 300 sec respectively, while that in *nap1*Δ cells recovered by 30 and 40% at the same time points, indicating a higher exchange rate of Cdc3 molecules between the septin ring and the cytoplasmic pool in *nap1*Δ cells than in WT cells. It

suggests that the septin ring assembled in the absence of Nap1 is less stable and exchanges subunits with the cytoplasmic pool more frequently than a normal septin ring.

In summary, the results above indicate that Nap1 plays an important role in determining the localization, organization and dynamics of the septins in *C. albicans*.

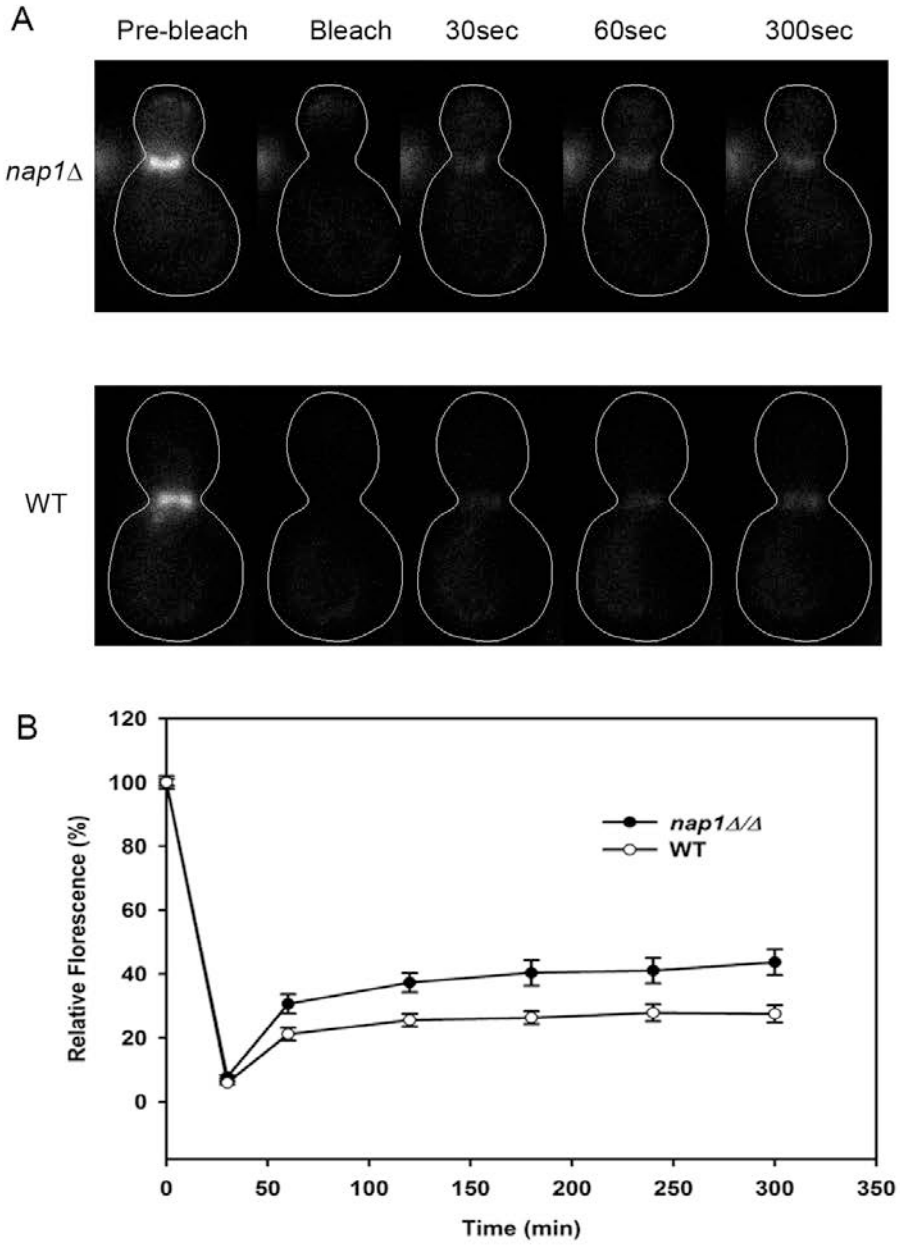

Figure 4.8 FRAP analysis of WT and *nap1*Δ mutants

(A) Cells were incubated at 30°C, and Cdc3 GFP full ring bleach was carried out. Images were taken at indicated time points. (B) Relative fluorescence recoveries were calculated using ImageJ. Error bar stands for 1 standard deviation between 3 triplicates of experiments. p value<0.05.

4.3.7 Cdc3 phospho-regulation is impaired in *nap1*Δ cells

As described in **Chapter 3**, Cdc3 undergoes cell-cycle-dependent phosphorylation, in which dephosphorylation coincides with the disassembly of old septin rings and re-phosphorylation with the assembly of new ones. Since *NAP1* deletion causes severe defects in septin organization and localization, I wondered whether the phospho-regulation of Cdc3 is affected as well. In asynchronous cultures, Cdc3 in *nap1*Δ mutants showed lower intensity in the hyper-phosphorylated end compared to that in WT (**Fig. 4.9A**). To further address this question, I prepared *nap1*Δ G1 cells that express Cdc3-GFP to start a synchronous yeast culture at both 30 and 37°C. Aliquots of cells were harvested at 0, 60, 120, 180 and 270 min followed by 2D WB analysis in which Cdc3 was detected with anti-GFP antibodies. The phosphorylation pattern of Cdc3 in *nap1*Δ cells was compared with that in WT cells. At 0 min, 7 spots of Cdc3 were detected in the *nap1*Δ cells in contrast to 10 spots in the WT cells (**Fig. 4.9B**). At 30°C, Cdc3 dephosphorylation was near the peak at 60 min in both WT and *nap1*Δ cells although it appeared to be moderately stronger in the mutant cells. At 120 min, a significant difference was observed in the abundance of different isoforms between the WT and *nap1*Δ cells: the least phosphorylated Cdc3 isoforms were much more abundant in the *nap1*Δ cells than in the WT cells. The same experiment was repeated at 37°C at which the *nap1*Δ mutant shows a stronger phenotype. Strikingly, in the *nap1*Δ mutants, the strong dephosphorylation of Cdc3 that normally occurs at 60 min was nearly completely blocked, and its rephosphorylation between 60 and 180 min was drastically enhanced with all the 5 least phosphorylated isoforms being undetectable at 180 min. Together, the results indicate that Nap1 plays a critical role in determining the cell-cycle-dependent

phosphorylation and dephosphorylation of Cdc3, thus influencing the structure and function of the septins.

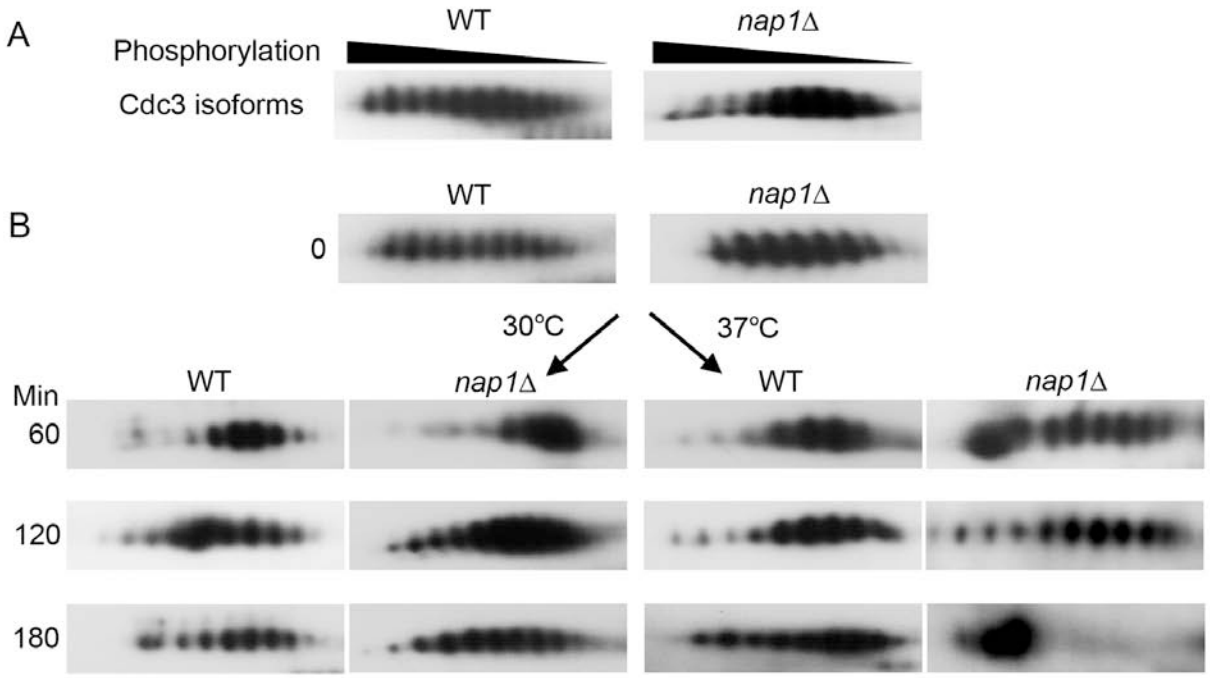

Figure 4.9 Impaired Cdc3 phosphorylation in *nap1*Δ mutants

(A) Phosphorylation pattern of Cdc3 in asynchronous WT and *nap1*Δ cells at 30°C. RThe pattern of phosphatase-treated Cdc3 can be found in **Fig. 3.1**. (B) Phosphorylation pattern of Cdc3 in WT and *nap1*Δ Cells at 30°C and 37°C. Elutriated G1 cells were released into GMM for growth at 30°C or 37°C and aliquots of cells were collected at the indicated time points. Cdc3 spots were aligned by the position of protein markers.

4.3.8 FCF treatment stabilizes septin structure in *NAP1* deleted cells

Forchlorfenuron (FCF) is a small-molecule drug used in agriculture as a cytokinin. It has been reported to induce abnormal septin fiber assembly by suppressing septin dynamics and stabilizing septin polymers in both yeast and mammalian cells. Since the FRAP results from **Fig. 4.8** demonstrated that the septin ring in *nap1*Δ is less stable, I wanted to determine whether FCF could ameliorate the defects of the *NAP1* deletion. Treatment of WT cells with 25 μM FCF indeed caused formation of thick septin filaments in the cell periphery similar to observations made in *S. cerevisiae* and mammalian cells (DeMay et al., 2010; Hu et al., 2008; Iwase et al., 2004) (**Fig. 4.10A** arrowhead). However, the cells were able to go through the cell cycle without significant problems other than a slight delay in budding. Interestingly, treatment of *nap1*Δ G1 cells with 25 μM FCF blocked the germ-tube-like growth induced by incubation at 37°C in YPD and the cells were able to produce normal-looking buds (**Fig. 4.10B**); and highly elongated cells were not observed in the culture after overnight growth in the presence of FCF, although moderate cell swelling and cytokinesis/cell separation defects were obvious (**Fig. 4.10B**). However, the random cortical localization of Cdc3 was still observed in *nap1*Δ mutants at both 30 and 37°C. The results suggest that FCF's interaction with the septins may have improved the structure and function of the septin ring at the neck, thus suppressing the aberrant polarized growth in *nap1*Δ cells. The effect of the septin-specific drug on *nap1*Δ cells also suggests that septin defects be primarily responsible for the morphological abnormalities in the *nap1*Δ mutant. Interestingly, FCF treatment of cells under hyphal-induction conditions, caused the formation of multiple

short surface protrusions and prevented normal hyphal growth in both WT and *nap1*Δ cells (**Fig. 4.10C**).

I next examined whether the FCF treatment restored Cdc3 phosphorylation in *nap1*Δ G1 cells and thus suppressed the morphological defects. To answer this question, I obtained *nap1*Δ G1 cells by elutriation and released them into medium containing 25 μM FCF at 37°C and collected samples at timed intervals for 2D WB analysis. The result in **Figure 4.10D** shows that FCF treatment did not change the pattern of Cdc3 phosphorylation in *nap1*Δ cells under this condition. The data suggest that FCF's interaction with the septins might be able to bypass the damaging effect from the loss of *NAP1* without restoring the Cdc3 phosphoregulation and preventing Cdc3 cortical deposits.

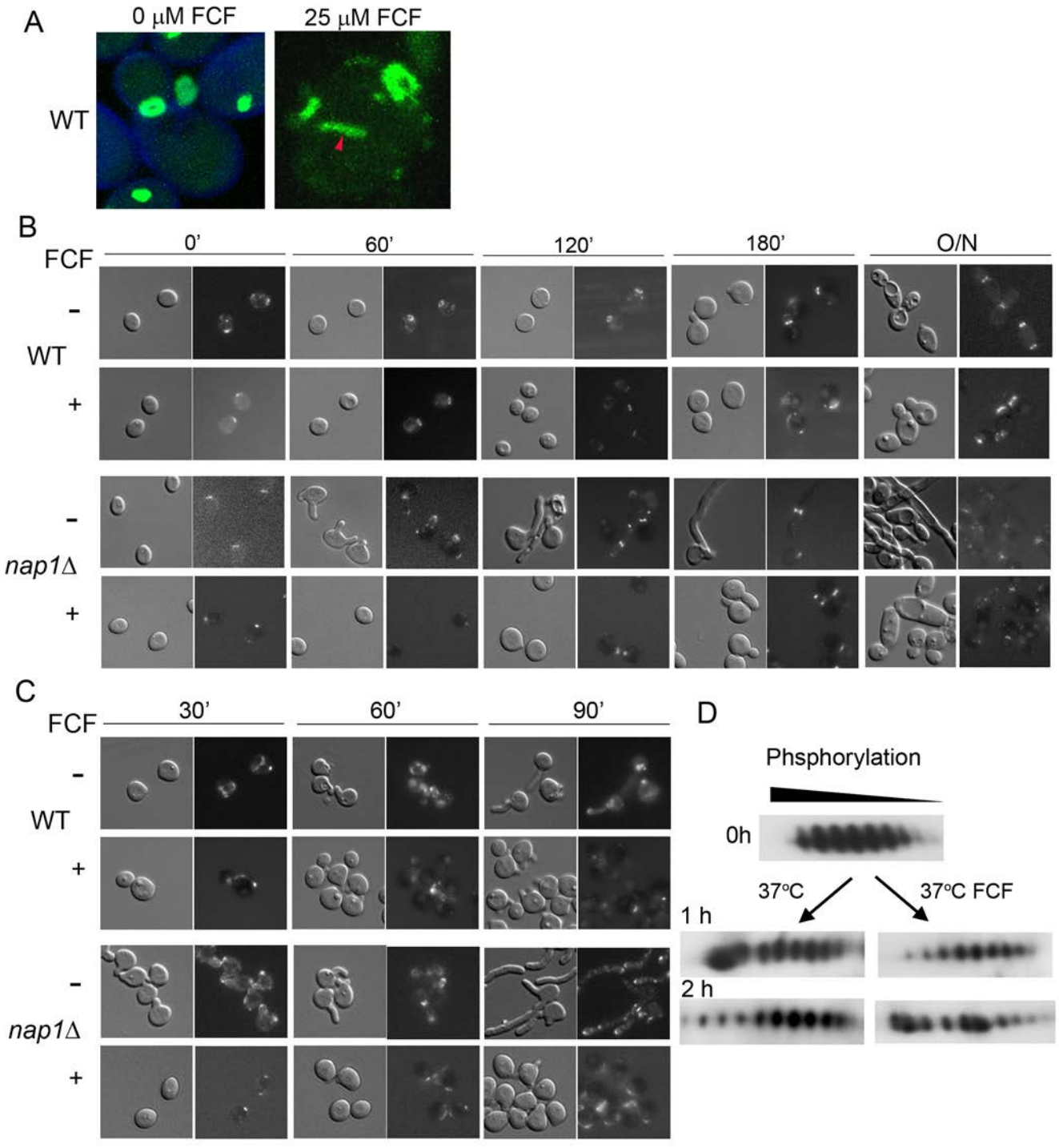

Figure 4.10 FCF treatment can partially restore the defects in *nap1*Δ cells

(A) Asynchronous WT cells before and after treatment with 25 μm FCF at 30°C in YPD. Green fluorescence indicates Cdc3-GFP. Blue fluorescence indicates cell wall. Red arrowheads indicate Cdc3 filaments. (B) WT and *nap1*Δ G1 cells treated with 25 μm FCF at 37^{o}C in YPD. Aliquots of cells were collected at the indicated time points. (C) WT and *nap1*Δ G1 cells were treated with 25 μm FCF at 37°C in YPD with 20% serum. Aliquots of cells were collected at indicated time points. (D) 2D WB of Cdc3 in *nap1*Δ G1 cells at 37°C in YPD with or without 25 μm FCF. Aliquots of cells were collected at indicated time points.

4.4 Phosphorylation of Nap1 is critical for its function in septin organization

4.4.1 Nap1 is a phospho-protein

Previous data in *S. cerevisiae* showed that Nap1 is a substrate of Casein Kinase 2 (Calvert et al., 2008). To test whether Nap1 is a phospho-protein, immunoprecipitated Nap1 was subjected to 2D WB analysis. **Figure 4.11A** shows that the untreated Nap1 yielded 6 spots, while the λ phosphatase treatment abolished 4 of the 6 spots and generated a strong spot near the basic end of the gel, consistent with dephosphorylation of Nap1 (Sinha et al., 2007). The two spots resistant to λ phosphatase may be due to other types of protein modifications.

To identify the phosphorylated residues in Nap1, 1L overnight culture of cells expressing HA-tagged Nap1 was harvested and immunopurified using anti-HA beads. The band corresponding to Nap1-HA on SDS-PAGE was excised and subjected to mass spectrometry (MS) phospho-mapping. The mapping results showed phosphorylation on 12 serine and threonine residues. Interestingly, 10 of the phospho-residues are clustered

within the first 60 amino acids at the N terminus (**Fig. 4.11B**). Mutational replacement of the 10 Ser/Thr residues with Ala abolished most of the Nap1 phospho-isoforms on 2D WT (**Fig. 4.11A, bottom panel**).

Together, I have demonstrated that Nap1 is a phosphoprotein, and its phosphorylation mainly occurs near the N terminal end.

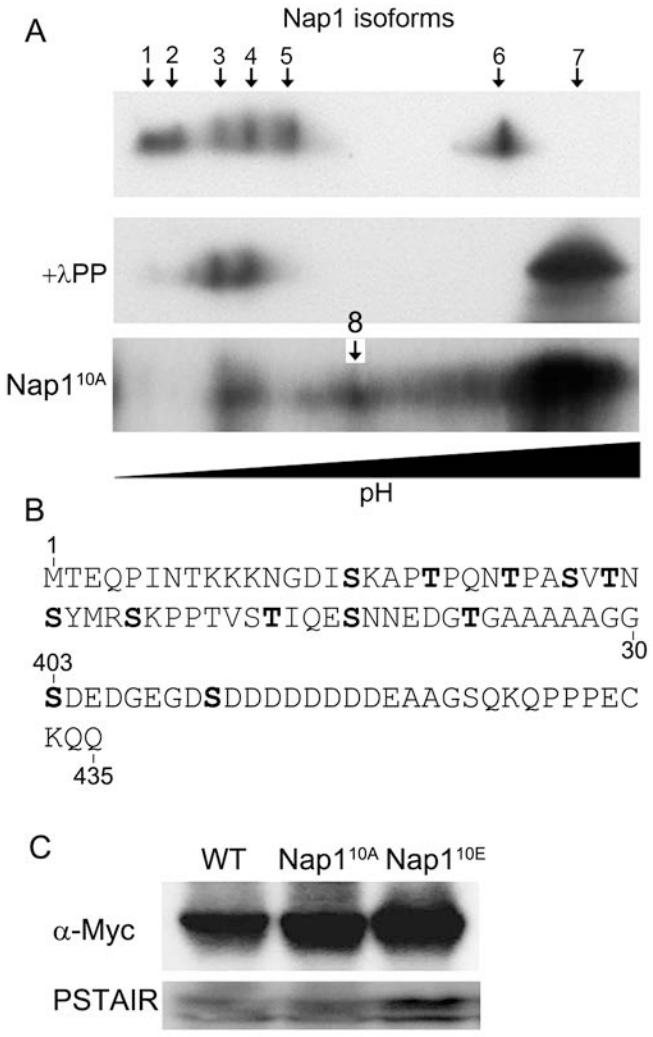

Figure 4.11 Nap1 is a phospho-protein

(A) 2D WB analysis of immuneprecipitated Nap1-HA with or without λ phosphatase treatment and Nap1^{10A}. (B) MS phosphomapping of Nap1 identified 12 phospho-Ser and Thr residues which are indicated in bold. (C) WB analysis of Nap1-Myc, Nap1^{10A}-Myc and Nap1^{10E}-Myc. Cdc28 was used as loading control.

4.4.2 Nap1 phosphorylation status affects cell morphology

What is the physiological significance of Nap1 phosphorylation? To address this question, I mutated all 10 Ser and Thr residues in the N terminus to either the unphosphorylatable Ala (A) or the phosphomimetic glutamic acid (E). The mutated versions of *NAP1* were integrated into the *nap1*Δ mutant at the native promoter. Western blot analysis confirmed that Nap1 proteins were expressed to comparable levels (**Fig. 4.11C**) **Fig. 4.11A**). Microscopic examination of cells grown at 30°C and 37°C showed that the $nap1^{10A}$ allele could partially rescue the filamentous phenotype of the *nap1*Δ mutant: both the percentage of elongated cells and the degree of cell elongation were significantly reduced (**Fig. 4.12A**). The $nap1^{10A}$ allele also abolished the germ-tube like growth of the *nap1*Δ mutant at 37°C, although 30% of the cells generated a highly elongated bud. In comparison, the $nap1^{10E}$ cells exhibited rather normal yeast growth at both temperatures except a moderate degree of cell enlargement. Together, the results suggest that Nap1 phosphorylation has a role in determining the cell shape.

I next examined the cellular localization of GFP-tagged $Nap1^{10A}$ and $Nap1^{10E}$. $Nap1^{10E}$ exhibited generally the same localization pattern as the WT Nap1 through the cell cycle except that $Nap1^{10E}$ also showed random cortical localization in the form of patches and small circles (**Fig. 4.12B**). In comparison, $Nap1^{10A}$ exhibited a strong and largely even cytoplasmic localization, although localization to the bud neck could be seen in some cells (**Fig. 4.12B** arrowheads); perhaps, the strong cytoplasmic signal obscured the bud neck signal. Taken together, the data indicate that Nap1 phosphorylation may have a role in regulating Nap1 localization.

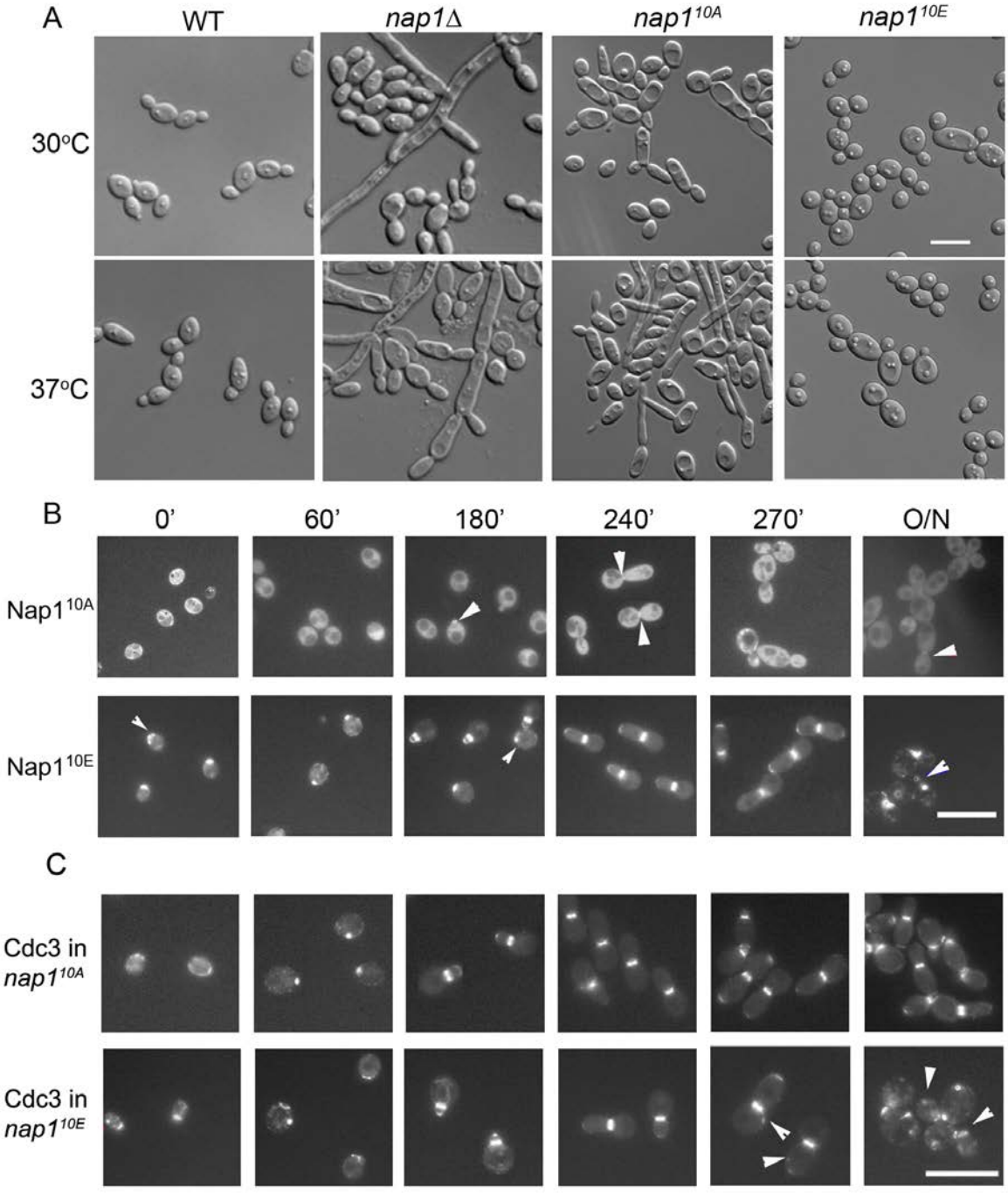
A
WT
nap1Δ
nap1^10A
nap1^10E
30°C
37°C
B
0'
60'
180'
240'
270'
O/N
Nap1^10A
Nap1^10E
C
Cdc3 in nap1^10A
Cdc3 in nap1^10E

Figure 4.12 Morphology of *nap1^{10A}* and *nap1^{10E}* mutants

(A) Cells of WT, *nap1*Δ, *nap1^{10A}* and *nap1^{10E}* strains were grown in YPD at 30 and 37°C overnight. (B) Localization of Nap1^{10A}-GFP and Nap1^{10E}-GFP through one cell cycle and in cells of an overnight culture. G1 cells were obtained and released into GMM for growth at 30°C. Aliquots of cells were collected at the indicated time points for fluorescence microscopy. Arrowheads in Nap1^{10A} panel indicate Nap1^{10A}-GFP signals at the bud neck. Arrowheads in Nap1^{10E} panel indicate Nap1^{10E}-GFP mislocalization. (C) Localization of Cdc3-GFP in *nap1^{10A}* and *nap1^{10E}* mutants. G1 cells were obtained and released to GMM for growth at 30°C. Aliquots of cells were collected at the indicated time points for fluorescence microscopy. Arrowheads in panel *nap1^{10E}* indicate abnormal Cdc3-GFP localization in *nap1^{10E}* cells. Bars = 10 μm.

4.4.3 Cdc3 localization is affected in *nap1^{10E}* mutants

Next I wanted to determine whether the 10A and 10E mutations of Nap1 affect septin localization by tagging Cdc3 with GFP in the mutants. I found that Cdc3-GFP localized normally in *nap1^{10A}* cells throughout the cell cycle at 30°C, exhibiting no increase in cytoplasmic localization like Nap1^{10A} itself (**Fig. 4.12C**). Interestingly, Cdc3 in *nap1^{10E}* cells formed numerous random cortical patches similar to Nap1^{10E}-GFP and Cdc3 in *nap1*Δ cells (**Fig. 4.12C**). The data suggests that Nap1 phosphorylation affects its own localization as well as that of the septins.

4.5 Discussion

In this chapter, I have introduced *C. albicans* ORF19.7501 as an orthologue of the Nucleosome Assembly Protein 1 (Nap1) of *S. cerevisiae*. Deletion of *NAP1* in *C. albicans* leads to filamentous and invasive growth. The increase of temperature exacerbates the severity of the abnormal growth. Nap1-GFP has never been observed in the nucleus, not even in the mutant in which the putative nuclear export signal is mutated. Thus, the defects of *nap1*Δ mutants are unlikely due to the loss of its nuclear function. Nap1 is a component of the septin complex and plays a role in its organization and localization. Disturbance of the septin structure by deletion of *CDC10* or *CDC11* or shutoff of *GIN4* expression all abolishes the neck localization of Nap1. *NAP1* also interacts with *CDC10* genetically, since deletion of the two genes together results in more severe defects than deletion of any individual gene. Absence of Nap1 causes an increase in septin ring dynamics and formation of random Cdc3 patches and partial circles in the cell cortex. The observation that delocalization of Cdc3 only occurs in mother cells but

not in daughter cells of the *nap1*Δ mutant suggests defects in the disassembly of the old ring and/or septins' higher propensity for aggregation in the mother cell. Time-lapse microscopic studies indicate that both occur. Cdc3 rephosphorylation, which coincides with the new ring assembly, is impaired in *nap1*Δ cells.

4.5.1 The defects of the *nap1*Δ mutant is not due to the loss of its nuclear functions

Although Nap1 was originally identified to be a histone assembly protein in *S. cerevisiae*, deletion of the gene only causes mild cell elongation (Longtine et al., 2000). Deletion or mutation of its NES prevents its cytoplasmic localization, thus resulting in mitotic delay in a mitotic cyclin-dependent manner (Miyaji-Yamaguchi et al., 2003). The findings in the budding yeast confirm that Nap1 plays many roles outside the nucleus through its numerous binding partners (Zlatanova et al., 2007). In *C. albicans*, I found that similar to the budding yeast, Nap1 does not show detectable nuclear localization at any stage of the cell cycle. Deletion of NLS or disruption of NES has little effect on Nap1 localization or the cell morphology. Thus, it is likely that the majority of Nap1 protein does not enter the nucleus and its nuclear function, if any, is minimal.

4.5.2 Nap1's role in filamentous growth

Previous studies in *S. cerevisiae* have demonstrated the involvement of Nap1 in septin organization through Gin4, because Gin4 cannot localize to the bud neck in the absence of *NAP1* (Altman and Kellogg, 1997; Okuzaki et al., 1997). This was later supplemented by the possibility that Nap1 affects septin organization directly which in turn ensures an efficient recruitment of Gin4 to the bud neck (Longtine et al., 2000). In *C.*

albicans, the senario is quite different since deletion of *GIN4* results in complete disruption of septin complex organization (unpublished results in Dr. Yue Wang laboratory) and loss of Nap1 neck localization. Therefore, in *C. albicans* Gin4 most likely works upstream of septins and Nap1 as a master regulator.

In this work, I demonstrated that *NAP1* deleted cells are more prone to hyphal induction and form constitutive pseudohyphae under conditions for yeast growth. This filamentous growth phenotype is likely caused by destabilized septin structures in the absence of *NAP1*. This model is supported by results of FCF treatment of *nap1*Δ cells. The FCF-induced septin stability can restore normal budding and largely rescues the pseudohyphal morphology in *nap1*Δ cells. FRAP results also demonstrated a more rapid exchange of Cdc3 between cytoplasm and the septin complex at the neck. Therefore, the data suggest that Nap1 is involved in the regulation of the septin ring by stabilizing the septin structure. The involvement of septins in polarized growth has been implicated in numerous studies in mammalian cells, *S. cerevisiae* and *C. albicans* (Spiliotis et al., 2008; Roemer et al., 1996; Bi et al., 2000; Gladfelter et al., 2005; Gale et al., 2001; Luedeke et al., 2005; Li et al., 2007). Previous studies by Li et al. (2007) proposed that in *C. albicans* and *S. cerevisiae* septins mainly localize to two sites where cell growth happens: amorphous aggregation at the bud tip and highly organized septin rings at the bud neck. There is evidence that septins have an intrinsic ability to attract secretory vesicles to direct polarized growth. Septins at the hyphal tip or bud tip participate in attracting exocytosis to drive tip extension, while septins at the bud neck attract exocytosis for growth in the region adjacent to the neck. Septins at the tip dominate during hyphal growth, while the neck septins prevail during yeast growth. Thus, the balance between

the two septin pools plays an important role in determining whether daughter cells will grow apically or isotropically. Since septins at the neck are known to form highly organized structures while those at the tip aggregate in an amorphous manner, the neck septins and its ability to attract exocytosis are more sensitive to disruptions than the septins at the tip. This explains why nearly all mutations affecting septins cause bud elongation in both *C. albicans* and *S. cerevisiae*. In this study, I have shown that Nap1 colocalizes and coprecipitates with septins and that deleting *NAP1* causes mislocalization of septins. Therefore, the constitutive filamentous growth and enhanced sensitivity to hyphal induction in *nap1*Δ cells is most likely the result of impairment in septin organization and function.

4.5.3 Nap1 regulates Cdc3 localization and phosphorylation

In addition to constitutive filamentous growth, deletion of *NAP1* also affects Cdc3 localization and phosphorylation. In *nap1*Δ mutants, Cdc3 forms random cortical patches both before bud emergence and during bud enlargement. Cdc3 also forms similar patches in WT cells before bud emergence but at a lower frequency, and importantly most of these patches are disassembled prior to successful assembly of the septin ring at the presumptive budding site. Interestingly, these random cortical patches are not seen during bud enlargement in WT cells. These observations indicate that WT cells have a mechanism that disassembles ectopically formed cortical septin patches and prevents their formation during bud expansion. My data suggest that Nap1 is an important component of this mechanism.

As demonstrated in **Chapter 3**, Cdc3 undergoes cell cycle dependent phosphorylation, and constitutive phosphorylation at S422 mimicked by substitution with Glu severely impairs septin organization and function. Interestingly, I observed that deletion of *NAP1* strongly affects Cdc3 phosphorylation particularly at 37°C where Cdc3 exhibits significantly enhanced phosphorylation accompanied by strong phenotypic defects. Thus, I propose that Nap1 plays an important role in septin assembly/disassembly and organization by regulating Cdc3 phosphorylation during the cell cycle.

Consistent with the findings in *S. cerevisiae* (Calvert et al., 2008), CaNap1 is also a phospho-protein. Mass spectrometry analysis revealed 10 phospho-Ser/Thr residues that are clustered within the first 60 amino acids in the N-terminal end. Mutating the 10 residues to non-phosphorylatable Ala abolishes Nap1's localization at the bud neck and causes filamentous growth, while mutating the 10 residues to the phosphomimetic Glu results in random deposition of Cdc3 in the cell cortex but normal neck localization of Nap1. Thus, Nap1 phosphorylation not only controls its localization, but also different aspects of its function. The kinase(s) responsible for Nap1 phosphorylation has not been explored in this thesis. However, there are several candidates, such as the septin-associated kinases Gin4, Elm1 and Cla4 and casein kinase 2 (Calvert et al., 2008). This is certaily an important issue to be addressed to gain a full understandin of Nap1's role in the regulation of septins in future studies.

Chapter 5 Conclusion and Perspectives

5.1 Cdc3 project

In the Cdc3 project, I found that the *C. albicans* septin Cdc3 undergoes cell cycle dependent phosphorylation and that phosphorylation at a single amino acid S422 plays a critical role in determining septin organization and function. Cdc3 exhibits the highest level of phosphorylation in early G1 cells, followed by a period of dephosphorylation. After the cells traverse the START, Cdc3 phosphorylation increases gradually through the rest of the cell cycle and peaks around the time of cytokinesis. Phospho-mapping by mass spectrometry identified phosphorylation on several residues, and subsequent mutational studies indicated that phosphorylation on S422 may play a key role in regulating septin organization and stability. The phosphomimetic S422D mutation causes gross disorganization of septin structures, severe cytokinetic defects, dramatic cell elongation, and inability of Cdc3 to localize to the bud neck. The nonphosphorylatable S422A mutation causes a much weaker phenotype, and $Cdc3^{S422A}$ can localize to the bud neck although it also forms random cortical patches and circles. Coimmunoprecipitation experiments demonstrate that the S422D mutation greatly weakens Cdc11's association with the septin complex and causes premature dissociation of Cdc11 from the ring. I found that the septin-associated kinase Gin4 is involved in the phosphorylation of Cdc3, but it remains to be determined whether it includes S422. Using the analog-sensitive *cdc28as* mutant did not reveal any significant difference in Cdc3 phosphorylation between 1NM PP1-treated and untreated cells, indicating that Cdc28 is not involved. Interestingly, mutating S422 of Cdc3 to alanine causes disappearance of multiple phosphoisoforms, suggesting that phosphorylation of S422 may facilitate further

phosphorylation at other sites. Thus, S422 appears to be a major determinant of the overall phosphorylation level of Cdc3. The data from **Chapter 3** strongly supports that S422 serves as a critical site of control that regulates septin assembly/disassembly, organization and stability in a cell cycle dependent manner.

In the model I proposed in **Fig. 3.7**, Cdc3 phosphorylation and dephosphorylation, in which S422 is a key determinant, is temporally controlled during the cell cycle: it is phosphorylated in early G1, dephosphorylated in late G1 and rephosphorylated progressively throughout S, G2 and M phases until the time of cytokinesis when most Cdc3 molecules are phosphorylated.

This model not only offers a possible link between septin phosphorylation and behavior, but also incorporated the molecular event of Cdc11 dissociating from the septin ring triggered by the overall phosphorylation of Cdc3. Cdc3 phosphorylation causes disassembly of the long, cross-connected septin filaments in the old septin ring into short oligomers in early G1; and at the same time it also prevents premature assembly of septin oligomers into new rings. When cells approach the START, cell cycle signals trigger a rapid dephosphorylation of Cdc3, which removes the hindrance for septin oligomers to assemble into long, cross-connected filaments, thus forming a new ring at the presumptive bud site. After the cells have entered the cell cycle, rephosphorylation of Cdc3 occurs in a progressive manner and reaches the highest level near the end of M phase. The slow and progressive rephosphorylation of Cdc3 may be important for maintaining the stability and integrity of the septin structure during the cell cycle. Only when the overall phosphorylation level of Cdc3 rises above a threshold level, the septin structure will be significantly destabilized thus initiating the process of disassembly.

The search for the kinases and phosphatases was unsuccessful. The strategy adopted is by first searching for kinases and phosphatases whose activation time coincides with the phosphorylation and dephosphorylation of Cdc3. The deletion mutants of these genes with GFP labeled Cdc3 were generated afterwards. The phosphorylation profile of Cdc3 was then examined in these mutants and compared to that in WT. This method identified Gin4 as a potential kinase. After validating with in vitro kinase assay, the effect of Gin4 turned out to be secondary. The current searching method still revolves around the same cascade of experimental approach.

5.2 Nap1 project

In this project, I have introduced *C. albicans* ORF19.7501 as an orthologue of the Nucleosome Assembly Protein 1 (Nap1) of *S. cerevisiae*. Deletion of *NAP1* in *C. albicans* leads to filamentous and invasive growth. The increase of temperature exacerbates the severity of the abnormal growth. Nap1-GFP has never been observed in the nucleus, not even in the mutant in which the putative nuclear export signal is mutated. Thus, the defects of *nap1*Δ mutants are unlikely due to the loss of its nuclear function. Nap1 is a component of the septin complex and plays a role in its organization and localization. Disturbance of the septin structure by deletion of *CDC10* or *CDC11* or shutoff of *GIN4* expression all abolishes the neck localization of Nap1. *NAP1* also interacts with *CDC10* genetically, since deletion of the two genes together results in more severe defects than deletion of any individual gene. Absence of Nap1 causes an increase in septin ring dynamics and formation of random Cdc3 patches and partial circles in the cell cortex. The observation that delocalization of Cdc3 only occurs in mother cells but

not in daughter cells of the *nap1*Δ mutant suggests defects in the disassembly of the old ring and/or septins' higher propensity for aggregation in the mother cell. Time-lapse microscopic studies indicate that both occur. Cdc3 rephosphorylation, which coincides with the new ring assembly, is impaired in *nap1*Δ cells.

In this work, I first demonstrated that *NAP1* deleted cells are more prone to hyphal induction and form constitutive pseudohyphae under conditions for yeast growth. This filamentous growth phenotype is likely caused by destabilized septin structures in the absence of *NAP1*. I then showed that deletion of *NAP1* affects Cdc3 localization. In *nap1*Δ mutants, Cdc3 forms random cortical patches both before bud emergence and during bud enlargement. Cdc3 also forms similar patches in WT cells before bud emergence but at a lower frequency, and importantly most of these patches are disassembled prior to successful assembly of the septin ring at the presumptive budding site. Interestingly, these random cortical patches are not seen during bud enlargement in WT cells. These observations indicate that WT cells have a mechanism that disassembles ectopically formed cortical septin patches and prevents their formation during bud expansion. My data suggest that Nap1 is an important component of this mechanism. In addition to its effect on the localization of Cdc3, absence of *NAP1* also strongly affects the phosphorylation of Cdc3, especially at 37^{o}C. Therefore, it is evident that Nap1 plays an important role in septin assembly/disassembly and organization by regulating Cdc3 phosphorylation during the cell cycle.

References

Alonso-Monge, R., Navarro-García, F., Molero, G., Diez-Orejas, R., Gustin, M., Pla, J., Sánchez, M., and Nombela, C. (1999). Role of the mitogen-activated protein kinase Hog1p in morphogenesis and virulence of Candida albicans. J Bacteriol *181*, 3058-3068.
Altman, R., and Kellogg, D. (1997). Control of mitotic events by Nap1 and the Gin4 kinase. J Cell Biol *138*, 119-130.
Asano, S., Park, J.E., Yu, L.R., Zhou, M., Sakchaisri, K., Park, C.J., Kang, Y.H., Thorner, J., Veenstra, T.D., and Lee, K.S. (2006). Direct phosphorylation and activation of a Nim1-related kinase Gin4 by Elm1 in budding yeast. J Biol Chem *281*, 27090-27098.
Asleson, C.M., Bensen, E.S., Gale, C.A., Melms, A.S., Kurischko, C., and Berman, J. (2001). Candida albicans INT1-induced filamentation in Saccharomyces cerevisiae depends on Sla2p. Mol Cell Biol *21*, 1272-1284.
Barral, Y., Mermall, V., Mooseker, M.S., and Snyder, M. (2000). Compartmentalization of the cell cortex by septins is required for maintenance of cell polarity in yeast. Mol Cell *5*, 841-851.
Bensen, E.S., Clemente-Blanco, A., Finley, K.R., Correa-Bordes, J., and Berman, J. (2005). The mitotic cyclins Clb2p and Clb4p affect morphogenesis in Candida albicans. Mol Biol Cell *16*, 3387-3400.
Berman, J. (2006). Morphogenesis and cell cycle progression in Candida albicans. Curr Opin Microbiol *9*, 595-601.
Berman, J., and Sudbery, P.E. (2002). Candida Albicans: a molecular revolution built on lessons from budding yeast. Nat Rev Genet *3*, 918-930.
Bertin, A., McMurray, M.A., Grob, P., Park, S.S., Garcia, G., Patanwala, I., Ng, H.L., Alber, T., Thorner, J., and Nogales, E. (2008). Saccharomyces cerevisiae septins: supramolecular organization of heterooligomers and the mechanism of filament assembly. Proc Natl Acad Sci U S A *105*, 8274-8279.
Bertin, A., McMurray, M.A., Thai, L., Garcia, G., Votin, V., Grob, P., Allyn, T., Thorner, J., and Nogales, E. (2010). Phosphatidylinositol-4,5-bisphosphate promotes budding yeast septin filament assembly and organization. J Mol Biol *404*, 711-731.
Bishop, A., Lane, R., Beniston, R., Chapa-y-Lazo, B., Smythe, C., and Sudbery, P. (2010). Hyphal growth in Candida albicans requires the phosphorylation of Sec2 by the Cdc28-Ccn1/Hgc1 kinase. EMBO J *29*, 2930-2942.
Biswas, S., Van Dijck, P., and Datta, A. (2007). Environmental sensing and signal transduction pathways regulating morphopathogenic determinants of Candida albicans. Microbiol Mol Biol Rev *71*, 348-376.
Bloom, J., Cristea, I.M., Procko, A.L., Lubkov, V., Chait, B.T., Snyder, M., and Cross, F.R. (2010). Global analysis of CDC14 phosphatase reveals diverse roles in mitotic processes. J Biol Chem.
Bouquin, N., Barral, Y., Courbeyrette, R., Blondel, M., Snyder, M., and Mann, C. (2000). Regulation of cytokinesis by the Elm1 protein kinase in Saccharomyces cerevisiae. J Cell Sci *113 (Pt 8)*, 1435-1445.
Calderone, R.A., and Fonzi, W.A. (2001). Virulence factors of Candida albicans. Trends Microbiol *9*, 327-335.

Calvert, M.E., Keck, K.M., Ptak, C., Shabanowitz, J., Hunt, D.F., and Pemberton, L.F. (2008). Phosphorylation by casein kinase 2 regulates Nap1 localization and function. Mol Cell Biol *28*, 1313-1325.
Carlisle, P.L., and Kadosh, D. (2010). Candida albicans Ume6, a filament-specific transcriptional regulator, directs hyphal growth via a pathway involving Hgc1 cyclin-related protein. Eukaryot Cell *9*, 1320-1328.
Carroll, C.W., Altman, R., Schieltz, D., Yates, J.R., and Kellogg, D. (1998). The septins are required for the mitosis-specific activation of the Gin4 kinase. J Cell Biol *143*, 709-717.
Caudron, F., and Barral, Y. (2009). Septins and the lateral compartmentalization of eukaryotic membranes. Dev Cell *16*, 493-506.
Caviston, J.P., Longtine, M., Pringle, J.R., and Bi, E. (2003). The role of Cdc42p GTPase-activating proteins in assembly of the septin ring in yeast. Mol Biol Cell *14*, 4051-4066.
Chapa y Lazo, B., Bates, S., and Sudbery, P. (2005). The G1 cyclin Cln3 regulates morphogenesis in Candida albicans. Eukaryot Cell *4*, 90-94.
Cid, V.J., Adamiková, L., Sánchez, M., Molina, M., and Nombela, C. (2001). Cell cycle control of septin ring dynamics in the budding yeast. Microbiology *147*, 1437-1450.
Clemente-Blanco, A., González-Novo, A., Machín, F., Caballero-Lima, D., Aragón, L., Sánchez, M., de Aldana, C.R., Jiménez, J., and Correa-Bordes, J. (2006). The Cdc14p phosphatase affects late cell-cycle events and morphogenesis in Candida albicans. J Cell Sci *119*, 1130-1143.
Crampin, H., Finley, K., Gerami-Nejad, M., Court, H., Gale, C., Berman, J., and Sudbery, P. (2005). Candida albicans hyphae have a Spitzenkörper that is distinct from the polarisome found in yeast and pseudohyphae. J Cell Sci *118*, 2935-2947.
Damagnez, V., and Cottarel, G. (1996). Candida albicans CDK1 and CYB1: cDNA homologues of the cdc2/CDC28 and cdc13/CLB1/CLB2 cell cycle control genes. Gene *172*, 137-141.
Davis, D., Wilson, R.B., and Mitchell, A.P. (2000). RIM101-dependent and-independent pathways govern pH responses in Candida albicans. Mol Cell Biol *20*, 971-978.
De Virgilio, C., DeMarini, D.J., and Pringle, J.R. (1996). SPR28, a sixth member of the septin gene family in Saccharomyces cerevisiae that is expressed specifically in sporulating cells. Microbiology *142 (Pt 10)*, 2897-2905.
De Wulf, P., Montani, F., and Visintin, R. (2009). Protein phosphatases take the mitotic stage. Curr Opin Cell Biol *21*, 806-815.
DeMay, B.S., Meseroll, R.A., Occhipinti, P., and Gladfelter, A.S. (2010). Cellular requirements for the small molecule forchlorfenuron to stabilize the septin cytoskeleton. Cytoskeleton (Hoboken) *67*, 383-399.
Dobbelaere, J., and Barral, Y. (2004). Spatial coordination of cytokinetic events by compartmentalization of the cell cortex. Science *305*, 393-396.
Dobbelaere, J., Gentry, M.S., Hallberg, R.L., and Barral, Y. (2003). Phosphorylation-dependent regulation of septin dynamics during the cell cycle. Dev Cell *4*, 345-357.
Dong, A., Zhu, Y., Yu, Y., Cao, K., Sun, C., and Shen, W.H. (2003). Regulation of biosynthesis and intracellular localization of rice and tobacco homologues of nucleosome assembly protein 1. Planta *216*, 561-570.

Egelhofer, T.A., Villén, J., McCusker, D., Gygi, S.P., and Kellogg, D.R. (2008). The septins function in G1 pathways that influence the pattern of cell growth in budding yeast. PLoS One *3*, e2022.
Eisman, B., Alonso-Monge, R., Román, E., Arana, D., Nombela, C., and Pla, J. (2006). The Cek1 and Hog1 mitogen-activated protein kinases play complementary roles in cell wall biogenesis and chlamydospore formation in the fungal pathogen Candida albicans. Eukaryot Cell *5*, 347-358.
Enserink, J.M., and Kolodner, R.D. (2010). An overview of Cdk1-controlled targets and processes. Cell Div *5*, 11.
Ernst, J.F. (2000). Transcription factors in Candida albicans - environmental control of morphogenesis. Microbiology *146 (Pt 8)*, 1763-1774.
Estey, M.P., Di Ciano-Oliveira, C., Froese, C.D., Bejide, M.T., and Trimble, W.S. (2010). Distinct roles of septins in cytokinesis: SEPT9 mediates midbody abscission. J Cell Biol *191*, 741-749.
Farkasovsky, M., Herter, P., Voss, B., and Wittinghofer, A. (2005). Nucleotide binding and filament assembly of recombinant yeast septin complexes. Biol Chem *386*, 643-656.
Faty, M., Fink, M., and Barral, Y. (2002). Septins: a ring to part mother and daughter. Curr Genet *41*, 123-131.
Fidel, P.L. (1999). Host defense against oropharyngeal and vaginal candidiasis: Site-specific differences. Rev Iberoam Micol *16*, 8-15.
Field, C.M., al-Awar, O., Rosenblatt, J., Wong, M.L., Alberts, B., and Mitchison, T.J. (1996). A purified Drosophila septin complex forms filaments and exhibits GTPase activity. J Cell Biol *133*, 605-616.
Finger, F.P. (2005). Reining in cytokinesis with a septin corral. Bioessays *27*, 5-8.
Flescher, E.G., Madden, K., and Snyder, M. (1993). Components required for cytokinesis are important for bud site selection in yeast. J Cell Biol *122*, 373-386.
Fujii-Nakata, T., Ishimi, Y., Okuda, A., and Kikuchi, A. (1992). Functional analysis of nucleosome assembly protein, NAP-1. The negatively charged COOH-terminal region is not necessary for the intrinsic assembly activity. J Biol Chem *267*, 20980-20986.
Gal, T.Z., Glazer, I., Sherman, A., and Koltai, H. (2005). Protein interaction of nucleosome assembly protein 1 and casein kinase 2 during desiccation response in the insect-killing nematode Steinernema feltiae IS-6. J Parasitol *91*, 691-693.
Gladfelter, A.S., Bose, I., Zyla, T.R., Bardes, E.S., and Lew, D.J. (2002). Septin ring assembly involves cycles of GTP loading and hydrolysis by Cdc42p. J Cell Biol *156*, 315-326.
Gladfelter, A.S., Pringle, J.R., and Lew, D.J. (2001). The septin cortex at the yeast mother-bud neck. Curr Opin Microbiol *4*, 681-689.
Gonzalez, M.E., Makarova, O., Peterson, E.A., Privette, L.M., and Petty, E.M. (2009). Up-regulation of SEPT9_v1 stabilizes c-Jun-N-terminal kinase and contributes to its pro-proliferative activity in mammary epithelial cells. Cell Signal *21*, 477-487.
González-Novo, A., Correa-Bordes, J., Labrador, L., Sánchez, M., Vázquez de Aldana, C.R., and Jiménez, J. (2008). Sep7 is essential to modify septin ring dynamics and inhibit cell separation during Candida albicans hyphal growth. Mol Biol Cell *19*, 1509-1518.

Gow, N.A., Knox, Y., Munro, C.A., and Thompson, W.D. (2003). Infection of chick chorioallantoic membrane (CAM) as a model for invasive hyphal growth and pathogenesis of Candida albicans. Med Mycol *41*, 331-338.
Hartwell, L.H. (1971). Genetic control of the cell division cycle in yeast. IV. Genes controlling bud emergence and cytokinesis. Exp Cell Res *69*, 265-276.
Hawser, S., and Islam, K. (1996). Spectrophotometric determination of the morphogenetic transformation by synchronous Candida albicans: effects of antifungal agents. J Antimicrob Chemother *38*, 67-73.
Hazan, I., Sepulveda-Becerra, M., and Liu, H. (2002). Hyphal elongation is regulated independently of cell cycle in Candida albicans. Mol Biol Cell *13*, 134-145.
Hu, Q., Nelson, W.J., and Spiliotis, E.T. (2008). Forchlorfenuron alters mammalian septin assembly, organization, and dynamics. J Biol Chem *283*, 29563-29571.
Hull, C.M., and Johnson, A.D. (1999). Identification of a mating type-like locus in the asexual pathogenic yeast Candida albicans. Science *285*, 1271-1275.
Hull, C.M., Raisner, R.M., and Johnson, A.D. (2000). Evidence for mating of the "asexual" yeast Candida albicans in a mammalian host. Science *289*, 307-310.
Ishimi, Y., and Kikuchi, A. (1991). Identification and molecular cloning of yeast homolog of nucleosome assembly protein I which facilitates nucleosome assembly in vitro. J Biol Chem *266*, 7025-7029.
Ishimi, Y., Kojima, M., Yamada, M., and Hanaoka, F. (1987). Binding mode of nucleosome-assembly protein (AP-I) and histones. Eur J Biochem *162*, 19-24.
Ishimi, Y., Sato, W., Kojima, M., Sugasawa, K., Hanaoka, F., and Yamada, M. (1985). Rapid purification of nucleosome assembly protein (AP-I) and production of monoclonal antibodies against it. Cell Struct Funct *10*, 373-382.
Ito, T., Tyler, J.K., Bulger, M., Kobayashi, R., and Kadonaga, J.T. (1996). ATP-facilitated chromatin assembly with a nucleoplasmin-like protein from Drosophila melanogaster. J Biol Chem *271*, 25041-25048.
Iwase, M., Luo, J., Nagaraj, S., Longtine, M., Kim, H.B., Haarer, B.K., Caruso, C., Tong, Z., Pringle, J.R., and Bi, E. (2006). Role of a Cdc42p effector pathway in recruitment of the yeast septins to the presumptive bud site. Mol Biol Cell *17*, 1110-1125.
Iwase, M., Okada, S., Oguchi, T., and Toh-e, A. (2004). Forchlorfenuron, a phenylurea cytokinin, disturbs septin organization in Saccharomyces cerevisiae. Genes Genet Syst *79*, 199-206.
Jackson, L.P., Reed, S.I., and Haase, S.B. (2006). Distinct mechanisms control the stability of the related S-phase cyclins Clb5 and Clb6. Mol Cell Biol *26*, 2456-2466.
John, C.M., Hite, R.K., Weirich, C.S., Fitzgerald, D.J., Jawhari, H., Faty, M., Schläpfer, D., Kroschewski, R., Winkler, F.K., Walz, T., *et al.* (2007). The Caenorhabditis elegans septin complex is nonpolar. EMBO J *26*, 3296-3307.
Kadota, J., Yamamoto, T., Yoshiuchi, S., Bi, E., and Tanaka, K. (2004). Septin ring assembly requires concerted action of polarisome components, a PAK kinase Cla4p, and the actin cytoskeleton in Saccharomyces cerevisiae. Mol Biol Cell *15*, 5329-5345.
Kellogg, D.R., Kikuchi, A., Fujii-Nakata, T., Turck, C.W., and Murray, A.W. (1995). Members of the NAP/SET family of proteins interact specifically with B-type cyclins. J Cell Biol *130*, 661-673.

Kellogg, D.R., and Murray, A.W. (1995). NAP1 acts with Clb1 to perform mitotic functions and to suppress polar bud growth in budding yeast. J Cell Biol *130*, 675-685.
Kinoshita, M., Field, C.M., Coughlin, M.L., Straight, A.F., and Mitchison, T.J. (2002). Self- and actin-templated assembly of Mammalian septins. Dev Cell *3*, 791-802.
Kozubowski, L., Larson, J.R., and Tatchell, K. (2005). Role of the septin ring in the asymmetric localization of proteins at the mother-bud neck in Saccharomyces cerevisiae. Mol Biol Cell *16*, 3455-3466.
Kumar, M.J., Jamaluddin, M.S., Natarajan, K., Kaur, D., and Datta, A. (2000). The inducible N-acetylglucosamine catabolic pathway gene cluster in Candida albicans: discrete N-acetylglucosamine-inducible factors interact at the promoter of NAG1. Proc Natl Acad Sci U S A *97*, 14218-14223.
Káposzta, R., Tree, P., Maródi, L., and Gordon, S. (1998). Characteristics of invasive candidiasis in gamma interferon- and interleukin-4-deficient mice: role of macrophages in host defense against Candida albicans. Infect Immun *66*, 1708-1717.
Lankenau, S., Barnickel, T., Marhold, J., Lyko, F., Mechler, B.M., and Lankenau, D.H. (2003). Knockout targeting of the Drosophila nap1 gene and examination of DNA repair tracts in the recombination products. Genetics *163*, 611-623.
Lee, J.M., and Greenleaf, A.L. (1991). CTD kinase large subunit is encoded by CTK1, a gene required for normal growth of Saccharomyces cerevisiae. Gene Expr *1*, 149-167.
Li, M., Strand, D., Krehan, A., Pyerin, W., Heid, H., Neumann, B., and Mechler, B.M. (1999). Casein kinase 2 binds and phosphorylates the nucleosome assembly protein-1 (NAP1) in Drosophila melanogaster. J Mol Biol *293*, 1067-1084.
Liao, S.M., Zhang, J., Jeffery, D.A., Koleske, A.J., Thompson, C.M., Chao, D.M., Viljoen, M., van Vuuren, H.J., and Young, R.A. (1995). A kinase-cyclin pair in the RNA polymerase II holoenzyme. Nature *374*, 193-196.
Liu, H., Köhler, J., and Fink, G.R. (1994). Suppression of hyphal formation in Candida albicans by mutation of a STE12 homolog. Science *266*, 1723-1726.
Liu, J., and Kipreos, E.T. (2000). Evolution of cyclin-dependent kinases (CDKs) and CDK-activating kinases (CAKs): differential conservation of CAKs in yeast and metazoa. Mol Biol Evol *17*, 1061-1074.
Lo, H.J., Köhler, J.R., DiDomenico, B., Loebenberg, D., Cacciapuoti, A., and Fink, G.R. (1997). Nonfilamentous C. albicans mutants are avirulent. Cell *90*, 939-949.
Longtine, M.S., and Bi, E. (2003). Regulation of septin organization and function in yeast. Trends Cell Biol *13*, 403-409.
Longtine, M.S., Fares, H., and Pringle, J.R. (1998). Role of the yeast Gin4p protein kinase in septin assembly and the relationship between septin assembly and septin function. J Cell Biol *143*, 719-736.
Longtine, M.S., Theesfeld, C.L., McMillan, J.N., Weaver, E., Pringle, J.R., and Lew, D.J. (2000). Septin-dependent assembly of a cell cycle-regulatory module in Saccharomyces cerevisiae. Mol Cell Biol *20*, 4049-4061.
Luedeke, C., Frei, S.B., Sbalzarini, I., Schwarz, H., Spang, A., and Barral, Y. (2005). Septin-dependent compartmentalization of the endoplasmic reticulum during yeast polarized growth. J Cell Biol *169*, 897-908.
López-Ribot, J.L. (2005). Candida albicans biofilms: more than filamentation. Curr Biol *15*, R453-455.

Lörincz, A.T., and Reed, S.I. (1984). Primary structure homology between the product of yeast cell division control gene CDC28 and vertebrate oncogenes. Nature *307*, 183-185.
Magee, B.B., and Magee, P.T. (1997). WO-2, a stable aneuploid derivative of Candida albicans strain WO-1, can switch from white to opaque and form hyphae. Microbiology *143 (Pt 2)*, 289-295.
Magee, P.T. (2010). Fungal pathogenicity and morphological switches. Nat Genet *42*, 560-561.
Malic, S., Hill, K.E., Ralphs, J.R., Hayes, A., Thomas, D.W., Potts, A.J., and Williams, D.W. (2007). Characterization of Candida albicans infection of an in vitro oral epithelial model using confocal laser scanning microscopy. Oral Microbiol Immunol *22*, 188-194.
McBryant, S.J., and Peersen, O.B. (2004). Self-association of the yeast nucleosome assembly protein 1. Biochemistry *43*, 10592-10599.
McMurray, M.A., Bertin, A., Garcia, G., Lam, L., Nogales, E., and Thorner, J. (2011). Septin filament formation is essential in budding yeast. Dev Cell *20*, 540-549.
McMurray, M.A., and Thorner, J. (2009a). Reuse, replace, recycle. Specificity in subunit inheritance and assembly of higher-order septin structures during mitotic and meiotic division in budding yeast. Cell Cycle *8*, 195-203.
McMurray, M.A., and Thorner, J. (2009b). Septins: molecular partitioning and the generation of cellular asymmetry. Cell Div *4*, 18.
Mendenhall, M.D., and Hodge, A.E. (1998). Regulation of Cdc28 cyclin-dependent protein kinase activity during the cell cycle of the yeast Saccharomyces cerevisiae. Microbiol Mol Biol Rev *62*, 1191-1243.
Miyaji-Yamaguchi, M., Kato, K., Nakano, R., Akashi, T., Kikuchi, A., and Nagata, K. (2003). Involvement of nucleocytoplasmic shuttling of yeast Nap1 in mitotic progression. Mol Cell Biol *23*, 6672-6684.
Morschhäuser, J., Michel, S., and Staib, P. (1999). Sequential gene disruption in Candida albicans by FLP-mediated site-specific recombination. Mol Microbiol *32*, 547-556.
Mortensen, E.M., McDonald, H., Yates, J., and Kellogg, D.R. (2002). Cell cycle-dependent assembly of a Gin4-septin complex. Mol Biol Cell *13*, 2091-2105.
Nagaraj, S., Rajendran, A., Jackson, C.E., and Longtine, M.S. (2008). Role of nucleotide binding in septin-septin interactions and septin localization in Saccharomyces cerevisiae. Mol Cell Biol *28*, 5120-5137.
Odds, F.C. (1985). Morphogenesis in Candida albicans. Crit Rev Microbiol *12*, 45-93.
Oh, Y., and Bi, E. (2010). Septin structure and function in yeast and beyond. Trends Cell Biol.
Ohkuni, K., Shirahige, K., and Kikuchi, A. (2003). Genome-wide expression analysis of NAP1 in Saccharomyces cerevisiae. Biochem Biophys Res Commun *306*, 5-9.
Okuzaki, D., Tanaka, S., Kanazawa, H., and Nojima, H. (1997). Gin4 of S. cerevisiae is a bud neck protein that interacts with the Cdc28 complex. Genes Cells *2*, 753-770.
Ozsarac, N., Bhattacharyya, M., Dawes, I.W., and Clancy, M.J. (1995). The SPR3 gene encodes a sporulation-specific homologue of the yeast CDC3/10/11/12 family of bud neck microfilaments and is regulated by ABFI. Gene *164*, 157-162.
Pan, F., Malmberg, R.L., and Momany, M. (2007). Analysis of septins across kingdoms reveals orthology and new motifs. BMC Evol Biol *7*, 103.

Park, H.O., and Bi, E. (2007). Central roles of small GTPases in the development of cell polarity in yeast and beyond. Microbiol Mol Biol Rev *71*, 48-96.
Park, Y.J., and Luger, K. (2006a). Structure and function of nucleosome assembly proteins. Biochem Cell Biol *84*, 549-558.
Park, Y.J., and Luger, K. (2006b). The structure of nucleosome assembly protein 1. Proc Natl Acad Sci U S A *103*, 1248-1253.
Perepnikhatka, V., Fischer, F.J., Niimi, M., Baker, R.A., Cannon, R.D., Wang, Y.K., Sherman, F., and Rustchenko, E. (1999). Specific chromosome alterations in fluconazole-resistant mutants of Candida albicans. J Bacteriol *181*, 4041-4049.
Rabkin, J.M., Oroloff, S.L., Corless, C.L., Benner, K.G., Flora, K.D., Rosen, H.R., and Olyaei, A.J. (2000). Association of fungal infection and increased mortality in liver transplant recipients. Am J Surg *179*, 426-430.
Ramage, G., VandeWalle, K., López-Ribot, J.L., and Wickes, B.L. (2002). The filamentation pathway controlled by the Efg1 regulator protein is required for normal biofilm formation and development in Candida albicans. FEMS Microbiol Lett *214*, 95-100.
Richards, M.J., Edwards, J.R., Culver, D.H., and Gaynes, R.P. (1999). Nosocomial infections in medical intensive care units in the United States. National Nosocomial Infections Surveillance System. Crit Care Med *27*, 887-892.
Richardson, H., Lew, D.J., Henze, M., Sugimoto, K., and Reed, S.I. (1992). Cyclin-B homologs in Saccharomyces cerevisiae function in S phase and in G2. Genes Dev *6*, 2021-2034.
Rocha, C.R., Schröppel, K., Harcus, D., Marcil, A., Dignard, D., Taylor, B.N., Thomas, D.Y., Whiteway, M., and Leberer, E. (2001). Signaling through adenylyl cyclase is essential for hyphal growth and virulence in the pathogenic fungus Candida albicans. Mol Biol Cell *12*, 3631-3643.
Rodal, A.A., Kozubowski, L., Goode, B.L., Drubin, D.G., and Hartwig, J.H. (2005). Actin and septin ultrastructures at the budding yeast cell cortex. Mol Biol Cell *16*, 372-384.
Rogner, U.C., Spyropoulos, D.D., Le Novère, N., Changeux, J.P., and Avner, P. (2000). Control of neurulation by the nucleosome assembly protein-1-like 2. Nat Genet *25*, 431-435.
Sato, T., Watanabe, T., Mikami, T., and Matsumoto, T. (2004). Farnesol, a morphogenetic autoregulatory substance in the dimorphic fungus Candida albicans, inhibits hyphae growth through suppression of a mitogen-activated protein kinase cascade. Biol Pharm Bull *27*, 751-752.
Satyanarayana, A., and Kaldis, P. (2009). Mammalian cell-cycle regulation: several Cdks, numerous cyclins and diverse compensatory mechanisms. Oncogene *28*, 2925-2939.
Seider, K., Heyken, A., Lüttich, A., Miramón, P., and Hube, B. (2010). Interaction of pathogenic yeasts with phagocytes: survival, persistence and escape. Curr Opin Microbiol *13*, 392-400.
Seufert, W., Futcher, B., and Jentsch, S. (1995). Role of a ubiquitin-conjugating enzyme in degradation of S- and M-phase cyclins. Nature *373*, 78-81.
Shcheprova, Z., Baldi, S., Frei, S.B., Gonnet, G., and Barral, Y. (2008). A mechanism for asymmetric segregation of age during yeast budding. Nature *454*, 728-734.

Sherlock, G., Bahman, A.M., Mahal, A., Shieh, J.C., Ferreira, M., and Rosamond, J. (1994). Molecular cloning and analysis of CDC28 and cyclin homologues from the human fungal pathogen Candida albicans. Mol Gen Genet *245*, 716-723.
Simon, M., Seraphin, B., and Faye, G. (1986). KIN28, a yeast split gene coding for a putative protein kinase homologous to CDC28. EMBO J *5*, 2697-2701.
Sinha, I., Wang, Y.M., Philp, R., Li, C.R., Yap, W.H., and Wang, Y. (2007). Cyclin-dependent kinases control septin phosphorylation in Candida albicans hyphal development. Dev Cell *13*, 421-432.
Sirajuddin, M., Farkasovsky, M., Hauer, F., Kühlmann, D., Macara, I.G., Weyand, M., Stark, H., and Wittinghofer, A. (2007). Structural insight into filament formation by mammalian septins. Nature *449*, 311-315.
Sirajuddin, M., Farkasovsky, M., Zent, E., and Wittinghofer, A. (2009). GTP-induced conformational changes in septins and implications for function. Proc Natl Acad Sci U S A *106*, 16592-16597.
Skaar, J.R., and Pagano, M. (2009). Control of cell growth by the SCF and APC/C ubiquitin ligases. Curr Opin Cell Biol *21*, 816-824.
Soll, D.R. (1997). Gene regulation during high-frequency switching in Candida albicans. Microbiology *143 (Pt 2)*, 279-288.
Steer, W.M., Abu-Daya, A., Brickwood, S.J., Mumford, K.L., Jordanaires, N., Mitchell, J., Robinson, C., Thorne, A.W., and Guille, M.J. (2003). Xenopus nucleosome assembly protein becomes tissue-restricted during development and can alter the expression of specific genes. Mech Dev *120*, 1045-1057.
Sudbery, P., Gow, N., and Berman, J. (2004). The distinct morphogenic states of Candida albicans. Trends Microbiol *12*, 317-324.
Sudbery, P.E. (2001). The germ tubes of Candida albicans hyphae and pseudohyphae show different patterns of septin ring localization. Mol Microbiol *41*, 19-31.
Takizawa, P.A., DeRisi, J.L., Wilhelm, J.E., and Vale, R.D. (2000). Plasma membrane compartmentalization in yeast by messenger RNA transport and a septin diffusion barrier. Science *290*, 341-344.
Tang, C.S., and Reed, S.I. (2002). Phosphorylation of the septin cdc3 in g1 by the cdc28 kinase is essential for efficient septin ring disassembly. Cell Cycle *1*, 42-49.
Toh-e, A., Tanaka, K., Uesono, Y., and Wickner, R.B. (1988). PHO85, a negative regulator of the PHO system, is a homolog of the protein kinase gene, CDC28, of Saccharomyces cerevisiae. Mol Gen Genet *214*, 162-164.
Tyers, M., Tokiwa, G., and Futcher, B. (1993). Comparison of the Saccharomyces cerevisiae G1 cyclins: Cln3 may be an upstream activator of Cln1, Cln2 and other cyclins. EMBO J *12*, 1955-1968.
van de Veerdonk, F.L., Kullberg, B.J., and Netea, M.G. (2010). Pathogenesis of invasive candidiasis. Curr Opin Crit Care *16*, 453-459.
Versele, M., Gullbrand, B., Shulewitz, M.J., Cid, V.J., Bahmanyar, S., Chen, R.E., Barth, P., Alber, T., and Thorner, J. (2004). Protein-protein interactions governing septin heteropentamer assembly and septin filament organization in Saccharomyces cerevisiae. Mol Biol Cell *15*, 4568-4583.
Versele, M., and Thorner, J. (2004). Septin collar formation in budding yeast requires GTP binding and direct phosphorylation by the PAK, Cla4. J Cell Biol *164*, 701-715.

Vrabioiu, A.M., Gerber, S.A., Gygi, S.P., Field, C.M., and Mitchison, T.J. (2004). The majority of the Saccharomyces cerevisiae septin complexes do not exchange guanine nucleotides. J Biol Chem *279*, 3111-3118.
Wang, A., Raniga, P.P., Lane, S., Lu, Y., and Liu, H. (2009). Hyphal chain formation in Candida albicans: Cdc28-Hgc1 phosphorylation of Efg1 represses cell separation genes. Mol Cell Biol *29*, 4406-4416.
Warenda, A.J., Kauffman, S., Sherrill, T.P., Becker, J.M., and Konopka, J.B. (2003). Candida albicans septin mutants are defective for invasive growth and virulence. Infect Immun *71*, 4045-4051.
Warenda, A.J., and Konopka, J.B. (2002). Septin function in Candida albicans morphogenesis. Mol Biol Cell *13*, 2732-2746.
Weirich, C.S., Erzberger, J.P., and Barral, Y. (2008). The septin family of GTPases: architecture and dynamics. Nat Rev Mol Cell Biol *9*, 478-489.
Wightman, R., Bates, S., Amornrrattanapan, P., and Sudbery, P. (2004). In Candida albicans, the Nim1 kinases Gin4 and Hsl1 negatively regulate pseudohypha formation and Gin4 also controls septin organization. J Cell Biol *164*, 581-591.
Wilson, L.S., Reyes, C.M., Stolpman, M., Speckman, J., Allen, K., and Beney, J. (2002). The direct cost and incidence of systemic fungal infections. Value Health *5*, 26-34.
Xu, X.L., Lee, R.T., Fang, H.M., Wang, Y.M., Li, R., Zou, H., Zhu, Y., and Wang, Y. (2008). Bacterial peptidoglycan triggers Candida albicans hyphal growth by directly activating the adenylyl cyclase Cyr1p. Cell Host Microbe *4*, 28-39.
Yao, S., Neiman, A., and Prelich, G. (2000). BUR1 and BUR2 encode a divergent cyclin-dependent kinase-cyclin complex important for transcription in vivo. Mol Cell Biol *20*, 7080-7087.
Yoon, H.W., Kim, M.C., Lee, S.Y., Hwang, I., Bahk, J.D., Hong, J.C., Ishimi, Y., and Cho, M.J. (1995). Molecular cloning and functional characterization of a cDNA encoding nucleosome assembly protein 1 (NAP-1) from soybean. Mol Gen Genet *249*, 465-473.
Zheng, X., and Wang, Y. (2004). Hgc1, a novel hypha-specific G1 cyclin-related protein regulates Candida albicans hyphal morphogenesis. EMBO J *23*, 1845-1856.
Zheng, X.D., Lee, R.T., Wang, Y.M., Lin, Q.S., and Wang, Y. (2007). Phosphorylation of Rga2, a Cdc42 GAP, by CDK/Hgc1 is crucial for Candida albicans hyphal growth. EMBO J *26*, 3760-3769.
Zilberberg, M.D., Shorr, A.F., and Kollef, M.H. (2008). Secular trends in candidemia-related hospitalization in the United States, 2000-2005. Infect Control Hosp Epidemiol *29*, 978-980.
Zlatanova, J., Seebart, C., and Tomschik, M. (2007). Nap1: taking a closer look at a juggler protein of extraordinary skills. FASEB J *21*, 1294-1310.